NASA Tech Briefs

Official Publication of
National Aeronautics and
Space Administration
Volume 15 Number 5

Transferring Technology
to Industry and
Government

May 1991

Lasers Track Fast Fluid Flows

NOW THAT 10GB FITS ON AN 8MM TAPE, WHAT ARE YOU WAITING FOR?

You don't need to wait hours to change tapes.

You don't need to wait months for other storage technologies to catch up.

One 8mm tape drive will already deliver more than they promise.

It's the digital CY-8200, now with optional data compression. And you can get it exclusively from Contemporary Cybernetics Group.

True "Plug-And-Play" Compatibility With:

Alliant	DEC 3100	IBM S/36	Pertec
Alpha Micro	DEC HSC	IBM AS/400	Plexus
Altos	DEC Q-Bus	Macintosh	Prime
Apollo	DEC TU/TA81	NCR	Pyramid
Arix	DEC Unibus	Novell	Sequent
AT&T	Gould	PC 386/ix	Sun
Convergent	HP	PC MS-DOS	Unisys
Data General	IBM RT	PC Xenix/Unix	Wang

and more...

With data compression, the CY-8200 can quadruple the amount of data you can load on an 8mm cassette that fits neatly in your shirt pocket. Meaning the already tremendous savings in man hours, media costs, storage and shipping are multiplied by four.

Until now, the best 8mm drive on the market stored an impressive 2.5GB per tape at speeds up to 15 MB per minute.

Our data compression option allows you to write up to 10 GB per tape at up to 60 MB per minute. Completely unattended.

Of course, the data compression feature is switch-selectable, so you can turn off data compression to read and write standard 8mm tapes.

Plus it's a simple upgrade for the best tape drive built: our CY-8200. Offering a complete range of standard interfaces, a 2-line, 40-column display option, and optional security card encryption. And assuring you of full support and a 12-month warranty from the leader in advanced 8mm helical scan technology.

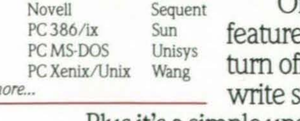

The CY-8200 with data compression will remain the best value in data storage for a long time to come. So now you've got many good reasons for calling us today at (804) 873-0900 and no good reason for waiting.

CONTEMPORARY CYBERNETICS Group

Rock Landing Corporate Center • 11846 Rock Landing • Newport News, Virginia 23606 • Phone (804) 873-0900 • FAX (804) 873-8836

Circle Reader Action No. 411

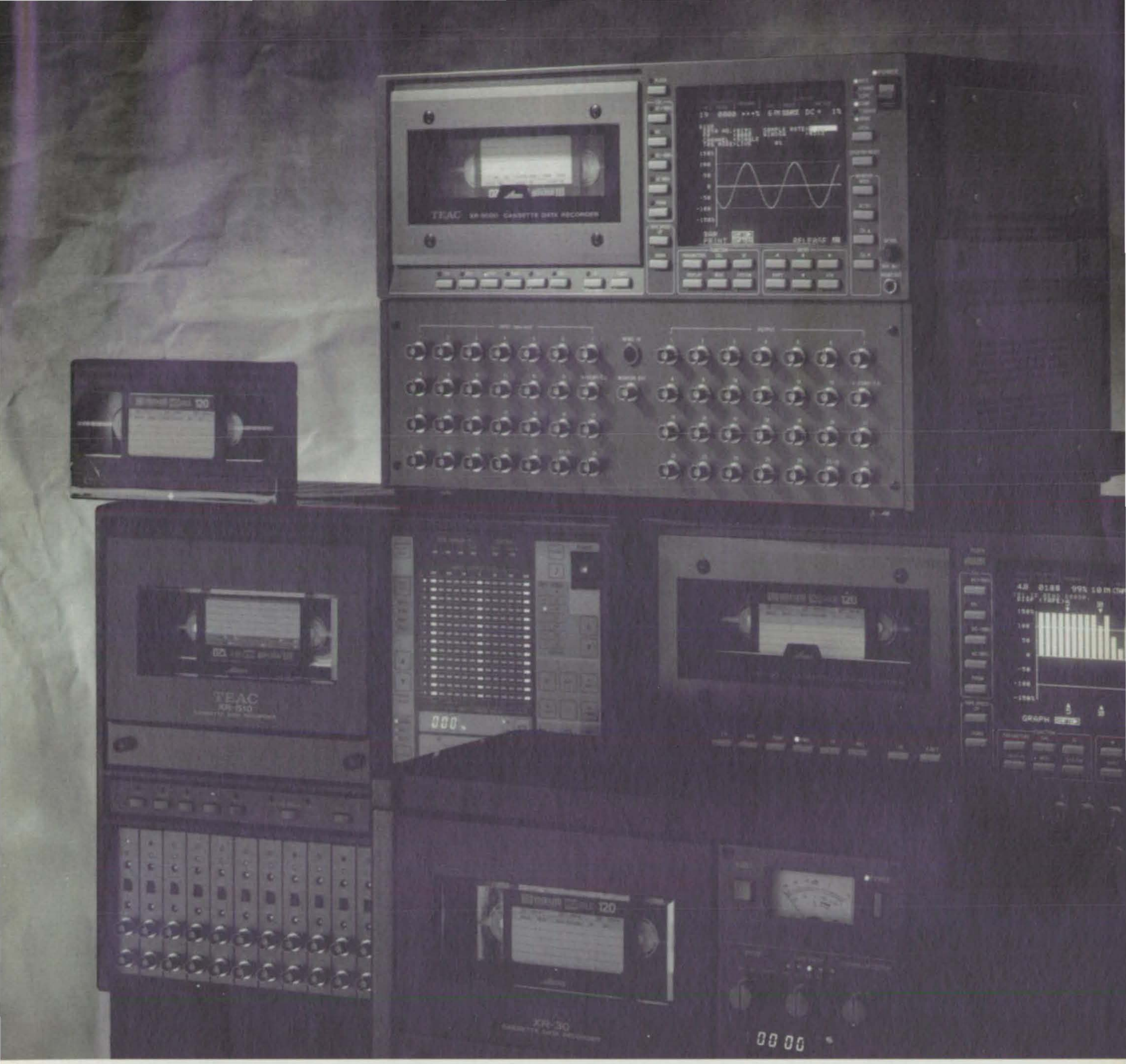

NOW TEAC'S XR SERIES IS 28-CHANNELS WIDE.

Introducing the world's first 28-channel VHS data recorder. The TEAC XR-9000. Now the performance and capacity of the larger open-reel decks are available with the convenience, economy and ease of operation of VHS cassettes. All within a lightweight, minimum foot print unit.

The XR-9000 offers TEAC's exclusive menu-driven on-screen display plus numerous auto-functions to provide a simple step-by-step setup procedure. You can use your computer to remotely control the XR-9000. And recorded data from the XR-9000 can be fed directly into a computer.

It's been over a decade since TEAC introduced the world's first VHS cassette data recorder. Since then, we've helped develop every major improvement in VHS data recording technology. Today we're building VHS data recorders from 7- to 28-channels with models available in Wide Band Groups I and II, plus interchangeable FM, Super FM DR, and PCM modules. And in an industry with little tolerance for error, TEAC's enviable record of performance and reliability is unsurpassed.

So, if you're looking for greater capacity, with the most variety of options and models, at the most efficient cost-per-channel, TEAC XR series data recorders is the only place you'll find it.

TEAC®

Information Products Division.

Circle Reader Action No. 344

The IBM RISC System/
The power you've been seeking

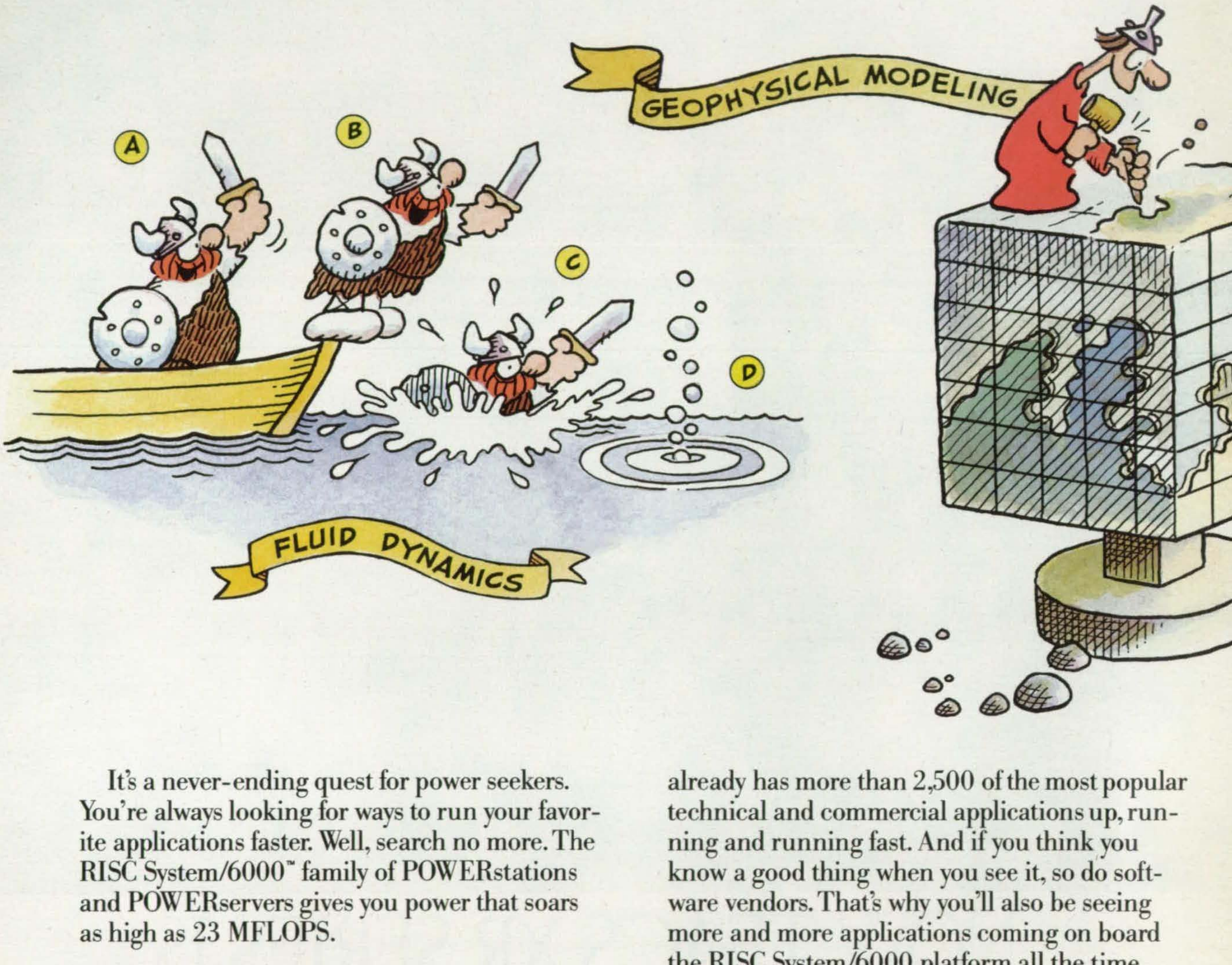

It's a never-ending quest for power seekers. You're always looking for ways to run your favorite applications faster. Well, search no more. The RISC System/6000™ family of POWERstations and POWERservers gives you power that soars as high as 23 MFLOPS.

	MFLOPS	MIPS	SPECmark™
POWERstation 320	8.5	29.5	24.6
DECstation 5000-200	3.7	24.2	18.5

When it comes to porting, your ship has come in. Of course, all the speed in the world wouldn't mean much without the applications you need. So the RISC System/6000 family already has more than 2,500 of the most popular technical and commercial applications up, running and running fast. And if you think you know a good thing when you see it, so do software vendors. That's why you'll also be seeing more and more applications coming on board the RISC System/6000 platform all the time. And if you like to build your own solutions, there's a full arsenal of enablers and relational data bases from leading vendors, as well as CASE tools and a host of popular programming languages.

A smorgasbord of solutions. Applications already announced include the IBM engineering design packages CADAM™, CAEDS™, CBDS™,

MFLOPS are the results of the double-precision, all FORTRAN Linpack test 100x100 array suite. The Dhrystone Version 1.1 test results are used to compute RISC System/6000 Integer MIPS value where 1,757 Dhrystones/second is 1 MIPS (Vax 11/780). SPECmark is a geometric mean of ten benchmark tests. All performance data are based on published benchmark information.

6000 family.
for all your applications.

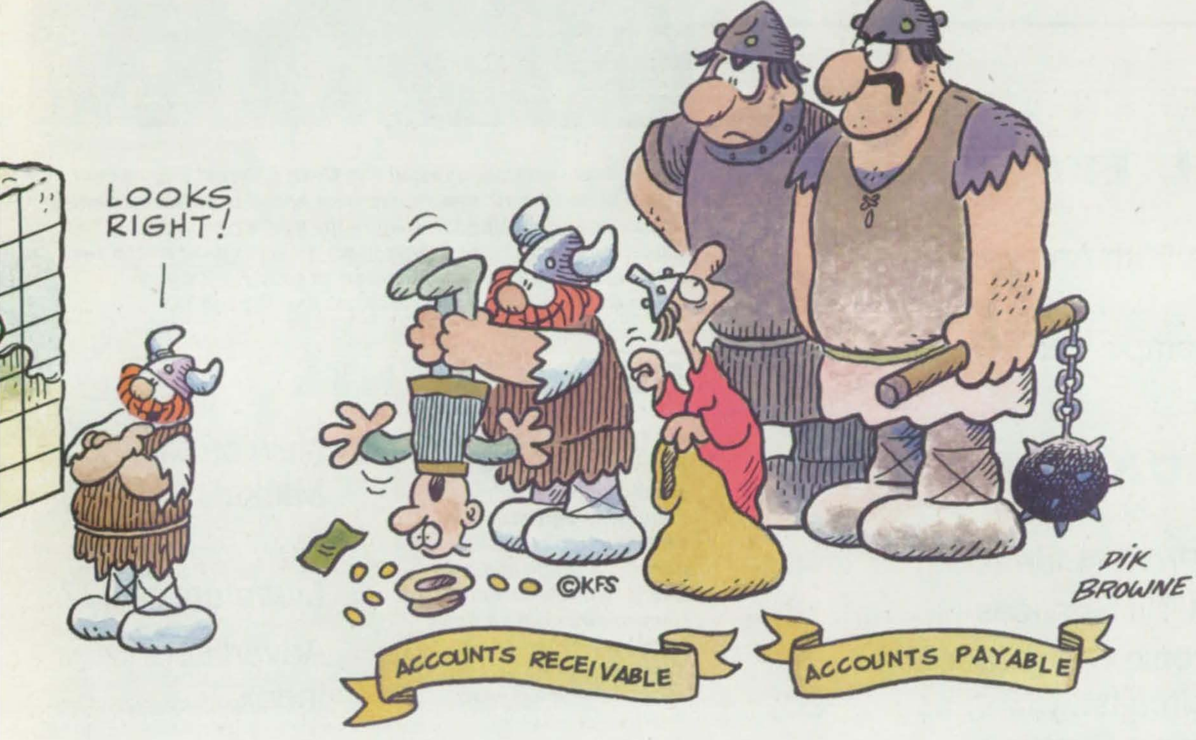

CATIA™ and AES. Also available are a broad spectrum of solutions from vendors like Valid Logic, MacNeal Schwendler, Swanson Analysis, SAS Institute, SPSS, Wavefront, Alias, Polygen, Cadence, Fluid Dynamics International, Western Atlas, ECL Petro and creare.X. Scientific and technical applications are available in areas like physics, structural analysis, chemistry, securities trading, mathematics, earth resources, operations research, visualization, graphics, technical publishing and more. There's also accounting software like FourGen and support for leading UNIX®-based office automation packages. And there are key industry applications for businesses in medical groups, retail stores, newspapers, pharmacies and many more.

Command enormous processing clout. The RISC System/6000 family is built to boost the performance of the software power seekers use most. It's got the best floating point processor in the business for numerically intensive applications, plus a new superscalar processor and incredible 3D graphics capabilities. To find out more, call your IBM marketing representative or IBM Business Partner. For literature, call 1 800 IBM-6676, ext. 990.

For the Power Seeker.

IBM®

NASA Tech Briefs

Transferring Technology to Industry and Government

May 1991
Volume 15 Number 5

BPA ABP

Photo courtesy Lewis Research Center

Lewis Research Center tested this Mach 5 aircraft engine inlet model in its 10' x 10' supersonic wind tunnel to validate computational codes developed to analyze the inlet's performance. The model may provide the design basis for inlets used on the next generation of supersonic transport aircraft. For more on the Lewis Center's propulsion research, turn to page 12.

SPECIAL FEATURES

TECHNICAL SECTION

DEPARTMENTS

On The Cover: NASA is employing laser spectroscopic techniques to simultaneously measure air temperature and density. A prime application is to track fluctuations in turbulent air flows inside wind tunnels. See the tech brief on page 43.
(Photo courtesy Ames Research Center)

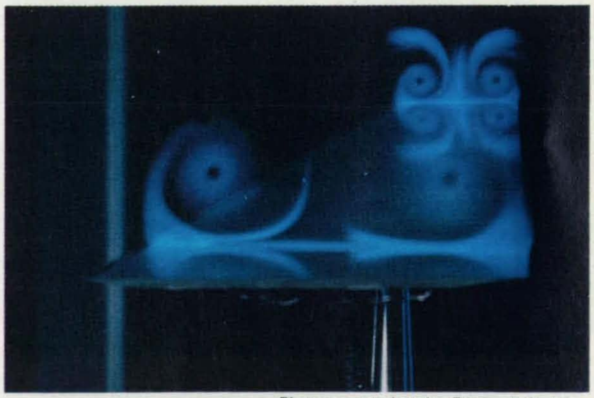

Photo courtesy Langley Research Center

A laser-based system designed to illuminate flows in the Langley Center's Basic Aerodynamics Research Tunnel may be reapplied in the art and construction industries. See page 30.

NASA Tech Briefs, ISSN 0145-319X, USPS 750-070, copyright © 1991 in U.S., is published monthly by Associated Business Publications Co., Ltd., 41 E. 42nd St., New York, NY 10017-5391. The copyrighted information does not include the individual tech briefs which are supplied by NASA. Editorial, sales, production and circulation offices at 41 East 42nd Street, New York, NY 10017-5391. Subscription for non-qualified subscribers in the U.S., Panama Canal Zone, and Puerto Rico, $75.00 for 1 year; $125.00 for 2 years; $200.00 for 3 years. Single copies $10.00. Foreign subscriptions one-year U.S. Funds $150.00. Remit by check, draft, postal, express orders or VISA, MasterCard, and American Express. Other remittances at sender's risk. Address all communications for subscriptions or circulation to NASA Tech Briefs, 41 East 42nd Street, New York, NY 10017-5391. Second-class postage paid at New York, NY and additional mailing offices. **POSTMASTER: please send address changes to NASA Tech Briefs, 41 E. 42nd Street, Suite 921, New York, NY 10017-5391.**

To show you what our new DataGraf recorder can do,

GOULD
Electronics

No matter how advanced your recorder is, it still has to meet your most basic recording needs. That's why our new DataGraf offers everything you'd expect from a computer-based recorder—plus unique hard copy output flexibility.

How advanced is DataGraf? It offers 16-channel recording capability, all in a rugged, portable package weighing less than forty pounds. With DataGraf, you can store events on disk and replay them as often as you like. You can also expand or compress traces, overlay signals, and even label key points.

What's more, using advanced waveform analysis software, DataGraf automatically analyzes your data, virtually eliminating the need for manual interpolation and long-hand math. Whether you're interested in the entire signal or just a specific section, the touch of a button will calculate Max/Min, Standard Deviation, dY/dX, RMS, and much more.

And when it comes to seeing your results on paper, DataGraf can output your traces to hundreds of printers, plotters and traditional oscillographic recorders.

It's exactly the kind of solution you'd expect from Gould, a company with over fifty years of recorder development experience. By applying new technology to the real needs of today's engineers, we've developed a unit that offers real advantages. Advantages that go beyond advanced features. Advantages you can put on paper.

Send for a free DataGraf demo disk. Use the coupon below, or fax your request to (216) 328-7400.

we put it on paper.

Free demo disk!

NTB 5/91

Yes! I'd like to see what DataGraf can do. Send me a free demo disk and product information package.

NAME: ______________ TITLE: ______________

COMPANY: ______________________________

STREET: ______________________________

CITY: ______________ STATE: ______ ZIP: __________

PHONE: ______________________________

Send to: Gould, Inc., Test and Measurement, 8333 Rockside Road, Valley View, Ohio 44125, or call (216) 328-7000. Fax: (216) 328-7400

The road to the future passes through San Jose this December as NASA, the Technology Utilization Foundation, and *NASA Tech Briefs* magazine host **Technology 2001**, the second national technology transfer conference and exposition. In three information-packed days, experts from top government research laboratories will reveal the latest innovations in five critical areas of technology: Computer Technology and Software Engineering, Electronics, Advanced Manufacturing, Materials Science, and Biotechnology and Life Sciences. Over 120 presentations in all...focusing on potential commercial applications of these new discoveries.

Between and after the symposia, visit the **Technology 2001** Exhibit Hall, featuring over 50,000 square feet of hands-on demonstrations by the federal laboratories, their contractors, and other high-tech companies and universities with leading-edge technologies available for license or sale.

Government research programs have created a $65 billion technology storehouse that's available to you now for use in developing new products and processes. Technology 2001 will show you how to tap into this amazing resource to improve your productivity and gain a vital competitive edge, and will introduce you to the nation's premier researchers and technology transfer experts. If you attend only one high-tech event this year, make it Technology 2001!

Register Early And Save

Register by June 1, 1991 and save up to 33 percent. Mail the form below with check payable to the Technology Utilization Foundation, or fax the form with complete credit card information to (212) 986-7864. You can register by phone by calling (212) 490-3999 (VISA and Mastercard accepted). Government organizations may register using a purchase order.

	Postmarked by 6/1	After 6/1
Complete Registration Package	$250	$300
Symposia/Exhibits Registration	$150	$200
One-Day Exhibits Only Reg.	$20	$30

Federal government employees are entitled to a 50% discount on above prices.

Complete Registration Package includes entrance to the symposia and exhibits for all three days, tickets to the opening wine and cheese reception on Monday evening, Dec. 2 and to the Excellence in Technology Transfer Awards Dinner on Wednesday evening, Dec. 4, and a copy of the **Technology 2001** Official Proceedings.
Symposia/Exhibits Registration includes access to the technical sessions and exhibits for all three days.

Tickets to the Awards Dinner may be purchased separately for $150 each. The dinner, a celebration of successful technology transfer to American industry, presents a unique opportunity to meet government leaders and industry executives in an elegant setting—the grand ballroom of the San Jose Fairmont Hotel.

Registrants may pick up their badges (and dinner tickets) in the registration area at the San Jose Convention Center, 150 West San Carlos St; registration confirmations will be sent via mail. All registrants automatically will be mailed the **Technology 2001** Preliminary Program, to be published in June.

Special Rates At San Jose's Finest Hotels

The following special rates have been negotiated for **Technology 2001** attendees:

	single	double
Fairmont Hotel (headquarter hotel) (800) 527-4727	$105	$105
Hyatt San Jose (408) 993-1234	$85	$105
The Red Lion (408) 453-4000	$80	$80
Hotel De Anza (800) 843-3700	$115	$130

Each of these hotels offers a limited number of government-rate rooms. Call for details.

For further information about Technology 2001, call Justina Cardillo or Joseph Pramberger at (212) 490-3999.

Technology 2001 Registration Form

Use a separate form or photocopy for each registrant. Type or print clearly.

Name ______________________

Title ______________________

Company ______________________

Address ______________________

City/St/Zip ______________________

Phone ______________________

❑ check enclosed   charge my: ❑ VISA ❑ Mastercard

Account No.______________________

Expiration: Mo._______ Yr._________

Signature______________________

Registration Fees:	By 6/1	After 6/1	
Complete Registration	$250	$300	$ ____
Symposia/Exhibits Reg.	$150	$200	$ ____
One-Day Exhibits Only (circle day: Tues. Wed. Thurs.)	$20	$30	$ ____
Technology Transfer Awards Dinner—$150			$ ____
Total: (Fed. govt. employees deduct 50%)			$ ____

Registrations and awards dinner reservations are transferable, and may be cancelled until Nov. 8, 1991 subject to a $50 cancellation fee. After that date no cancellations will be accepted and no money refunded.

Return with payment to: Technology Utilization Foundation, 41 East 42nd St., Suite 921, New York, NY 10017

NASA Tech Briefs

Official Publication of
National Aeronautics and
Space Administration

ABP BPA

NASA Tech Briefs:

Published by .... **Associated Business Publications**
Editor-in-Chief/Publisher .... **Bill Schnirring**
Associate Publisher .... **Frank Nothaft**
Editor .... **Joseph T. Pramberger**
Managing Editor .... **R.J Laer**
Assistant Editor .... **Kathleen Carrea**
Assistant Editor .... **Justina Cardillo**
Assistant Editor .... **Patrick Corbett**
Technical Advisor .... **Dr. Robert E. Waterman**
Production Manager .... **Rita Nothaft**
Traffic Manager .... **James E. Cobb**
Art Director .... **Pierre Granier**
Circulation Manager .... **Cheryl Cohen**
Advertising Coordinator .... **Daniel Murphy**
Telecommunications Specialist .... **Evelyn Mars**
Reader Service Manager .... **Sylvia Valentin**

Briefs & Supporting Literature:
Provided to National Aeronautics and Space Administration by
International Computers & Telecommunications, Inc.,
NY, NY with assistance from **Logical Technical Services**, NY, NY
Technical/Managing Editor .... **Ted Selinsky**
Art Director .... **Luis Martinez**
Administrator .... **Elizabeth Texeira**
Chief Copy Editor .... **Lorne Bullen**
Staff Writers/Editors .... **Dr. James Boyd, Dr. Larry Grunberger, Dr. Theron Cole, Jordan Randjelovich, George Watson, Oden Browne**
Graphics .... **Zinaida Gimpeleva, Vernald Gillman, Pamela Baynham, Charles Sammartano**
Editorial & Production .... **Bill Little, Ivonne Valdes, Susan Kyu Oh, Frank Ponce**

NASA:
NASA Tech Briefs are provided by the National Aeronautics and Space Administration, Technology Utilization Division, Washington, DC:
Administrator .... **Richard H. Truly**
Assistant Administrator for Commercial Programs .... **James T. Rose**
Deputy Assistant Administrator(Programs) .... **Frank E. Penaranda**
Deputy Director TU Division(Publications Manager) .... **Leonard A. Ault**
Manager, Technology Utilization Office, NASA Scientific and Technical Information Facility .... **Walter M. Heiland**

Associated Business Publications
41 East 42nd Street, Suite 921, New York, NY 10017-5391
(212) 490-3999 FAX (212) 986-7864
President .... **Bill Schnirring**
Executive Vice President .... **Frank Nothaft**
Vice President .... **Domenic A. Mucchetti**
Operations Manager .... **Rita Nothaft**
Controller .... **Felecia Lahey**
Systems Analyst .... **Patrick Wolfert**

Advertising:
New York Office:(212) 490-3999 FAX (212) 986-7864
Director of Advertising Sales .... **Domenic A. Mucchetti**
Account Executive (NY,NJ) .... **Brian Clerkin** at (201) 366-2751
Account Executive (VA,DC,MD,DE,WV) .... **John D. Floyd, CBC** at (215) 399-3265
Account Executive .... **Debby Crane** at (201) 967-9838
Account Executive (Midwest) .... **Paul Lesher,CBC** at (708) 501-4140
Account Executive (Northwest) .... **Bill Hague** at (206) 858-7575
Regional Sales Manager (South) .... **Douglas Shaller** at (212) 490-3999
Account Executives (Eastern MA,NH,ME,RI) .... **Paul Gillespie** at (508) 429-8907;**Bill Doucette** at (508) 429-9861
Account Executives (Western MA,CT,VT) .... **George Watts** at (413) 253-9881
Account Executives (Calif.,AZ,NV,NM)
for Area Codes 714/619 **Tom Murphy**
for Area Codes 213/818/805/602/702/505 **Robert D'Alexander** at (213) 372-2744
for Area Codes 408/415/916/209/707 **Elizabeth Cooper** at (415) 673-5123

NTBM-Research Center
Account Supervisor .... **Lourdes Del Valle**

PC MAGAZINE EDITORS' CHOICE
March 26, 1991
Graftool, Version 3.3

GRAFTOOL™

"extremely flexible, powerful, and easy-to-use" ..."the ultimate graphics package, fulfilling everybody's needs."

Reprinted with permission from PC Magazine, March 14th, 1989, Copyright ©1989 Ziff Communications Co. and PC Magazine, March, 26th, 1991 ©Ziff Communications Co.

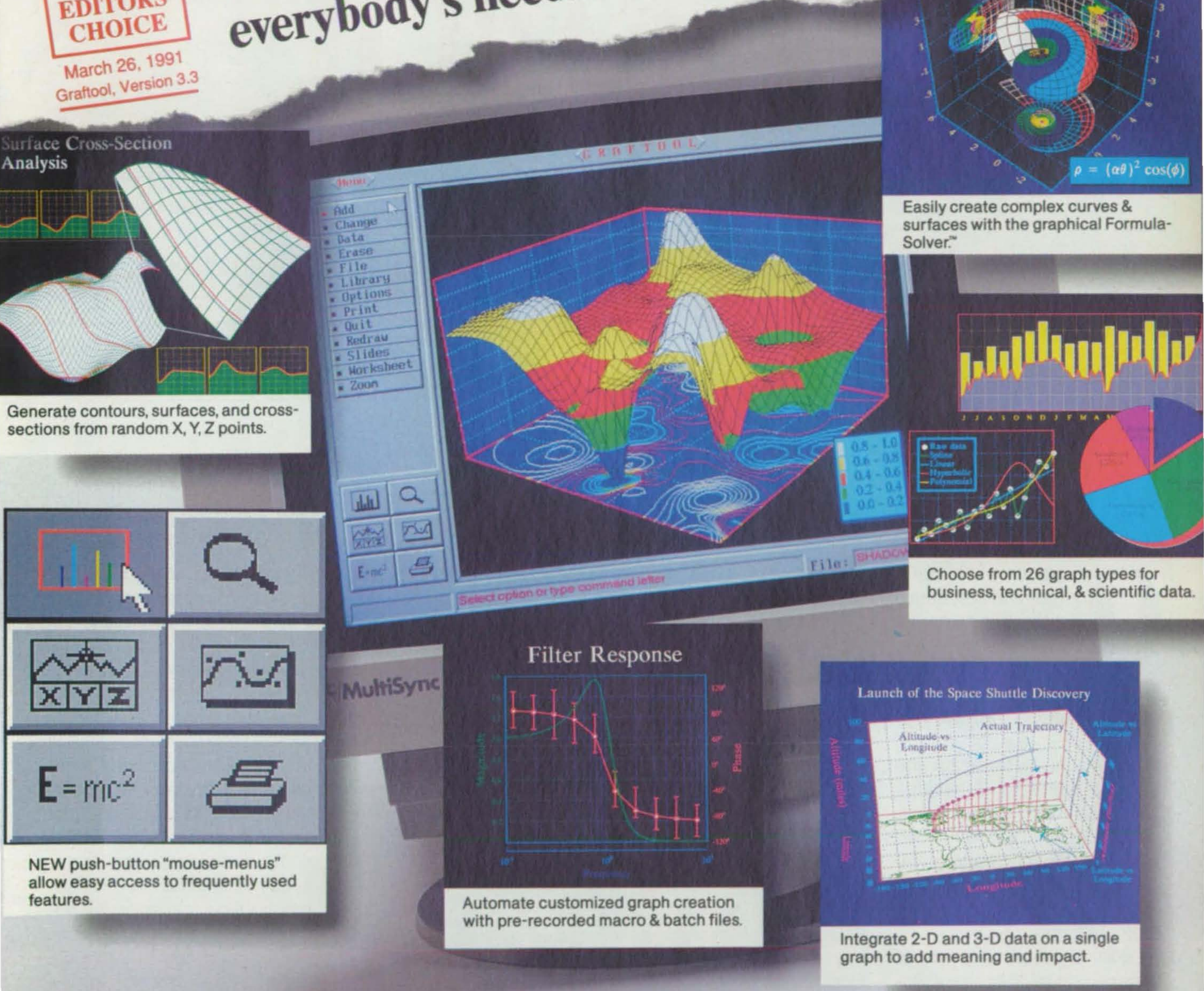

Presentation graphics and analysis for scientific users.

Your technical data requires more muscle and sophistication than basic business graphics and plotting packages can provide. It's simply a matter of using the right tool for the job. In addition to publication-quality graphics, you need powerful analysis tools and capabilities such as Graftool's ■ Intelligent Data Cursor™ to read out data points on curves & surfaces ■ Linear & non-linear curve-fitting ■ Unlimited zoom & rotation ■ Multiple axes in linear, log, or probability scales ■ Advanced data handling, allowing over 268,000,000 data points ■ Powerful scientific spreadsheet which can directly read your Lotus or ASCII files ■ Unrestricted placement of graphs & text ■ Direct compatibility with Microsoft Word & WordPerfect.

With Graftool, all this power and flexibility purr quietly under the hood, while pop-up menus and push-buttons bring an ease of use previously unheard of in scientific software. Just "point & process" with increased productivity and greater understanding.

GRAFTOOL – the right tool for your technical solutions.

GRAFTOOL $495.

■ Interactive demo available
■ Academic discounts.

3-D VISIONS
412 S. Pacific Coast Highway, Second Floor
Redondo Beach, CA 90277
Call: 1 (800) 729-4723, 1 (213) 540-8818
FAX: 1 (213) 540-3492

Circle Reader Action No. 669

5 0

LEWIS RESEARCH CENTER 1941-1991

A HALF-CENTURY OF TECHNOLOGY LEADERSHIP

On January 23, 1941, a group of dignitaries gathered in a muddy field adjacent to Cleveland Airport to break ground for a new airplane engine research laboratory. George W. Lewis, director of aeronautical research for the National Advisory Committee for Aeronautics, NASA's predecessor, drove a nickel-plated pick into the soil, marking the beginning of a major national resource that would one day bear his name.

Born amidst the urgency of impending war, the Lewis Center would evolve into a multifaceted, world-class research facility. By the end of World War II, Lewis was already deeply involved in testing the turbojet engine, a revolutionary form of aircraft propulsion which set the stage for advancements in rocketry and space technology. During the 1960s, Lewis developed the Centaur rocket, an upper-stage launch vehicle fueled by liquid hydrogen. Lewis' success with this dangerous propellant led to more than 100 Centaur flights and helped make the lunar landings a reality. With the energy crisis in the 1970s, the center expanded its work to include studies of wind and solar power, and new fuel-saving engine designs. In the 1980s, Lewis received two prestigious awards — the Collier Trophy and the Emmy — for outstanding achievements in propulsion and communications. Lewis' Icing Research Tunnel, the oldest and largest facility of its kind in the world, was declared an international historic mechanical engineering landmark in 1987.

Photo courtesy Lewis Research Center

Powering Freedom: Lewis engineers make final checks prior to plasma interaction tests with space station Freedom solar array panels.

Today, the Lewis Center continues its leadership in aerospace research and development. Lewis manages the design and development of space station Freedom's electrical power system, as well as the Advanced Communications Technology Satellite (ACTS), a joint NASA-industry project which promises to revolutionize telecommunications. With plans under way for numerous manned and unmanned space flights, Lewis researchers are studying the effects of low gravity on combustion, materials, and fluids. Moreover, the center is working to reduce the noise and emissions of future high-speed civil aircraft, and is involved in many fundamental research projects offering potential commercial applications in the communications, computer, automotive, and biomedical fields. Some of Lewis' current R&D efforts include:

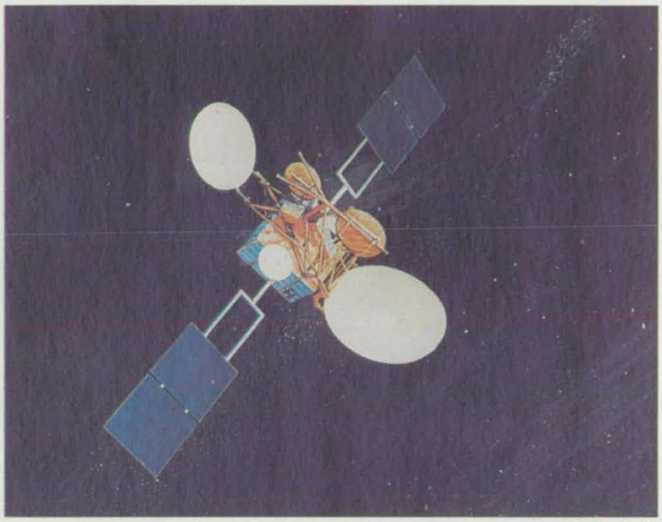

Photo courtesy Lewis

Slated for launch in 1992, the Advanced Communications Technology Satellite incorporates several innovative technologies — including a multiple-beam antenna system and on board digital switching — designed to make more effective use of available frequencies and to provide the capability for high-volume communications to small Earth terminals.

Arcjet Development. Lewis has the lead role in developing the arcjet thruster technology recently selected for stationkeeping on AT&T's Telstar 4 communications satellites. Arcjets are electrically-heated devices that produce thrust by expanding a hot gas in a nozzle to a high velocity. Low-power arcjets have captured the interest of satellite manufacturers because they are up to two times more fuel-efficient than present chemical engines and resistojet technology. The savings realized can be used to increase a satellite's on-orbit lifetime or payload mass. Alternatively, launch mass can be decreased to allow use of a smaller rocket booster.

Computational Materials Processing. A new laboratory at NASA Lewis applies computational techniques to materials science in order to improve processes, understand complex interactions, and produce more reliable materials. The laboratory employs advanced graphics workstations and is connected to supercomputers at Lewis and elsewhere. Work focuses on modifying programs developed for computational fluid dynamics or structural calculations to solve unique materials processing problems. The facility specializes in predicting the effects of gravitationally-driven convection on crystal growth from the liquid and the vapor. In one project, researchers modeled the fluid flow effects during growth of gallium arsenide semiconductors in space.

NASP Propulsion. For the National Aero-Space Plane (NASP) program — which seeks to build a hypersonic vehicle capable of taking off and landing horizontally like an airplane — Lewis conducts research in propulsion, high-temperature materials and structures, computational fluid dynamics, and cryogenics. Lewis leads the effort to develop "slush" hydrogen, a high-energy hydrogen slurry that will fuel the experimental vehicle. It is denser than liquid hydrogen and may result in smaller, lighter fuel tanks that could reduce NASP's takeoff weight by up to 30 percent. Lewis has modified a cryogenic facility to manufacture the slush hydrogen in 800-gallon batches, allowing researchers to explore production, transfer, and storage questions.

Stirling Engine Research. Under NASA's Civil Space Technology Initiative, Lewis is developing free-piston Stirling engines as a candidate power source for future space missions. This external combustion engine offers high reliability and long operating life because it has few moving parts, noncontacting gas bearings, and can be hermetically sealed. These attributes also make it attractive for terrestrial applications. Two industry teams are designing Advanced Stirling Conversion Systems for worldwide remote power applications. When coupled with a parabolic mirror to collect solar energy, the systems will deliver 25 kw of electricity to a power grid.

Structural Mechanics Applications. Lewis scientists are working with medical specialists from Case Western Reserve University to improve the performance of artificial knee joints. The project involves modifying aerospace computer codes for use in custom-designing prosthetic joint implants. With an optimally-designed fit, the patient's weight and joint movements would be evenly distributed on the supporting bone, eliminating the current problems of prosthesis loosening and bone deterioration. In the future, the codes not only will tell researchers what the optimum shape for the implant would be, but also which materials would be least likely to be rejected by the human body.

Superconductivity Studies. Over the past three years, the Lewis Center has investigated the application of new high-critical-temperature superconductors to electronic circuits for communications systems. Using thin films of yttrium barium copper oxide, Lewis researchers produced the first circuits able to operate at 33 to 37 GHz, a frequency range more than three times higher than attainable with previous circuits. Higher frequencies will allow satellites to process data at much faster rates, increasing the number of communications linkups they can handle.

In partnership with Argonne National Laboratory, Lewis is developing large-scale superconducting systems for aerospace propulsion and power applications, including power transmission, superconducting magnetic energy storage, and electromagnetic propulsion. To support these applications, research is under way to determine and improve the characteristics of superconducting materials in the space environment. ❑

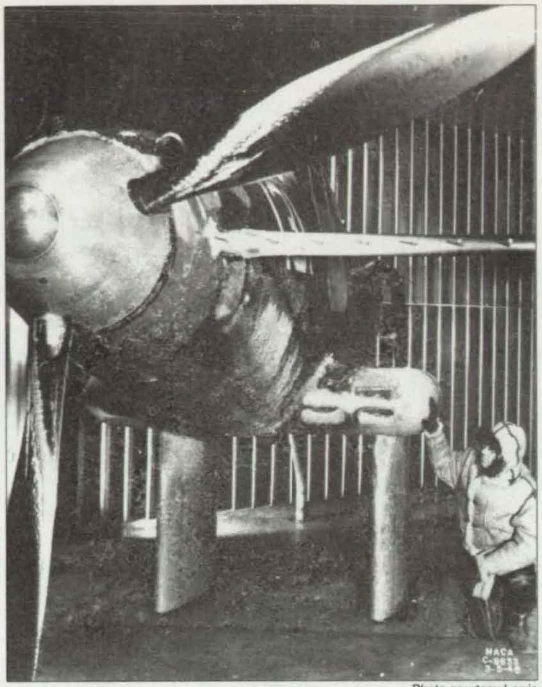

Photo courtesy Lewis

This 1945 photo shows the fuselage of a B-39 airplane mounted in Lewis' Icing Research Tunnel for the study of ice formation on rotating propellers. In 1987, the American Society of Mechanical Engineers designated the tunnel an international historic landmark.

For more information on the Lewis Center and its technology development programs, contact Anthony Ratajczak, Lewis Research Center Technology Utilization Office, Mail Stop 7-3, 21000 Brookpark Road, Cleveland, OH 44135.

New Product Ideas

New Product Ideas are just a few of the many innovations described in this issue of *NASA Tech Briefs* and having promising commercial applications. Each is discussed further on the referenced page in the appropriate section in this issue. If you are interested in developing a product from these or other NASA innovations, you can receive further technical information by requesting the TSP referenced at the end of the full-length article or by writing the Technology Utilization Office of the sponsoring NASA center (see page 18). NASA's patent-licensing program to encourage commercial development is described on page 18.

Segmented Arm for Positioning and Assembly

A proposed segmented robotic arm for positioning and assembly of components of large structures would contain motor-and-flywheel angular-momentum devices in each arm segment. The arm would be about 300 ft (90 m) long and could manipulate objects of up to about 1 million pounds (455 t).
(See page 58)

Mixed-Gas Sorption Joule–Thomson Refrigerator

A proposed mixed-gas Joule–Thomson refrigerator would include only one stage and no mechanical compressor. Compared with its predecessors, the refrigerator would be simpler, operate without vibrating, and consume less power in producing the same amount of cooling down to 70 K.
(See page 38)

High-Power Liquid-Metal Heat-Transfer Loop

A proposed closed-loop system for the transfer of thermal power would operate at relatively high differential pressure between the vapor and liquid phases of a liquid-metal working fluid. Because the system would contain no moving parts, it should be highly reliable and suited to long-term unattended operation.
(See page 36)

Higher-Performance Ambient-Temperature Heat Pipe

A porous wick added to the liquid channel improves the thermal performance of a heat pipe. Sintered aluminum powder now lines the liquid channel.
(See page 57)

Improved Planar Schottky Diode

Modified design and fabrication of a surface-channel planar Schottky diode reduce the parasitic capacitances to the theoretical minimum, eliminate the buried layer of conductive material between the anode contact and the semi-insulating substrate, and reduce the thickness of the diode chip.
(See page 24)

Tool for Robotic Resistive Roll Welding

Resistance-welding current starts and stops automatically according to force exerted against the workpiece, thanks to a roll-welding attachment for a robot. This simple, inexpensive attachment incorporates a modified commercial resistance-welding gun.
(See page 62)

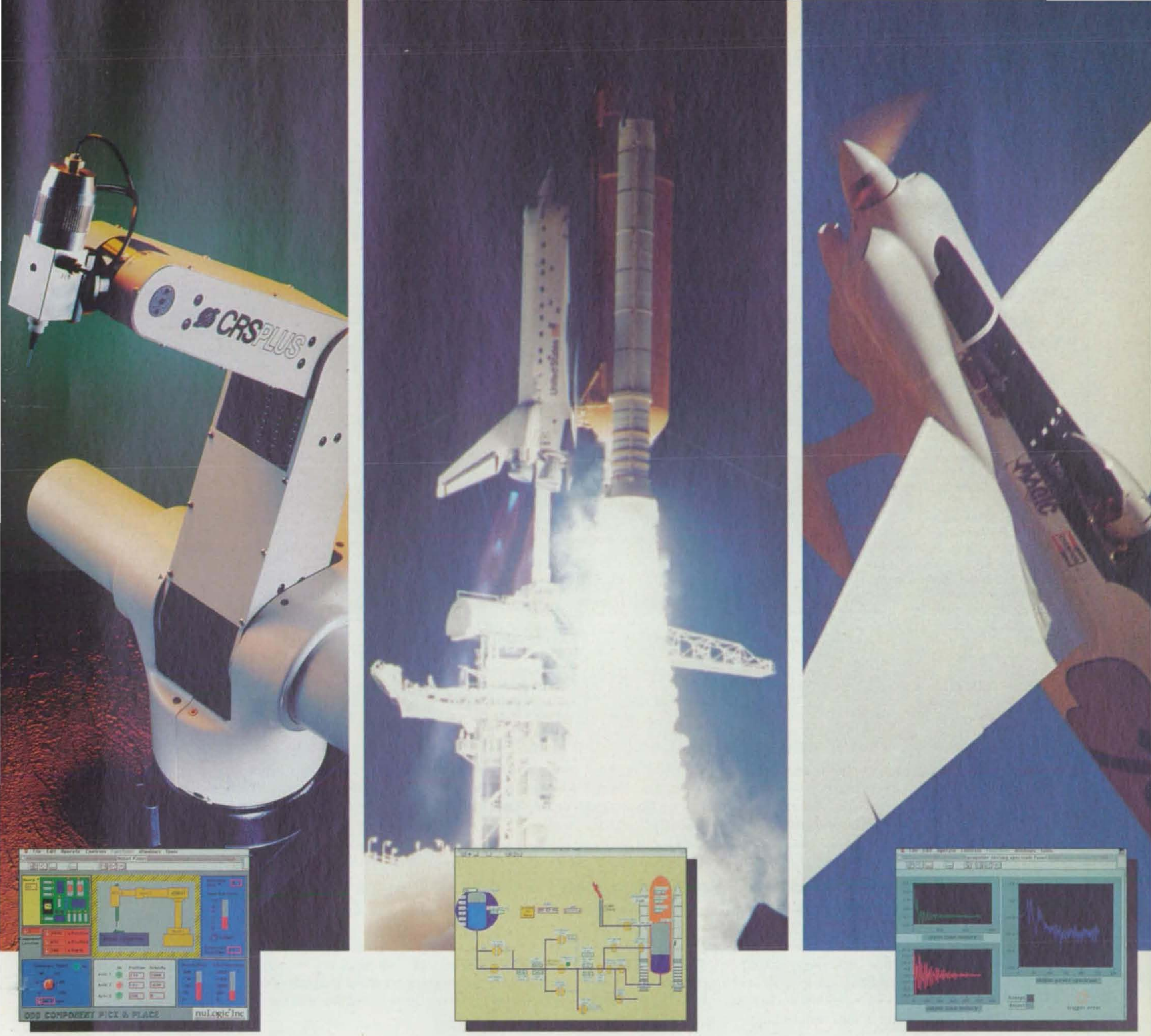

LabVIEW® 2
Where The Only Barrier Is Your Imagination.

By now, you are probably familiar with LabVIEW 2, the most celebrated application software for data acquisition and instrument control on the Macintosh. It recently won the *MacUser* magazine Editors' Choice award. Five years ago, LabVIEW introduced the combination of front panel interfaces and graphical programming. Today, engineers and scientists around the world are using LabVIEW 2 in a broad spectrum of applications.

Unlike other graphical packages, LabVIEW 2 does not sacrifice power and flexibility for ease of use. With LabVIEW 2, you quickly build block diagram programs and add your own blocks to expand upon our libraries. You also create front panel user interfaces and import pictures to customize the panels. Yet LabVIEW 2 virtual instruments run as quickly as compiled C programs.

If you thought LabVIEW 2 was just for test and measurement, call us to find out what LabVIEW 2 is really about.

For a free LabVIEW 2 Demo disk call:
(512) 794-0100 or
(800) 433-3488
(U.S. and Canada)

NATIONAL INSTRUMENTS®
The Software is the Instrument®

6504 Bridge Point Parkway
Austin, TX 78730-5039

Circle Reader Action No. 681

HOW YOU CAN BENEFIT FROM NASA's TECHNOLOGY UTILIZATION SERVICES

If you're a regular reader of TECH BRIEFS, then you're already making use of one of the low-and no-cost services provided by NASA's Technology Utilization (TU) Network. But a TECH BRIEFS subscription represents only a fraction of the technical information and applications/engineering services offered by the TU Network as a whole. In fact, when all of the components of NASA's Technology Utilization Network are considered, TECH BRIEFS represents the proverbial tip of the iceberg.

We've outlined below NASA's TU Network—named the participants, described their services, and listed the individuals you can contact for more information relating to your specific needs. We encourage you to make use of the information, access, and applications services offered by NASA's Technology Utilization Network.

How You Can Utilize **NASA's Industrial Applications Centers**—A nationwide network offering a broad range of technical services, including computerized access to over 100 million documents worldwide.

You can contact NASA's network of Industrial Applications Centers (IACs) for assistance in solving a specific technical problem or meeting your information needs. The "user friendly" IACs are staffed by technology transfer experts who provide computerized information retrieval from one of the world's largest banks of technical data. Nearly 500 computerized data bases, ranging from NASA's own data base to Chemical Abstracts and INSPEC, are accessible through the ten IACs located throughout the nation. The IACs also offer technical consultation services and/or linkage with other experts in the field. You can obtain more information about these services by calling or writing the nearest IAC. User fees are charged for IAC information services.

Aerospace Research Center (ARAC)
Indianapolis Center for Advanced Research
611 N. Capitol Avenue
Indianapolis, IN 46204
Dr. F. Timothy Janis, Director
(317) 262-5036

Central Industrial Applications Center/NASA (CIAC)
Rural Enterprises, Inc.
Post Office Box 1335
Durant, OK 74702
Dr. Dickie Deel, Director
(405) 924-5094
(800) 658-2823 (toll-free U.S.)

Science and Technology Research Center (STRC)
Post Office Box 12235
Research Triangle Park, NC 27709-2235
H.L. (Lynn) Reese, Director
(919) 549-0671

NASA Industrial Applications Ctr. 823 William Pitt Union
University of Pittsburgh
Pittsburgh, PA 15260
Lani Hummel
Executive Director
(412) 648-7000

Southern Technology Applications Center (STAC)
Post Office Box 24
Progress Ctr., One Progress Blvd.
Alachua, FL 32615
J. Ronald Thornton, Director
(904) 462-3913
(800) 354-4832 (FL only)
(800) 225-0308 (toll-free US)

NASA/UK Technology Technology Applications Center
University of Kentucky
109 Kinkead Hall
Lexington, KY 40506-0057
William R. Strong, Director
(606) 257-6322

NERAC, Inc.
One Technology Drive
Tolland, CT 06084
Dr. Daniel U. Wilde, President
(203) 872-7000

Technology Application Center (TAC)
University of New Mexico
Albuquerque, NM 87131
Dr. Stanley A. Morain, Director
(505) 277-3622

NASA Industrial Applications Center
University of Southern California
Research Annex
3716 South Hope Street
Los Angeles, CA 90007-4344
Robert Stark, Director
(213) 743-6132
(800) 642-2872 (CA only)
(800) 872-7477 (toll-free US)

NASA/SU Industrial Applications Center
Southern University Department of Computer Science
Post Office Box 9737
Baton Rouge, LA 70813-9737
Dr. John Hubbell, Director
(504) 771-6272
(504) 771-4950

If you represent a public sector organization with a particular need, you can contact NASA's Application Team for technology matching and problem solving assistance. Staffed by professional engineers from a variety of disciplines, the Application Team works with public sector organizations to identify and solve critical problems with existing NASA technology. **Technology Application Team, Research Triangle Institute, P.O. Box 12194, Research Triangle Park, NC 27709; *Dr. Doris Rouse, Director,* (919) 541-6980**

How You Can Access Technology Transfer Services At NASA Field Centers: **Technology Utilization Officers & Patent Counsels**—Each NASA Field Center has a Technology Utilization Officer (TUO) and a Patent Counsel to facilitate technology transfer between NASA and the private sector.

If you need further information about new technologies presented in NASA Tech Briefs, request the Technical Support Package (TSP). If a TSP is not available, you can contact the Technology Utilization Officer at the NASA Field Center that sponsored the research. He can arrange for assistance in applying the technology by putting you in touch with the people who developed it. If you want information about the patent status of a technology or are interested in licensing a NASA invention, contact the Patent Counsel at the NASA Field Center that sponsored the research. Refer to the NASA reference number at the end of the Tech Brief.

Ames Research Ctr.
Technology Utilization Officer:Geoffrey S. Lee
Mail Code 223-3
Moffett Field, CA 94035
(415) 604-4044
Patent Counsel:
Darrell G. Brekke
Mail Code 200-11
Moffett Field, CA 94035
(415) 604-5104

Lewis Research Center
Technology Utilization Officer: Anthony F. Ratajczak
Mail Stop 7-3
21000 Brookpark Road
Cleveland, OH 44135
(216) 433-2225
Patent Counsel:
Gene E. Shook
Mail Code LE-LAW
21000 Brookpark Road
Cleveland, OH 44135
(216) 433-5753

John C. Stennis Space Center
Technology Utilization Officer: Richard A. Galle (acting)
Code HA-32
Stennis Space Center, MS 39529
(601) 688-1929

John F. Kennedy Space Center
Technology Utilization Officer: Thomas M. Hammond
Mail Stop PT-PMO-A
Kennedy Space Center, FL 32899
(407) 867-3017
Patent Counsel:
Bill Sheehan
Mail Code PT-PAT
Kennedy Space Center, FL 32899
(407) 867-2544

Langley Research Ctr.
Technology Utilization Officer: Joseph J. Mathis Jr.
Deputy Head, TU Office
Mail Stop 139A
Hampton, VA 23665
(804) 864-2484
Patent Counsel:
George F. Helfrich
Mail Code 279
Hampton, VA 23665
(804) 864-3523

Goddard Space Flight Center
Technology Utilization Officer: Donald S. Friedman
Mail Code 702.1
Greenbelt, MD 20771
(301) 286-6242
Patent Counsel:
R. Dennis Marchant
Mail Code 204
Greenbelt, MD 20771
(301) 286-7351

Jet Propulsion Lab.
NASA Resident Office
Technology Utilization Officer: Arif Husain
Mail Stop 180-801
4800 Oak Grove Drive
Pasadena, CA 91109
(818) 354-4862
Patent Counsel:
Thomas H. Jones
Mail Code 180-801
4800 Oak Grove Drive
Pasadena, CA 91109
(818) 354-5179
Technology Utilization Mgr. for JPL: Dr. Norman L. Chalfin
Mail Stop 156-211
4800 Oak Grove Drive
Pasadena, CA 91109
(818) 354-2240

George C. Marshall Space Flight Center
Technology Utilization Officer: Ismail Akbay
Code AT01
Marshall Space Flight Center, AL 35812
(205) 544-2223
Fax (205) 544-3151
Patent Attorney:
Jerry L. Seemann
Mail Code CC01
Marshall Space Flight Center, AL 35812
(205) 544-0021

Lyndon B. Johnson Space Center
Technology Utilization Officer: Dean C. Glenn
Mail Code IC-4
Houston, TX 77058
(713) 483-3809
Patent Counsel:
Edward K. Fein
Mail Code AL3
Houston, TX 77058
(713) 483-4871

NASA Headquarters
Technology Utilization Officer: Leonard A. Ault
Code CU
Washington, DC 20546
(202) 557-5598
Assistant General Counsel for Patent Matters: Robert F. Kempf, Code GP
Washington, DC 20546
(703) 557-5598

A Shortcut To Software: **COSMIC®**—For software developed with NASA funding, contact COSMIC, NASA's Computer Software Management and Information Center. New and updated programs are announced in the Computer Programs section. COSMIC publishes an annual software catalog. For more information call or write: **COSMIC®**, 382 East Broad Street, Athens, GA 30602 *John A. Gibson, Dir.,* (404) 542-3265.

If You Have a Question..**NASA Scientific & Technical Information Facility** can answer questions about NASA's Technology Utilization Network and its services and documents. The STI staff supplies documents and provides referrals. Call, write or use the feedback card in this issue to contact: **NASA Scientific and Technical Information Facility,** Technology Utilization Office, P.O. Box 8757, Baltimore, MD 21240-0757. *Walter M. Heiland, Manager,* (301) 859-5300, Ext. 245.

Electronic Components and Circuits

Hardware, Techniques, and Processes

Flange Correction for Metal-to-Metal Contacts

Interfacial resistances can be extracted more accurately from four-terminal measurements.

NASA's Jet Propulsion Laboratory, Pasadena, California

An improved mathematical model provides a correction for the flange effect in estimating the resistance of a square contact between two metal layers from standard four-terminal measurements. The model is an extended version of one developed previously for a contact between a metal layer and a semiconductor layer, wherein the flange effect is important in the semiconductor layer only. Here the flange effect in both metal layers is significant.

As its name suggests, the flange effect occurs in the flanges — the regions of the metal layers in the vicinity of the contact — and is caused by the lateral flow of electrical current in these regions. In the one-flange (semiconductor/metal contact) model, the metal layer is represented by an equipotential plane, the contact zone is shrunken slightly from its true dimensions to a smaller equipotential core embedded in the semiconducting layer modeled as a two-dimensional resistive sheet, and a lumped resistor represents the interfacial resistance. The shrinkage of the core from the original contact zone is given by effective lengths of current flow under the contact derived from a one-dimensional-transmission-line model.

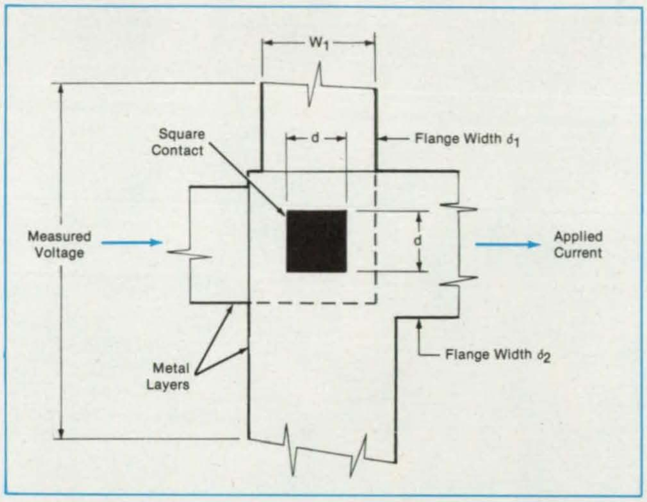

The **Four-Terminal Method** is a standard method for measuring the resistance of a contact like this one between the two metal layers. The resistance of the contact is determined by applying a current and measuring the voltage as shown, then making a correction for the geometry.

The two-flange (metal/metal contact) model is obtained by piecing together two one-flange models, one for each metal layer. Mathematically, this alters the effective lengths and implicity distributes the interfacial resistance between two one-flange problems. The two-flange model has been tested by comparison with numerical simulations and with experiments. The resistances predicted by the model were found to agree with those of the simulations at contact sizes of 1 and 4 μm but to disagree somewhat with those of the simulations at intermediate sizes. However, the predictions of the model agreed with measurements in the same size range.

This work was done by Udo Lieneweg and David J. Hannaman of Caltech for **NASA's Jet Propulsion Laboratory**. *For further information, Circle 8 on the TSP Request Card.*
NPO-18052

Thin, Lightweight Solar Cell

Features include enhanced resistance to ultraviolet light and to energetic charged particles.

Lewis Research Center, Cleveland, Ohio

An improved design for thin, lightweight solar photovoltaic cells with front contacts reduces the degradation of electrical output under exposure to energetic charged particles (protons and electrons). The design also increases the ability of the cells to maintain structural integrity under exposure to ultraviolet radiation by eliminating the ultraviolet-degradable adhesives that have been used to retain cover glasses in some prior designs.

The front (illuminated) surface of the semiconductor substrate of a cell contains rectangular grooves in which the back halves of interdigitated metal contact lines are embedded. The cell junctions lie on the surface, surrounding the metal contacts (see figure). The placement of all the junctions and contacts at the front (rather than placing some contacts at the back as in prior designs) provides shorter paths for the charge carriers generated by incident photons to travel to the junctions and contacts. The shortening of the paths decreases the probability of trapping of charge carriers by defects. Trapping degrades output, and the defects that cause trapping include those induced by energetic charged particles. Thus, this simple change of configuration helps to maintain output after exposure.

The front half of each contact line is formed in a mating rectangular groove in the back surface of the cover glass. The front surface of the cover glass contains triangular grooves aligned with the metal contacts. The triangular grooves refract the light incident on them away from the contacts and into the cell; without these grooves, the affected portion of the light would fall on the

metal contacts, where it would not generate charge carriers.

If the cells are made of semiconductors from groups III and V of the periodic table (e.g., GaAs or InP), they should be 5 to 10 μm thick. Single-crystal layers of such thicknesses can be made by a peeled-film technique. If the cells are made of silicon, they should be at least 30 μm thick. A typical cell is fabricated by the following sequence of steps:

1. The n^+ and p^+ regions of the semiconductor substrate are produced by diffusion of the dopants into the semiconductor, using photolithographic masking techniques to form the regions on the front surface.
2. An antireflection coat is deposited on the front surface of the semiconductor.
3. The grooves for the contacts are etched or laser-scribed into the front surface with the help of appropriate masks.
4. The metal contact material is deposited into these grooves and made flush with the top of the antireflection coating.
5. The aligned triangular and rectangular grooves are made in the upper and lower surfaces, respectively, of the cover glass.
6. By use of an appropriate masking technique in conjunction with plating, evaporation or other means, contact metal is deposited in the rectangular grooves, flush with the surface of the glass.
7. The cover glass and the semiconductor substrate are aligned so that their metal contacts coincide, then are joined by electrostatic bonding.
8. Multiple cells can be attached to a single large-area cover glass and interconnected with an appropriate pattern in the glass.
9. A backing layer, typically of Kapton (or equivalent) polyimide is attached to the back surface of the cell(s) by a silicone adhesive.

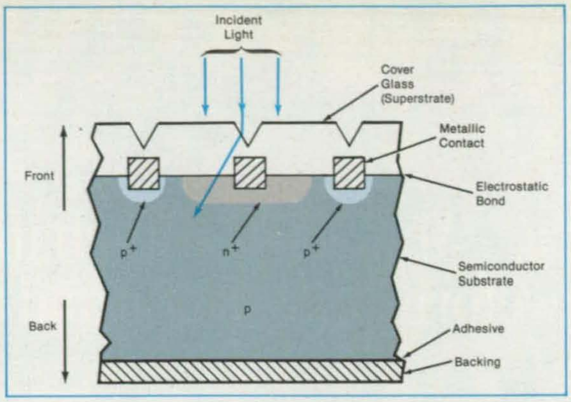

Interdigitated Front Contacts and front junctions are formed on the semiconductor substrate. Mating contacts are formed on the back surface of the cover glass. The cover glass and substrate are electrostatically bonded together.

This work was done by Henry W. Brandhorst, Jr., and Irving Weinberg of the **Lewis Research Center**. *For further information, Circle 159 on the TSP Request Card.*

This invention is owned by NASA, and a patent application has been filed. Inquiries concerning nonexclusive or exclusive license for its commercial development should be addressed to the Patent Counsel, Lewis Research Center [see page 18]. Refer to LEW-14959.

Doping To Reduce Base Resistances of Bipolar Transistors

A p/p^+ base-doping profile would reduce base resistance without reducing current gain.

NASA's Jet Propulsion Laboratory, Pasadena, California

A modified doping profile has been proposed to reduce the base resistances of bipolar transistors. Low base resistances are desirable for high-speed applications. Decreases in base resistances can also result in decreases in voltage drops along emitter/base junctions, with consequent decreases in the undesired crowding of emitter currents.

When base resistances are reduced by increasing the concentrations of dopants in the bases of bipolar transistors in the conventional manner, emitter efficiencies and current gains are reduced. The proposed base structure would reduce the base resistance without degrading the current gain. As shown in the figure, it would involve the placement of a p (or n) layer near the emitter and a p^+ (or n^+) layer near the collector in the case of an npn (or a pnp, respectively) transistor. The p (or n) layer near the emitter ensures a high emitter efficiency, and the resistance would be reduced by the incorporation of the p^+ or n^+ layer.

For example, the concentration of the dopant in, and the thickness of, the base of a typical npn bipolar transistor are 1×10^{18} cm^{-3} and 0.5 μm, respectively, and cause the sheet resistance of the base to be 200 ohms per square. The proposed low/high base profile of 1×10^{18} and 1×10^{20} cm^{-3} and thicknesses of 0.2 and 0.3 μm for the p and p^+ layers, respectively, would reduce the sheet resistance of the base to less than 30 ohms per square.

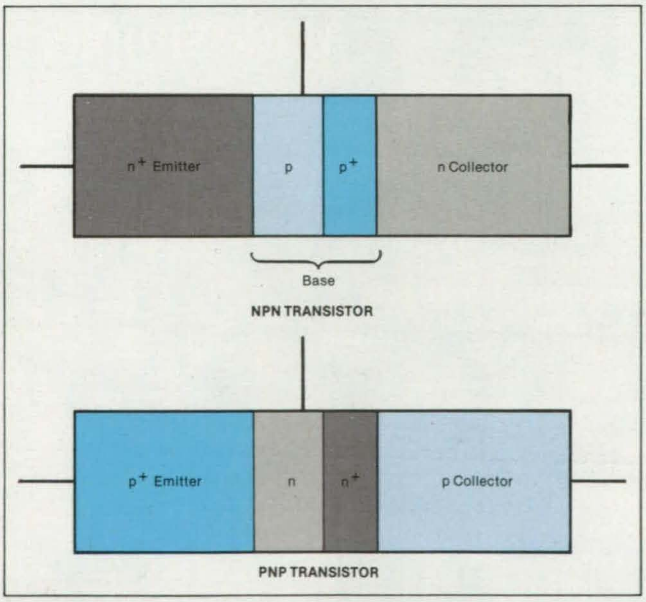

The **Proposed Low/High Doping Profile** would reduce the resistance of the base without reducing the current gain.

The proposed low/high base-doping profile could be realized by such low-temperature deposition techniques as molecular-beam epitaxy, ultra-high-vacuum chemical-vapor deposition, and limited-reaction epitaxy. These techniques can produce the desired doping profiles without excessive diffusion of dopant.

This work was done by True-Lon Lin of Caltech for **NASA's Jet Propulsion Laboratory**. *For further information, Circle 102 on the TSP Request Card.*
NPO-17948

We've Opened Minds To Ada

In just a few short months, Meridian has opened over 5000 minds to Ada.

Programmers who'd shied away from Ada, due to high prices and lengthy learning curves, have been quick to recognize the revolution Meridian's latest complete Ada development system, OpenAda, has set in motion.

At last, an Ada product that rivals the likes of TurboPascal® and C++.

"Meridian Software Systems slashed the price and raised the standard for PC based Ada development." –PC Week

OpenAda sets a new standard with an affordable, quick-start Ada development environment for the Macintosh® or PC. With hyper-text on-line help and a windowed editor, you'll quickly discover why Ada's not just for defense projects any more.

And for $299 or less you can't afford to pass up this opportunity to explore the industry's fastest growing language on a top quality development system.

"If you want to know what this language is all about, get OpenAda. It's the best low-cost Ada compiler around." –IEEE Computer

In an effort to prepare programmers for a transition to Ada, both corporate training programs and universities have added Ada to their curriculums, using OpenAda as the training vehicle.

It's the perfect choice. Even at this exceptional value, it's complete. For both training and development. It includes:

▪ compiler/linker ▪ debugger optimizer ▪ graphic interface ▪ Amake ▪ utility and Environment library ▪ ▪ Ada syntax-directed editor ▪ graphics/math library ▪ on-line LRM

To remain at the forefront of an evolving industry, you've got to know Ada. And OpenAda makes it easy for you to invest in your future.

You can trade-up to a full line of Ada development products, including PC (DOS AND UNIX), MACINTOSH, SUN, AND DIGITAL EQUIPMENT CORP. platforms. And you'll receive full value for your OpenAda purchase for two years. Meridian's renowned customer support is also available.

Order now. Call **1(800)221-2522.** If you wait, it will cost $495 to open your mind to Ada.

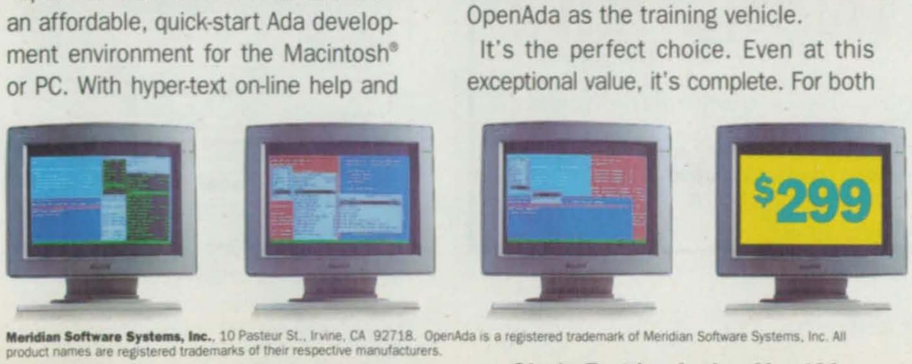

open Ada

Meridian Software Systems, Inc., 10 Pasteur St., Irvine, CA 92718. OpenAda is a registered trademark of Meridian Software Systems, Inc. All product names are registered trademarks of their respective manufacturers.

Circle Reader Action No. 496

Improved Planar Schottky Diode

Changes in the epitaxial layer structure and additional fabrication steps reduce conversion loss in millimeter and submillimeter mixers.

Goddard Space Flight Center, Greenbelt, Maryland

Modifications of the design and fabrication of a surface-channel planar Schottky diode (*NASA Tech Briefs*, Vol. 12, No. 7, pp. 22-23) reduce the parasitic capacitances to the theoretical minimum, eliminate the buried layer of conductive material between the anode contact and the semi-insulating substrate, and reduce the thickness of the diode chip. These improvements combine to reduce the conversion loss and noise of the diode in high-frequency mixer applications.

A thin layer of AlGaAs is added to the standard initial epitaxial-layer structure, as shown in part 1 of the figure. This layer acts as an etch stop during a later fabrication step.

After the surface-channel diode fabrication but before dicing, a polymer filler is injected into the etched surface channel on the wafer. This filler preserves the channel during subsequent fabrication steps by

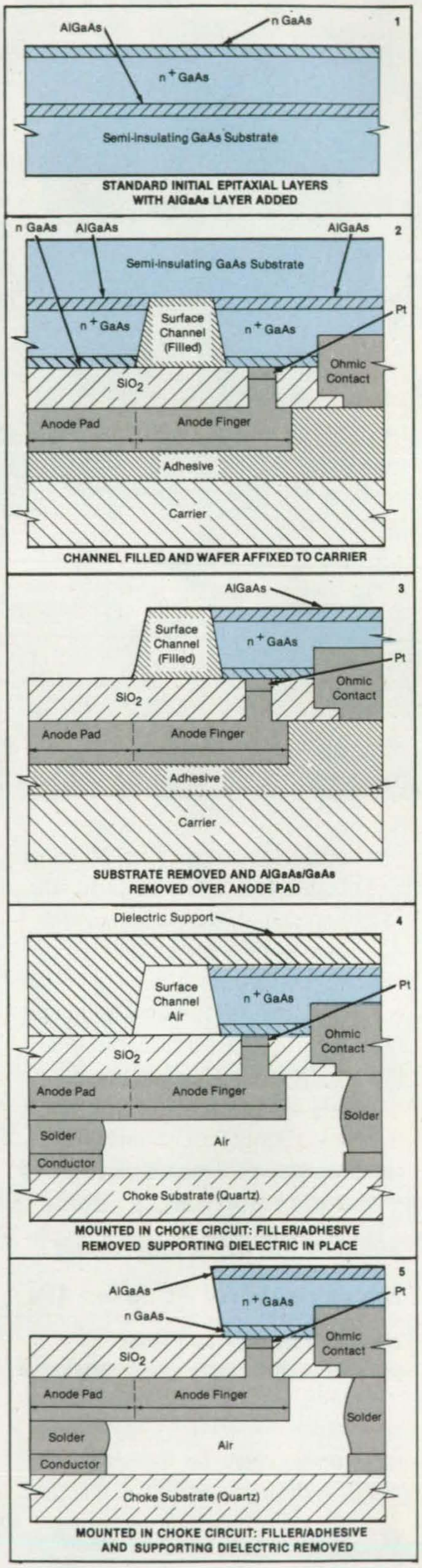

The Modified Planar Schottky Diode is shown at various stages in its fabrication.

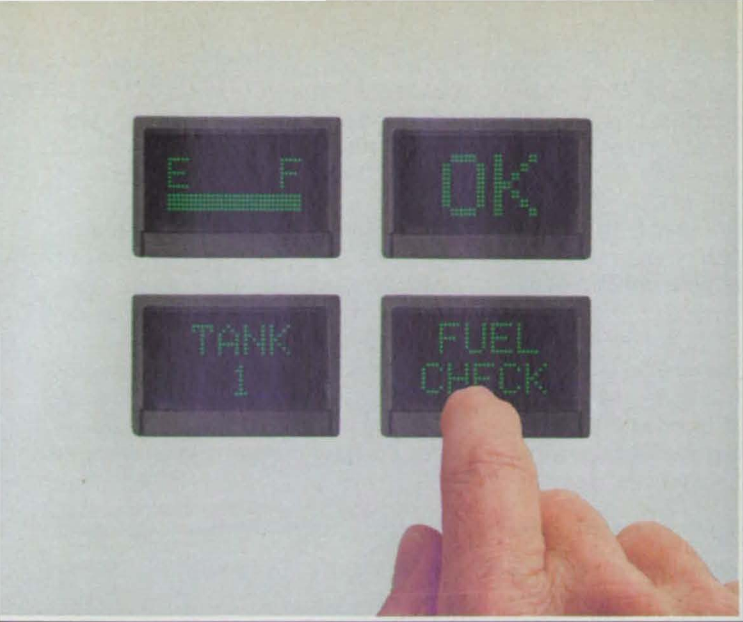

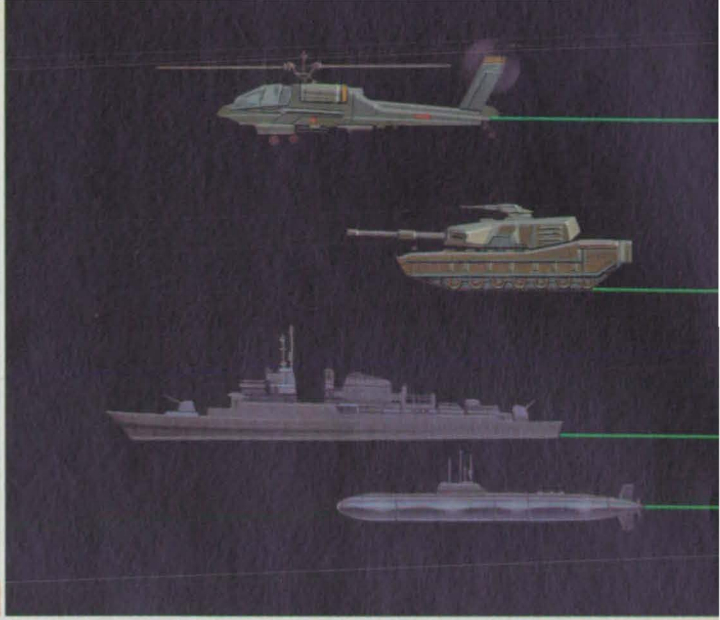

The programmable display system:

Design applications for land, sea or air.

Vivisun Series 2000, now the leading programmable display pushbutton system, interfaces the operator with the host computer. The user-friendly LED dot-matrix displays can display any graphics or alpha-numerics and are available in green, red or amber. They can efficiently guide the operator through any complex sequence with no errors and no wasted time.

They also simplify operator training as well as control panel design. One Vivisun Series 2000 programmable display system can do the work of 50 or more dedicated switches. In short, Vivisun Series 2000 gives the design engineer more control over the design.

Contact us today.

AEROSPACE OPTICS INC.
3201 Sandy Lane, Fort Worth, Texas 76112
(817) 451-1141 • Telex 75-8461 • Fax (817) 654-3405

Vivisun Series 2000 programmable displays. The intelligent communications system.

SERIES
VIVISUN 2000™

protecting it from other etchants. The filler may be the same material used as a temporary adhesive when the wafer is inverted and bonded to a carrier, as shown in part 2 of the figure, and may be injected at the same time. This filler/adhesive must be unaffected by photoresist and photoresist solvents but must be easily removed by other chemicals at the end of fabrication.

Once the wafer is bonded to the carrier, the semi-insulating substrate is etched away to the AlGaAs etch stop. The wafer is patterned with photoresist while still on the carrier, and the AlGaAs and GaAs above the anode contact pad are removed, as shown in part 3 of the figure. Because of the large size of the surface channel, this backside patterning is not critical in terms of alignment.

A thin [1- to 2-mil (25- to 50-μm)] layer of low dielectric-constant material, such as a polymer, spin-on glass, or quartz with adhesive, is applied to the wafer to provide support. The wafer is diced into individual chips while still bonded to the carrier. After removing the chips from the carrier and removing the surface channel filler, single chips are soldered or bonded to a choke structure in a "flip-chip" configuration. The diode chip may be used with the new support dielectric in place (see part 4 of figure) or, for absolute minimum parasitic capacitance and thickness, the support dielectric may be etched or dissolved away (see part 5 of figure).

This work was done by William Bishop and Robert Mattauch of the University of Virginia for **Goddard Space Flight Center**. *For further information, Circle 21 on the TSP Request Card.*

Inquiries concerning rights for the commercial use of this invention should be addressed to the Patent Counsel, Goddard Space Flight Center [see page 18]. Refer to GSC-13205.

Phototransistors for Long-Wavelength Infrared

Detection would be based on impurity-to-continuum transitions.

NASA's Jet Propulsion Laboratory, Pasadena, California

Phototransistors of a proposed new type would be used to detect photons that have wavelengths of 8 to 150 μm. Integrated-circuit imaging arrays of such phototransistors would be useful in infrared remote sensing.

A device of this type would be a silicon, germanium, or silicon/germanium phototransistor in which the junction between the collector and the base is lightly doped with impurities. In the case of the npn Si/Ge/Si phototransistor shown in the figure, the dopant would be one or more electron-donor material(s) in which the electron-energy states lie slightly below the bottom of the conduction band of silicon.

Photons of energy equal to or greater than the gap between these states and the conduction band would excite electrons from the donor states to the continuum of energy states in the conduction band. The electric field that arises from the application of the customary reverse bias to the collector/base junction would sweep these photoexcited electrons toward the collector.

The positive donor ions left by the photoexcitation would increase the forward bias across the emitter/base junction; this would cause electrons to be injected from the emitter to the base. If the lifetimes of the injected electrons exceeded the times of transit across the base, then most of this injected-electron current would be amplified by normal transistor action.

Although a phototransistor of this type could have a Ge or Si homostructure, a heterostructure containing both Si and Ge is preferred because it blocks the transport of holes and thereby contributes to the current gain. Blocking the hole current also decreases the dark current and its contribution to noise.

Another alternative configuration would include a blocked-impurity-band structure, which makes it possible to take advantage of concentrated doping without incurring the disadvantage of large leakage of current by conduction through the impurity band. In this case, the blocking layer (in which charges cannot travel in the impurity band) would be a thin, undoped layer grown on the collector side of the heavily doped active layer.

This work was done by Shmuel I. Borenstain of Caltech for **NASA's Jet Propulsion Laboratory**. *For further information, Circle 138 on the TSP Request Card.*
NPO-18029

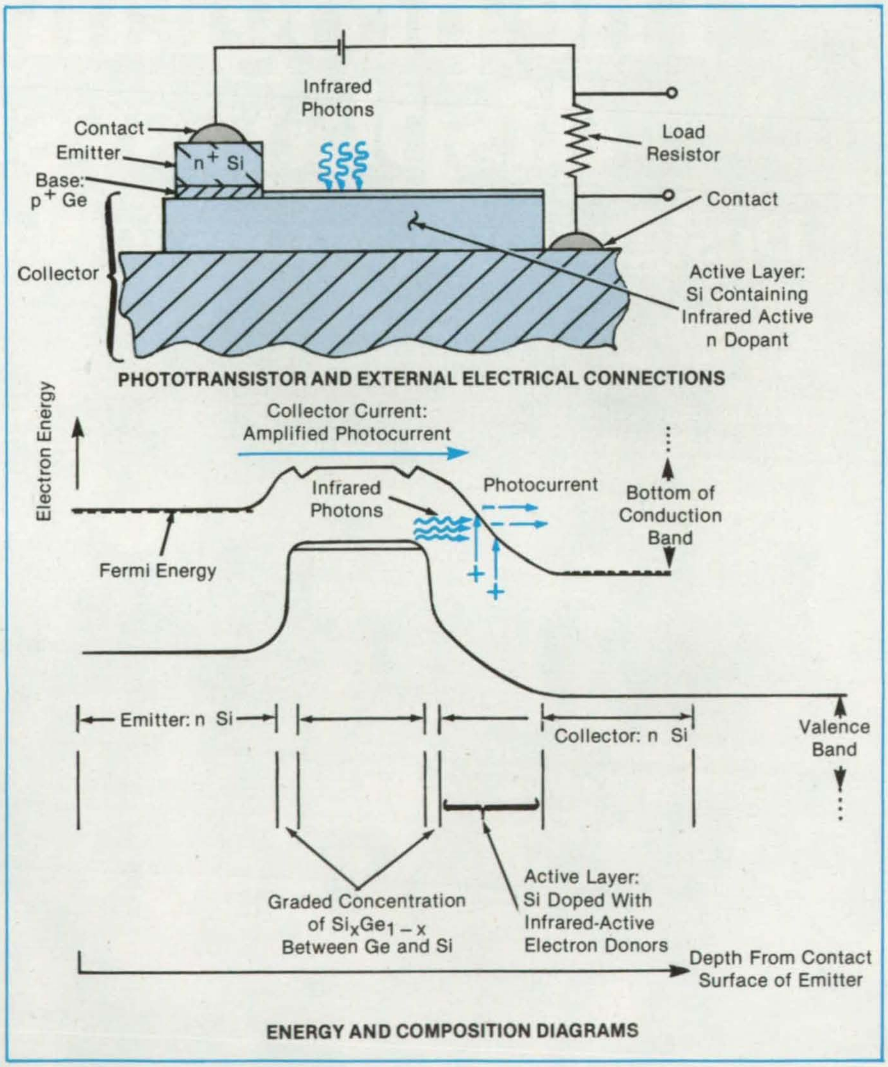

An **npn Phototransistor**, of several versions of a proposed new type, would include infrared-active electron-donor dopant in a thin layer at the collector/base junction.

Electronic Systems

Hardware, Techniques, and Processes

Books and Reports

Computer Processing of Tunable-Diode-Laser Spectra

Measurements in three channels are processed into spectra.

NASA's Jet Propulsion Laboratory, Pasadena, California

A tunable-diode-laser spectrometer that measures the transmission spectrum of a gas operates under the control of a computer, which also processes the measurement data. The laser beam is split into parts along three different paths: one through a germanium etalon, one through an absorption cell filled with a reference gas at low pressure, and one through an absorption cell filled with the specimen gas, the absorption or transmission spectrum of which one seeks to determine (see Figure 1). The computer tunes the laser in small increments of wavelength by increasing or decreasing the laser current in small steps. At each increment, three photodetectors measure the laser-beam powers that reach the ends of the paths.

These measurements are digitized, then processed as illustrated schematically in Figure 2. The measurement data represent raw transmission spectra that include the effects of instrumental distortion. The raw transmission spectrum of the etalon represents the interference-fringe pattern of the etalon, which defines a relative-wave-number scale and is used to linearize the wave-number scale via a polynomial interpolation procedure. An absolute-wave-number scale is derived from the spectrum of the reference gas, which is also used to determine the laser linewidth and to confirm the free spectral range of the etalon.

The spectrum of the specimen gas is normalized to a 100-percent-transmission baseline through polynomial fitting in the portions of the spectrum in which the density of absorption lines is low and, consequently, the 100-percent-transmission level is easily identified. To obtain this normalization in the portions of the spectrum in which the continuum absorption is high because the pressure of the specimen gas is high or because the spectral lines of the specimen gas are congested, a scan is performed with the specimen-gas absorption cell evacuated.

The spectral positions of spectral lines and maximums of the etalon fringes are obtained approximately via first- and second-derivative locating procedures and,

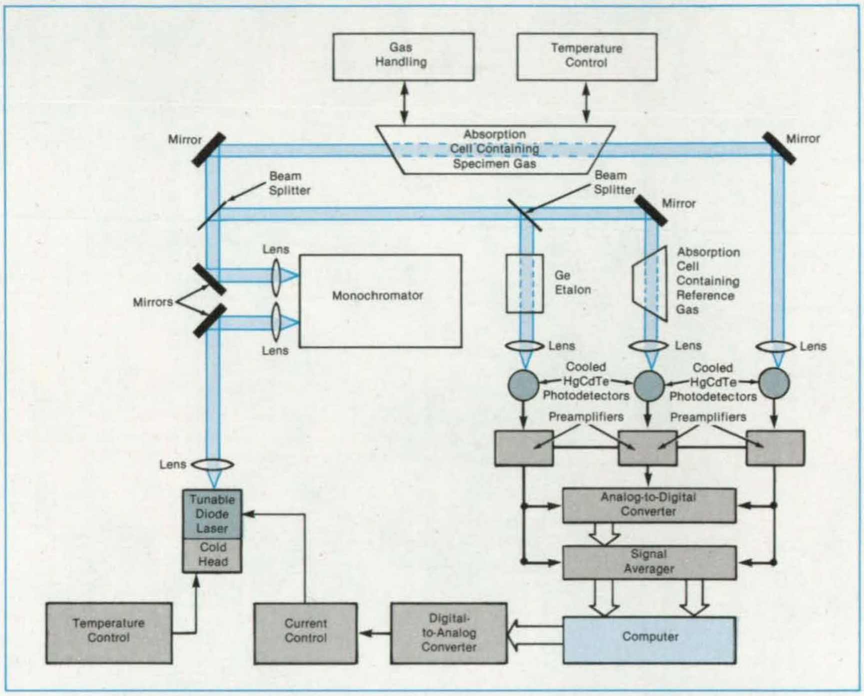

Figure 1. The **Computer Controls the Current** supplied to the tunable diode laser, thereby stepping it through small increments of wavelength while processing the spectral measurements at each step.

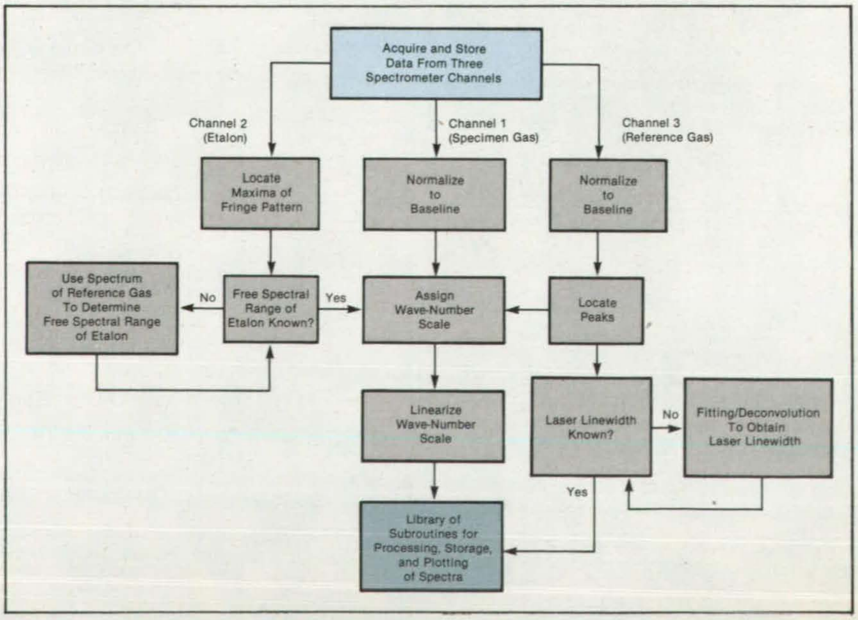

Figure 2. This **Flow Chart** illustrates the steps in the analysis of the raw spectral data.

(Actual Size)

In a nutshell,
it's the world's most advanced
microminiature camera.

As you can see, Toshiba's new microminiature color camera actually fits inside a peanut shell. But what's more incredible is what fits inside the camera.

It has the first and only ½" CCD that delivers 420,000 pixels for over 460 lines of horizontal resolution. It also has the only electronic shutter with 8 settings from 1/60 to 1/10,000 sec. Not to mention Y/C and composite video outputs and choice of 6 cable lengths from 2 to 30 meters. Also available are 5 lenses from super wideangle to telephoto. And C-mount adaptor.

So call 1-800-537-7045 [N.J., 201-628-8000, ext.3750] for more information on Toshiba's IK-M40A. You'll find out why buying any other microminiature camera would be nuts.

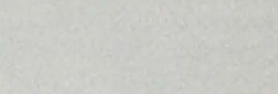

In Touch with Tomorrow

TOSHIBA

Toshiba Video Systems, 82 Totowa Road, Wayne NJ 07470

Circle Reader Action No. 393

when necessary, with the help of graphical input by the user. More accurate values for these positions are obtained via least-squares fitting procedures. A wave-number scale is assigned by using the known wavelengths or wave numbers of the spectral lines of the reference gas along with the free spectral range of the etalon. Nonlinearities in the wave-number scale are identified by observing irregularities in the numbers of data points that separate the etalon-fringe peaks. The computer program includes a library of routines for the general manipulation and plotting of spectra, least-squares fitting of direct-transmission and harmonic-absorption spectra, and deconvolution for determination of the laser linewidth and for removal of instrumental broadening of spectral lines.

This work was done by Randy D. May of Caltech for **NASA's Jet Propulsion Laboratory**. *For further information, Circle 123 on the TSP Request Card.*
NPO-18019

Twin-Mirrored-Galvanometer Laser-Light-Sheet Generator

Multiple, rotating laser-light sheets are generated to illuminate flows in wind tunnels.

Langley Research Center, Hampton, Virginia

Light sheets generated with either laser or noncoherent light sources have found many applications in the visualization of flows. However, previous systems were usually dedicated to specific viewing geometries. A new system was designed and developed to provide flexibility and adaptability to a wide range of applications. The design includes the capability to control the size and location of the laser-light sheet in real time, to generate horizontal or vertical sheets, to sweep the sheet repeatedly through a volume, to generate multiple sheets with controllable separation, and to rotate single or multiple laser-light sheets.

The galvanometer-mirror-based laser-light-sheet system (see figure) was developed for use in the Basic Aerodynamics Research Tunnel (BART) at NASA Langley Research Center. The system generates and positions single or multiple light sheets over aeronautical research models being tested in the low-speed tunnel.

The laser-light-sheet system is evolving. Initially, the system was configured to generate single horizontal or vertical laser-light sheets. The capability to generate multiple laser-light sheets or sweep the position of a single sheet was added next. The capability to rotate a single laser-light sheet by use of a sine/cosine potentiometer was then added. The capability to rotate multiple laser-light sheets was added by incorporating a rotation output in the multiple-sheet generator. The latest addition is a Bragg cell to remove spurious lines between the sheets.

The addition of each new capability was accomplished without compromising existing capabilities. The system is capable of producing up to 12 sheets of laser light at an angular divergence of ±20°. The maximum rate of scanning for any line is approximately 500 Hz. The rate of scanning of the generated line along the orthogonal axis is also controlled. The time-averaged line can be rotated to any desired degree.

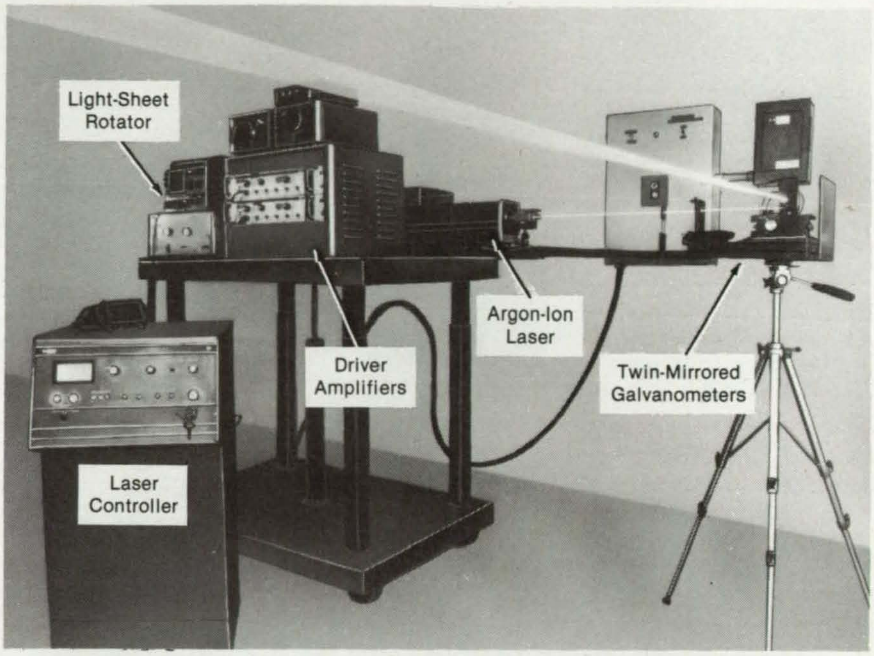

The **Light-Sheet System** includes electronic equipment and a laser mounted on an adjustable-height platform. The twin-mirrored galvanometer unit is supported by a tripod to reduce vibration.

When this system is used to illuminate smoke entrained in the flow over a delta-wing model, it reveals the vortical flow produced by the separation of the flow at the leading edge of the model. The light-sheet system has proved to be very adaptable and easy to use in sizing and positioning light sheets in wind-tunnel applications. Other possible applications include use in the construction industry to align beams of a building. Artistic or display applications are also possible.

This work was done by David B. Rhodes, John M. Franke, Stephen B. Jones, and Bradley D. Leighty of **Langley Research Center**. *Further information may be found in NASA TM-100587 [N88-25901], "A Twin-Mirrored Galvanometer Laser Light Sheet Generator."*

Copies may be purchased [prepayment required] from the National Technical Information Service, Springfield, Virginia 22161, Telephone No. (703) 487-4650. Rush orders may be placed for an extra fee by calling (800) 336-4700.
LAR-14248

Associative-Memory Array of Optical Logic Gates

Differences between binary input and memory images are measured in terms of Hamming distances.

NASA's Jet Propulsion Laboratory, Pasadena, California

An experimental optical associative-memory apparatus measures the similarity or dissimilarity between an input binary image and each of *M* binary images in memory. Using the Hamming distance as the measure of dissimilarity, it determines which (if any) of the memory images closely or most closely resembles the input image. It indicates this match by displaying an image (e.g., the recognized image or a symbol, word, number, or other substitute image) in real time on an output plane.

The apparatus contains a two-dimensional array of optical exclusive-OR gates, which are used to determine the Hamming distance between the input and memory images. Figure 1 illustrates the exclusive-OR function of a simplified (one-dimensional) array in which the input and memory images are binary column vectors. The array is illuminated from the input side with horizontally polarized light and the input and binary images, each of which is impressed on a spatial light modulator. The portions of each modulator wherein the intensity of the image represents binary "one" rotate the polarization by 90°, while those wherein the intensity represents binary "zero" do not change the polarization.

The light emerging from the memory-image spatial light modulator passes through an analyzer oriented for vertical polarization. In the spots where the input and memory images are both "zero" or both "one" (where they match), the output of the analyzer is dark and the contribution to the Hamming distance is zero. In the spots where the input and memory images differ (one of them is "zero" while the other is "one"), the output of the analyzer is bright and the contribution to the Hamming distance is 1.

Figure 2 illustrates the full two-dimensional apparatus. The input image is electronically made into *M* replicas that are impressed on the first spatial light modulator. Each of the *M* different memory images is impressed on the second spatial light modulator in a position corresponding to that of one of the replicas of the input image. An integrating lens (or, alternatively, an array of lenslets) focuses the exclusive-OR output image from each of the *M* pairs of input and memory images onto one of *M* photodetectors. The output of each photodetector is proportional to the Hamming distance between the images in the pair; an electronic circuit determines which one represents the shortest Hamming distance and signals an associative-recall module to display the corresponding output image.

This work was done by Tien-Hsin Chao of Caltech for **NASA's Jet Propulsion Laboratory**. *For further information, Circle 129 on the TSP Request Card.*

This invention is owned by NASA, and a patent application has been filed. Inquiries concerning nonexclusive or exclusive license for its commercial development should be addressed to the Patent Counsel, NASA Resident Office-JPL [see page 18]. Refer to NPO-17997.

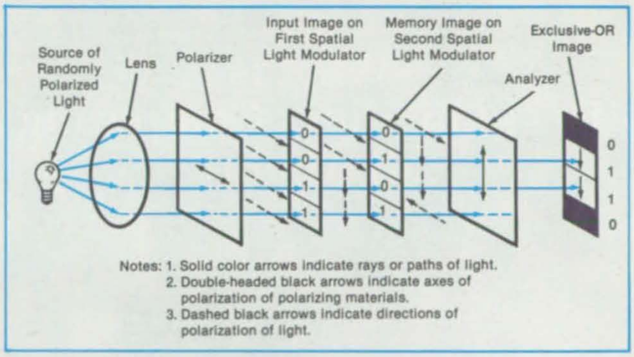

Figure 1. This **Column of Optical Exclusive-OR Gates** produces an output image that is dark where the input and memory images match and bright where they do not match. Thus, each segment of the output image represents a "zero" or "one" contribution to the Hamming distance between the input and memory images.

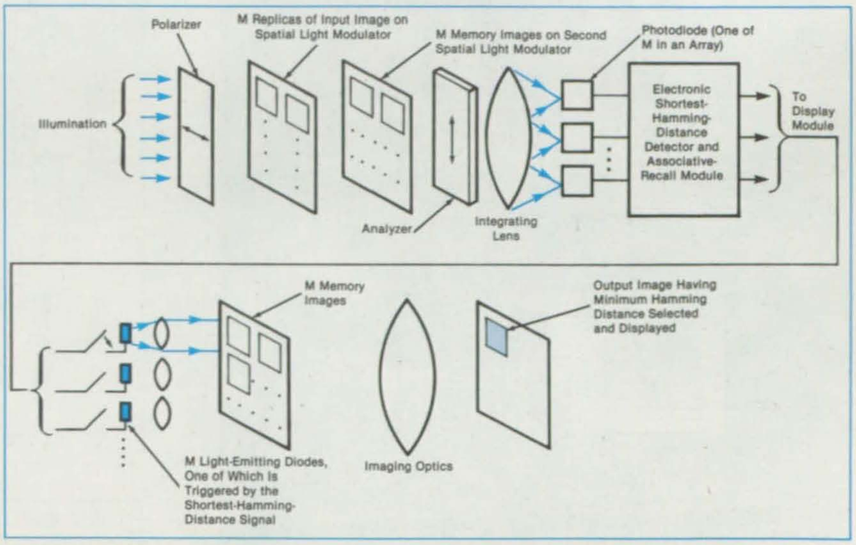

Figure 2. The **Optical Associative-Memory Apparatus**, operating on the principle illustrated in simplified form in Figure 1, finds which (if any) of *M* memory images resembles or most closely resembles the input image.

Deep FIFO Surge Buffer

A data-acquisition system temporarily accepts data at a higher rate.

Ames Research Center, Moffett Field, California

A first-in/first-out (FIFO) buffer temporarily stores short surges of data generated by a data-acquisition system at an excessively high rate and releases the data at a lower rate suitable for processing by a computer. The size and complexity of the FIFO buffer are reduced while its capacity is enhanced by the use of newly developed, sophisticated integrated circuits and by a "byte-folding" scheme that doubles the effective depth and data rate.

The system (see Figure 1) allows for tradeoff between the number of data channels (up to 64) and the sampling rate in each channel, each of which is equipped with its own sample-and-hold and 16-bit analog-to-digital converter circuits. The computer can accept 16-bit data at a maximum rate of only 500,000 pulses per second, whereas the 64 channels of the data-acquisition system operating at full capacity can generate data at 2,839,040 pulses per second. The FIFO buffer must be capable of storing the difference (2,339,040 pulses per second) during a burst 2.95 seconds long.

Each channel is equipped with a unit of FIFO memory that includes a FIFO random-access-memory (RAM) controller, two memory arrays, each containing four 8×32 K static RAM integrated circuits, and latching registers (see Figure 2). Peripheral programmable-array-logic integrated circuits are used to route clock signals to and from the FIFO RAM controller, the input and output latching registers, and the static RAM memory array.

The principle of operation is as follows: At the end of each analog-to-digital conversion, an "end-of-conversion" pulse triggers a flip-flop and sends a "write" request to the FIFO RAM controller. This toggles "write" data into the latching registers and enables double-speed operation of the writing port. The data are strobed in and out sequentially to make one 16-bit $\times$ 128 Kbyte writing/reading cycle. The FIFO RAM controller reads data from the memory array when it receives a "read request" in the form of an "output enable" signal from the computer.

This work was done by Gerald Temple, Marc Siegel, and Zwie Amitai of **Ames Research Center**. *For further information, Circle 71 on the TSP Request Card.*
ARC-12159

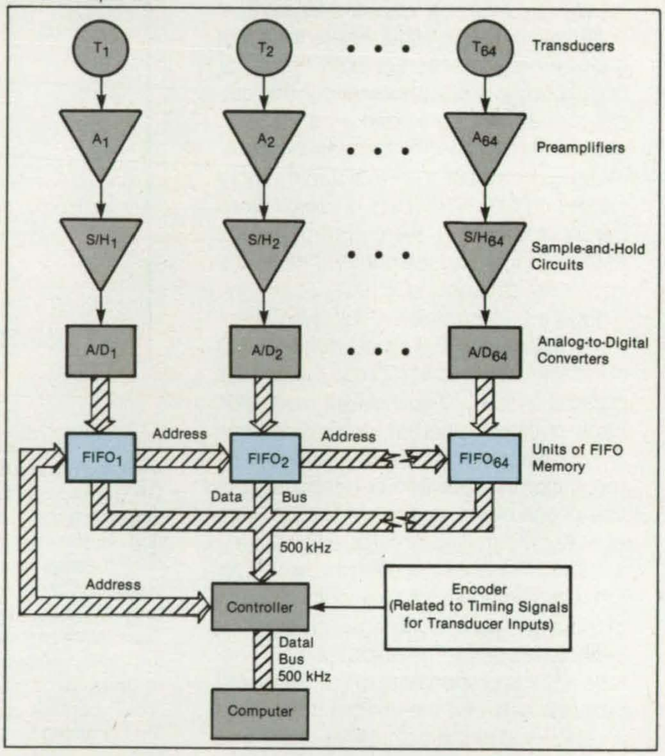

Figure 1. The **Data-Acquisition System** includes a unit of FIFO memory in each channel of incoming data. The FIFO buffer, consisting mostly of the collection of these FIFO memory units, stores large surges of incoming data and releases them to the computer at a lower rate that it can handle.

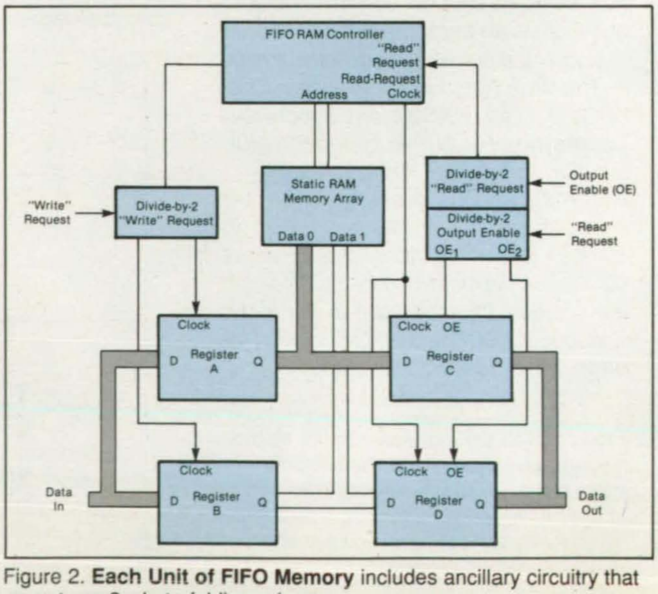

Figure 2. **Each Unit of FIFO Memory** includes ancillary circuitry that executes a 2 x byte-folding scheme.

FINALLY! TELEDYNE RELAY QUALITY FOR JUST $6.00*

We're pleased to introduce optimum price/performance in a DPDT relay designed for very dense packaging in cost-conscious commercial applications.

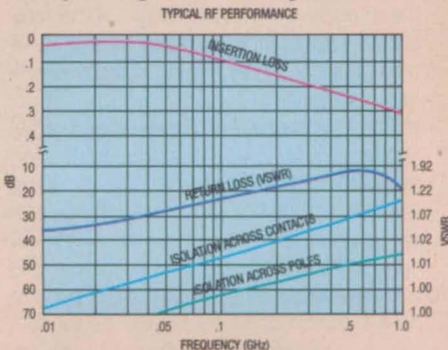

Our 172 Centigrid® uses TO-5 relay technology to provide high overall reliability and excellent resistance to environmental extremes. It's available at an unusually affordable quantity/price, thanks to vertical integration and automation in our manufacturing operations. Three models are offered in a basic DPDT configuration.

Applications include telecommunications, test instruments, mobile communications, aeronautical electronics, attenuators and automatic test equipment.

Inherently low intercontact capacitance and contact circuit losses make the 172 Series an excellent RF switch for frequencies well into the UHF spectrum as shown above.

DETAILED ELECTRICAL SPECIFICATIONS (@ 25°C)

GENERIC PART NUMBERS		172-5	172-12	172-26
Coil Voltage (VDC)	Nom.	5.0	12.0	26.5
	Max.	5.8	16.0	32.0
Coil Resistance (ohms ± 20%)		64	400	1600
Pick-up Voltage (VDC, Max.) Pulse Operation		3.8	9.0	18.0
Coil Operating Power at Nominal Voltage (Milliwatts)		405	360	440
Contact Load Ratings (DC)	Resistive: 1 Amp/28VDC Inductive: 200 mA/28VDC (320mH) Lamp: 100 mA/28VDC			
Contact Load Ratings (AC)	Resistive: 600 mA/115VAC, 400 Hz (Case ungrounded); 400 mA/115VAC, 60 Hz (Case ungrounded) 200 mA/115VAC, 60 and 400 Hz, (Case grounded)			

For complete technical information, application assistance and quantity pricing, call us at 1-800-284-7007 or FAX us at 213-779-9161 today.

TELEDYNE RELAYS
Innovations In Switching Technology

TELEDYNE RELAYS, 12525 Daphne Avenue, Hawthorne, California 90250

Circle Reader Action No. 537

*Priced at $6.00–$7.00 in quantities of 5,000 or more, depending upon specific model purchased. And, still very affordable in smaller quantities.

Physical Sciences

Hardware, Techniques, and Processes

Books and Reports

Microwave Brightness of Land Surfaces From Outer Space

Effects of roughness of surface, moisture in soil, and vegetation are included.

NASA's Jet Propulsion Laboratory, Pasadena, California

A mathematical model approximates the microwave radiation emitted by land surfaces that travels to a microwave radiometer in outer space. This is one of a number of such models developed in recent years for the interpretation of microwave imagery of the Earth to obtain the distributions of various chemical, physical, and biological characteristics across its surface. In this case, the model is intended primarily for use in mapping the moisture content of soil and the fraction of the Earth covered by vegetation.

The theoretical basis of this development is a general mathematical model of microwave brightness temperatures over land. The general model takes account of the altitude and viewing angle of the radiometer; the polarization and frequency of the radiation; the upwelling and downwelling radiation that originates in the atmosphere; the downwelling background radiation from outer space; and the attenuation and scattering in the atmosphere, including the effects of water vapor, clouds, and precipitation (see figure). The general model includes submodels that characterize the microwave appearance of the soil surface as a function of its moisture, roughness, and temperature. Other submodels characterize the vegetative land cover as a function of its temperature, moisture content, a single scattering albedo, structure, and the percentage of surface covered.

The general mathematical model is changed to express the brightness temperatures in terms of the ratios between the power densities received in vertical and horizontal polarizations in the various radiometric frequency bands. These polarization ratios depend primarily on the moisture content and percentage of vegetative cover, which one seeks to map, and upon the surface roughness, which one does not seek to map. That is to say, the use of these polarization ratios reduces the influence of the surface-temperature and atmospheric effects that are undesired in this mapping problem, leaving only the roughness of the surface as the major undesired feature. The surface-roughness submodel includes an approximate equation for the microwave reflectivity as a function of the microwave frequency, the root-mean-square roughness height, and the spatial frequency of the roughness. Because of this equation, one can use spatial-frequency effects in the observed polarization ratios to separate, at least partially, the surface-roughness effects from the soil-moisture effects.

The model was applied to measurements made by the Scanning Multichannel Microwave Radiometer (SMMR) aboard the Nimbus 7 satellite at five frequencies from 6.6 to 37 GHz and in both polarizations. The model was found to be useful in evaluating the effects of atmospheric water vapor and clouds at the SMMR frequencies, and in showing that microwave radiometry can be a very efficient technique for monitoring changes in soil moisture and vegetation, at least in semiarid areas.

A remaining problem is to find a suitable and reliable way of combining measurements made at different frequencies, to isolate the different parameters through their varying influences as functions of the microwave frequency. The model shows that the lower frequencies are best adapted to the monitoring of soil-moisture and canopy-water contents. The higher microwave frequencies are useful for monitoring the water content of vegetation only where the vegetative cover is very sparse. However, the higher spatial resolutions available at the higher microwave frequencies are desirable. The Advanced Very-High-Resolution Radiometer (AVHRR) of the National Oceanic and Atmospheric Administration could provide additional information on vegetative cover, thereby making possible the retrieval of soil-moisture values from the SMMR measurements. Moreover, the joint use of SMMR and AVHRR data will probably make it possible to monitor changes of the land surface during intervals of 5 to 10 years, providing significant data for mathematical models of the evolution of the climate.

This work was done by Yann H. Kerr and Eni G. Njoku of Caltech for **NASA's Jet Propulsion Laboratory**. *For further information, Circle 45 on the TSP Request Card.* *NPO-17739*

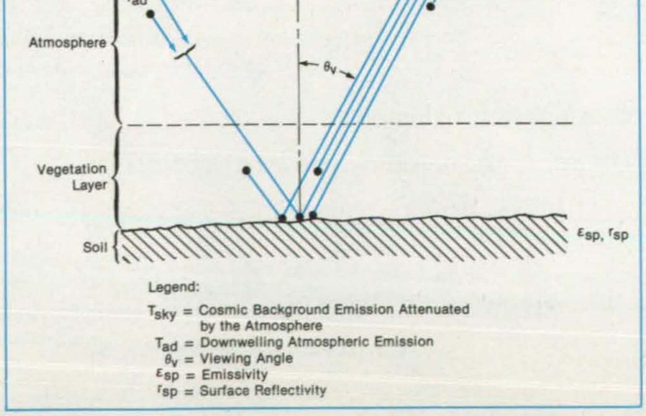

The **Microwave Brightness Temperature** is computed by accounting for the emission, scattering, and attenuation of radiation in the atmosphere, in vegetation, and on the ground.

High-Power Liquid-Metal Heat-Transfer Loop

A permselective barrier would sustain a high differential pressure and a consequent high rate of pumping.

NASA's Jet Propulsion Laboratory, Pasadena, California

A proposed closed-loop system for the transfer of thermal power would operate at relatively high differential pressure between the vapor and liquid phases of a liquid-metal working fluid. The higher differential pressure could be used to pump the fluid at a higher rate, thereby increasing the output thermal power. Inasmuch as the system would contain no moving parts, it should be highly reliable and well suited to long-term unattended operation.

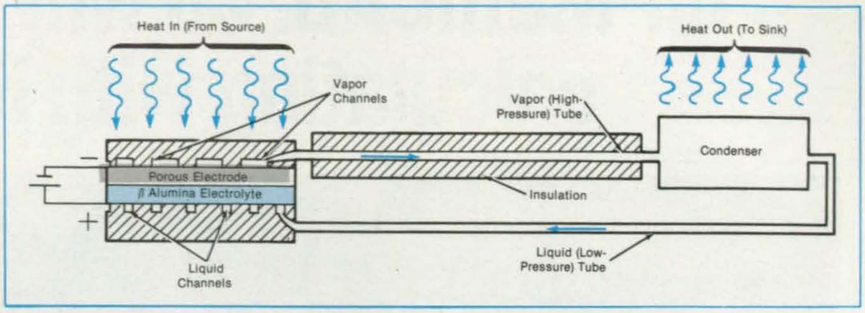

The **High-Power Liquid-Metal Heat-Transfer Loop** would resemble a "capillary-pumped" liquid-metal heat-transfer loop except that the electric field across a permselective barrier of β alumina (instead of the capillary force in a wick) would keep the liquid and vapor separate at the heat-input end.

The system is based partly on the same principle that underlies the operation of heat pipes and capillary pumped loops. All such heat-transfer loops are essentially heat engines in which the sources are slightly hotter than the sinks are, and the power produced by the expansion of the working fluid upon vaporization at a source is consumed in pumping the fluid around the loop. The term "capillary pumped loop" is misleading in that the capillary force does not pump the fluid: instead, it acts within a wick to provide a meniscus that serves as a barrier between the liquid and vapor. One major disadvantage of a capillary-type device is that the maximum differential pressure it can sustain is determined by the capillary force, and any attempt to increase it is inhibited by the practical difficulty of making smaller pores and by the tendency of small pores to become clogged over a long time.

In the proposed loop, the wick would be replaced by the combination of a porous electrode and a permselective barrier. In the version shown in the figure, the fluid would be sodium, and the barrier material would be β alumina solid electrolyte, which conducts sodium ions (but not neutral atoms) preferentially to electrons. The liquid zone would be the low-pressure zone, the vapor zone would be the high-pressure zone, and heat from the source would be transferred into the high-pressure zone near the porous electrode.

A positive electric potential (with respect to the porous electrode) would be applied to the liquid side of the β alumina electrolyte, giving rise to an electric field in the electrolyte that would tend to force sodium

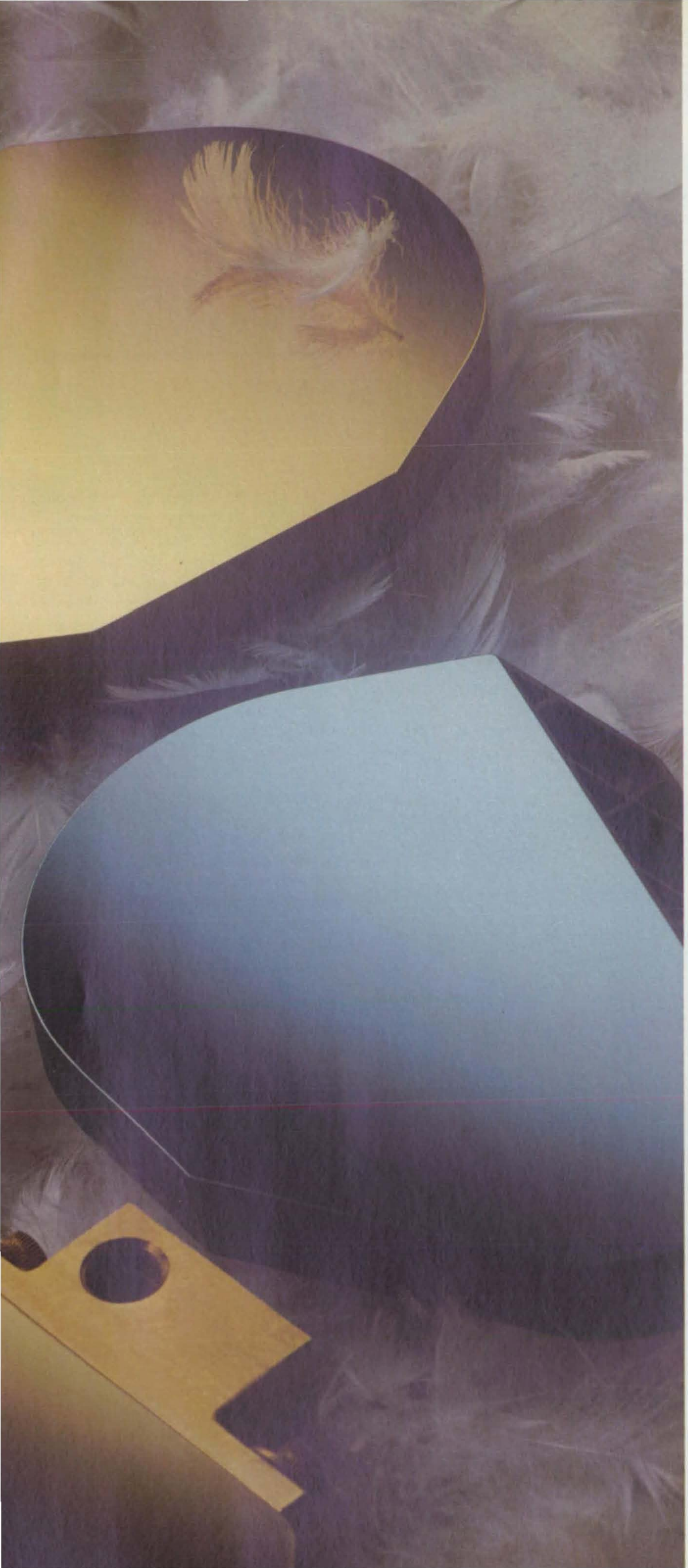

High Performance Without The Heavy Cost.

Now you can improve on the stiffness and weight advantages of beryllium—and save cost, too. With advanced CERAFORM® silicon carbide mirrors from United Technologies Optical Systems.

CERAFORM® silicon carbide mirrors offer significantly reduced thermal distortion and a superior package of optical and performance properties:

Properties	Be	SiC(*)	Al	ULE™
Physical				
Density (g cm^{-3})	1.85	2.92	2.73	2.21
Mechanical				
Young's Modulus (GPa)	303	311	71	68
Microyield Stress (MPa)	35	(**)	98	24
Thermal				
CTE (10^{-6} K^{-1})	11.4	2.57	24.0	0.03
Diffusivity (cm^2 s^{-1})	0.52	0.80	0.96	0.008
Specific Heat (J kg^{-1} K^{-1})	1,880	670	900	766
Conductivity (W m^{-1} K^{-1})	180	156	237	1.3
Figures of Merit(***)	**Be**	**SiC(*)**	**Al**	**ULE™**
Structural (higher is better)				
Specific Stiffness (E/ρ)	164	107	26	31
Thermal (lower is better)				
1st Order Distortion (CTE/k)	0.063	0.017	0.101	0.023
Thermal Distortion (CTE/D)	22.2	3.26	25.0	3.92
Dim. Change (CTE • ρ/k)	118	48.1	276	51.0

(*) Values shown are for CERAFORM®.
(**) None detected prior to fracture. (***) For equal geometries.

Optical system engineers will also appreciate how efficiently complex, lightweight structures can be produced using our unique Precision Forming Process.

CERAFORM® silicon carbide mirror technology. *Weight* till you see what it can do for you.

For more information, contact Rich Drake, Program Development Manager, at 407-775-4500. P.O. Box 109660, West Palm Beach, Florida 33410-9660.

UNITED TECHNOLOGIES OPTICAL SYSTEMS

Circle Reader Action No. 331

ions from the liquid toward the vapor zone. This effect would oppose the differential pressure, which would otherwise force ions from the vapor zone back toward the liquid zone. Thus, if a suitable voltage were applied, the electrolyte-and-electrode combination would keep the liquid and vapor apart, playing the same role as that of the meniscus in a capillary device. In this device, however, the maximum sustainable differential pressure would be limited only by the strength of the electrode and solid electrolyte, and these parts could be made as thick as necessary to withstand the differential pressure required for pumping at the desired rate.

In addition, the electric potential could be varied to control the rate of pumping; a larger potential would produce a larger rate. If the applied potential were larger than required for the pressure balance at a given combination of input and output temperatures and rate of flow, then the extra potential would exert an extra pumping effect that would increase the rate of flow until a new pressure balance was reached.

This work was done by Pradeep Bhandari and Toshio Fujita of Caltech for **NASA's Jet Propulsion Laboratory**. *For further information, Circle 11 on the TSP Request Card.*

This invention is owned by NASA, and a patent application has been filed. Inquiries concerning nonexclusive or exclusive license for its commercial development should be addressed to the Patent Counsel, NASA Resident Office-JPL [see page 18]. Refer to NPO-18034.

Mixed-Gas Sorption Joule–Thomson Refrigerator

Features would include relative simplicity, less required power, and no vibration.

NASA's Jet Propulsion Laboratory, Pasadena, California

A proposed mixed-gas sorption Joule–Thomson refrigerator would provide cooling down to a temperature of 70 K. A typical prior Joule–Thomson refrigerator included multiple stages of chemisorption and/or physisorption, each containing a single gas. The proposed mixed-gas Joule–Thomson refrigerator would include only one stage and no mechanical compressor. Thus, the new refrigerator would be simpler, would operate without vibrating, and would consume less power in producing the same amount of cooling.

The concept of using a single stage and mixed gases to obtain the amount and degree of cooling that would otherwise require multiple stages of single-gas sorption and Joule–Thomson expansion is based on prior research in the enhanced Joule–Thomson effect in some dual-gas mixtures. For example, as described in a British patent published in 1973, the addition of hydrocarbons to nitrogen increases the Joule–Thomson cooling tenfold.

In the proposed refrigerator, the working fluid — a mixture of propane, methane, ethane, nitrogen, and neon gases — would be circulated by two physisorption compressors that would be alternately heated and cooled between temperatures of 275 and 500 K. At the stage of operation illustrated in the figure, the hydrocarbon gases would be preferentially adsorbed from the gas mixture entering the left physisorption compressor, while the less-adsorbable nitrogen and neon would mostly pass through the sorbent to the void space in this unit. At the same time, heating would drive the hydrocarbon gases out of the sorbent in the right physisorption compressor. The hydrocarbon gases would push the nitrogen and neon, and then some of itself out of the void space in this unit and into a surge-volume chamber, in which the gases would be remixed.

From the surge volume, the mixture would flow through two heat exchangers, in which it would be cooled by the gas mixture returning from the cold stage. Between the two heat exchangers, the gas mixture flowing toward the cold stage would be cooled further by a thermoelectric device, causing the hydrocarbon gases to begin to liquefy. The mixture would then pass through the Joule–Thomson valve, causing further cooling and liquefaction. The boiling of the liquid would provide cooling at 70 K in the cold stage, and the evaporated mixture would return through the heat exchangers and a low-pressure surge volume to the cooler sorption compressor. The combination of fluids remains as a liquid even though the hydrocarbons would individually freeze out if not in the mixture.

The same sorption principle of operation may be applicable in a compressor that would chemisorb oxygen or hydrogen from a mixture with helium, neon, and/or other nonreactive gases.

This work was done by Jack A. Jones, S. Walter Petrick, and Steven Bard of Caltech for **NASA's Jet Propulsion Laboratory**. *For further information, Circle 10 on the TSP Request Card.*

This invention is owned by NASA, and

Fast Computation + WYSIWYG Graphics + Programming + Debugger + X-Windows

When you add it all up

Fast 2-D and 3-D Graphics
- *Strip charts*
- *Multiple curves*
- *Postscript, EPS, HPGL output*
- *Extensive annotation*
- *Zoom, pan, move, rotate*
- *Perspective, light source*

Matrix Spreadsheet
- *Edit matrices*
- *Cell by cell operations*
- *Access math functions*
- *Scrollable window*
- *Cut, copy, paste data sets*

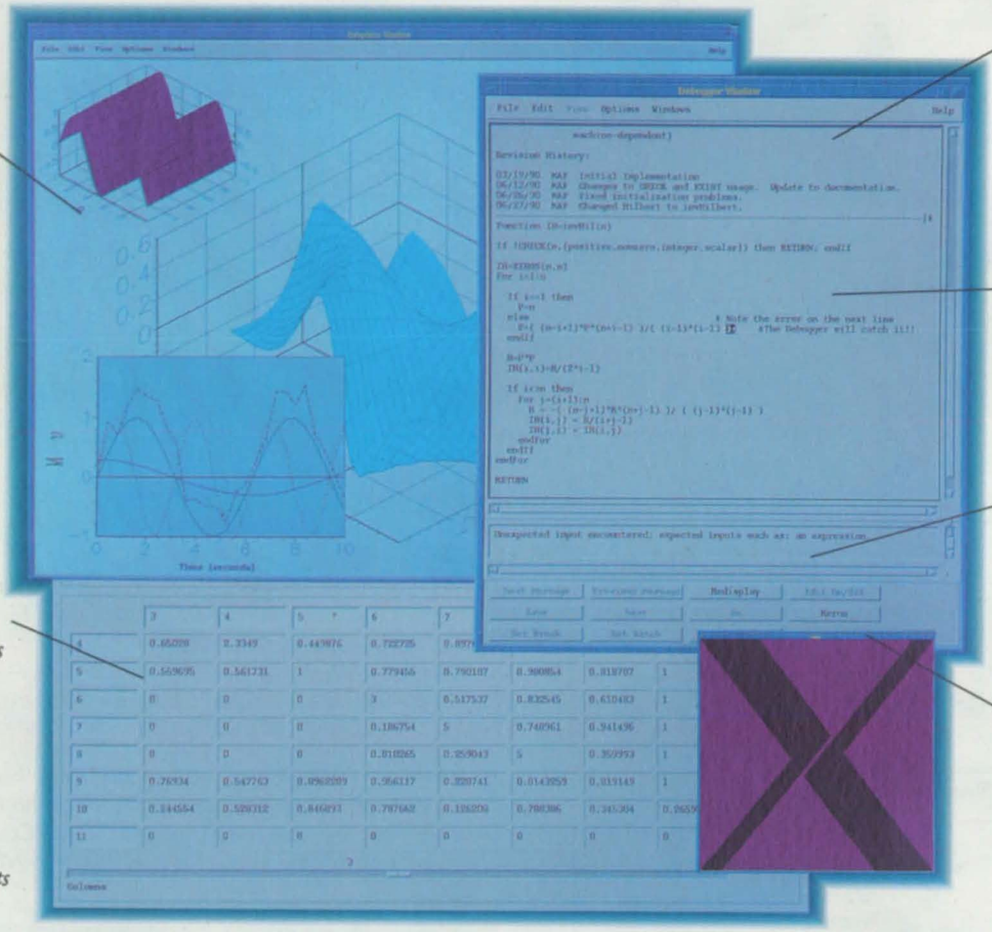

Object-Oriented Mathematics
- *Algorithms optimized for data types*
- *3-D matrices*
- *Strings, tables, lists*
- *200+ built-in math functions*

Open Architecture
- *Include your C or Fortran*
- *Import your data*
- *Use ISI's MathScript to add functions*

Interactive Script Debugger
- *Source level debugger*
- *Single step*
- *Break points*
- *Variable watch*

X-Windows User Interface
- *Industry standard*
- *Pull-down menus*
- *Hypertext HELP*
- *Mouse clicks*
- *Pop-up forms*
- *Multiple windows*
- *Data dictionary*

Xmath is the Answer

Manipulate your data with 100's of built-in functions. Develop new algorithms to find the answers you really need. Plot your results to show the world what you've done. All without a single line of Fortran or C.

Writers have word processors, financial analysts have spreadsheets, and now engineers and scientists have Xmath™ — the only object-oriented, mathematical analysis and scripting environment designed specifically for X-windows workstations. Xmath is the fastest math engine available today. Math functions, WYSIWYG 2-D and 3-D graphics, numerical programming, and a Motif interface are combined into an integrated engineering/scientific workbench. In one environment, you can interactively load, graph, and manipulate your data without writing a single line of code.

Xmath was designed to let you develop your own function libraries. With the built-in MathScript™ language, you can develop and debug numerical algorithms 10 to 100 times faster than with Fortran or C. The object-oriented nature of MathScript lets you capture 100's of lines of Fortran in a single command! And the friendly Motif user interface allows you to work with Xmath through pull-down menus, pop-up forms, and mouse clicks. Advanced function libraries written in MathScript are available for control design and signal processing.

Instead of spending your valuable time hacking out Fortran code, give us a call at **1-800-675-MATH** and we'll send you a **FREE Xmath Demo Diskette for workstations.** The diskette will convince you that Xmath is the best mathematical computation and graphics tool available.

integrated systems inc.
3260 Jay Street
Santa Clara, California 95054
Tel: (408) 980-1500 ▪ Fax: (408) 980-0400

Circle Reader Action No. 567

Technical Seminar: **Applications of Xmath**

May	June	July
14 Dayton, OH	4 Minneapolis, MN	16 Warren, MI
15 Atlanta, GA	5 Houston, TX	19 Dearborn, MI
17 Huntsville, AL	7 Orlando, FL	**August**
Contact Juli at ISI to sign up. Attendance is free of charge!	18 Toronto, ONT	13 Phoenix, AZ
	21 Montreal, QUE	15 Los Angeles, CA

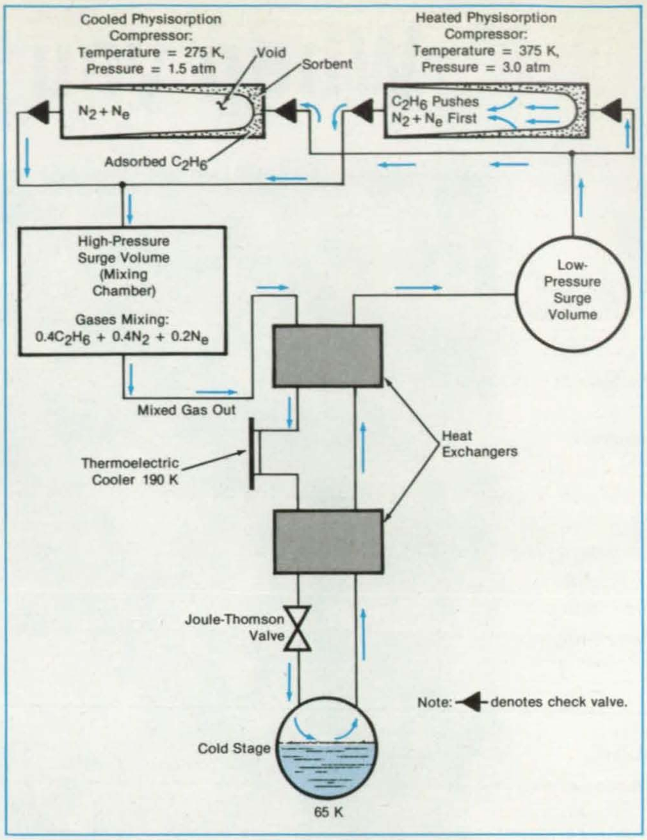

The **Mixed-Gas Joule-Thomson Refrigerator** would have only one two-compressor stage of physisorption and no mechanical compressor.

a patent application has been filed. Inquiries concerning nonexclusive or exclusive license for its commercial development should be addressed to the Patent Counsel, NASA Resident Office-JPL [see page 18]. Refer to NPO-17569.

Accounting for Nonlinearity in a Microwave Radiometer

Temperature is assumed to vary quadratically with the reading.

NASA's Jet Propulsion Laboratory, Pasadena, California

A simple mathematical technique has been found to account adequately for the nonlinear component of the response of a microwave radiometer. The underlying mathematical concept is not limited to this radiometric application; it is applicable to other measuring systems in which the re-

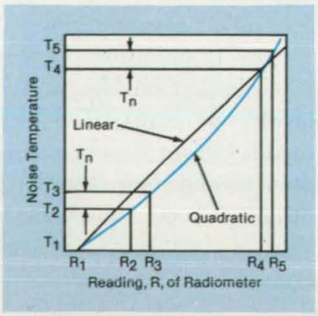

Five Prescribed Temperatures Are Measured to obtain the quadratic calibration curve for a radiometer. Two of the temperatures (T_1 and T_4) are those that would normally be used to obtain the less-accurate linear calibration curve. One of the temperatures (T_2) is the unknown that one seeks to measure. T_3 and T_5 represent measurements of T_2 and T_4, respectively, with added input from a noise diode at unknown temperature T_n.

lationships between the quantities to be determined and the readings of the instruments differ slightly from linearity.

The nominal linear relationship between the microwave temperature T (which is the quantity to be determined) and the reading R of the radiometer is $T = A+BR$, where A and B are calibration constants that can be determined by taking readings of calibration sources at two known temperatures. To account for the slight nonlinearity that is encountered in practice, it is assumed that the temperature varies quadratically with the reading:

$$T = A+BR+CR^2$$

Here, A and B have values slightly different from the values that they would have if the linear equation were used, and C is a new calibration constant that must be obtained from additional readings.

The following five-reading calibrating-and-temperature-measuring procedure based on the quadratic equation enables one to determine A, B, C, the temperature T_2 of the body under observation, and the temperature T_n of a diode noise source in the radiometer (see figure):

1. With the noise diode turned off, obtain reading R_1 by using the radiometer to measure the temperature of a calibration source at known temperature T_1.
2. With the noise diode off, aim the radiometer at the body under observation, obtaining reading R_2 for unknown temperature T_2.
3. Turn the noise diode on and again aim the radiometer at the body under observation, this time obtaining reading R_3 for unknown temperature $T_3 = T_2+T_n$.
4. Turn the noise diode off and obtain reading R_4 from a second calibration source at known temperature T_4.
5. Still using the second calibration source, turn the noise diode on and obtain reading R_5 at temperature $T_5 = T_4+T_n$.

The solution of the quadratic equations for the five readings yields the following equations for the desired quantities:

$$D = \frac{R_5^2-R_4^2-R_3^2+R_2^2}{R_5-R_4-R_3+R_2}$$

$$C = \frac{T_4-T_1}{R_4^2-R_1^2-(R_4-R_1)D}$$

$$B = -CD$$

$$A = T_1-BR_1-CR_1^2$$

$$T_2 = A+BR_2+BR_1^2$$

$$T_n = A+BR_3+CR_3^2-T_2$$

This work was done by Charles T. Stelzried of Caltech for **NASA's Jet Propulsion Laboratory**. *For further information, Circle 143 on the TSP Request Card. NPO-17451*

Books and Reports

These reports, studies, handbooks are available from NASA as Technical Support Packages (TSP's) when a Request Card number is cited; otherwise they are available from the National Technical Information Service.

Laser Spectroscopic Measurement of Temperature and Density

Development of techniques for measuring fluctuations in turbulent flows of air is reported.

A report discusses research on the use of laser-induced fluorescence in oxygen and Raman scattering in air for the simultaneous measurement of the temperature and density of air. The major intended application of these laser spectroscopic techniques is measurement of fluctuations of temperature and density in hypersonic flows in wind tunnels.

In the laser-induced-fluorescence technique, a pulsed ArF laser operating at a wavelength of 193 nm selectively excites one or more rotational spectral lines of O_2. The resulting fluorescence energy is proportional to the relative population of the selected initial energy state of the molecules (which population depends on temperature) and to the density of the air. The fluorescence takes place within a few picoseconds. The same laser beam used to excite the fluorescence gives rise to Raman scattering proportional to the density. Thus, the intensity of the Raman-scattered light indicates the density, while the ratio between the intensities of the fluorescence and the Raman-scattered light indicates the temperature.

The development of the laser-induced-fluorescence technique included the following steps:

1. Comparison of laser-induced fluorescence O_2 with other radiative processes excited in air by a broadband ArF laser;
2. Evaluation of the conditions that reduce the interferences of these processes with the measurement of temperature;
3. Development of a theoretical model of laser-induced-fluorescence, to be used in deducing the temperature from the fluorescence signal following each laser pulse;
4. Comparison of the predicted and experimentally determined dependence of the fluorescence signal upon temperature;
5. Assessment of the uncertainty associated with this technique under realistic conditions of hypersonic flow; and
6. The demonstration of the technique in slow, low-pressure, flows of cold air.

The development of the Raman technique included the investigation of the effect of tuning the narrow-band laser while monitoring the intensity of the Raman signal to detect resonances, estimation of the Raman intensity under realistic flow conditions, and the selection of the detection system to be used in these measurements.

The results of the research show that if detection is limited by photon-statistical noise, then at temperatures greater than 60 K and densities greater than 0.01 amagat, the uncertainties in the measurements of temperature and density can be less than 2 and 3 percent, respectively. The results also show that under the conditions that prevail in hypersonic wind tunnels, the measurements are unaffected by the heating of the air by the laser, collisional quenching, and (if the laser fluence is kept below 1.5 J/cm^2) nonlinear effects associated with multiphoton processes in O_2 and CO_2.

This work was done by Robert L. McKenzie of **Ames Research Center** *and Gabriel Laufer of Analatom Inc. To obtain a copy of the report, "Research and Development of a Laser Spectroscopic Technique To Measure Temperature and Density in Turbulent Air Flows," Circle 57 on the TSP Request Card.*
ARC-12719

Materials

Hardware, Techniques, and Processes

Making Solid Aromatic Polyimide Fibers

Under proper spinning conditions, voids are eliminated.

Langley Research Center, Hampton, Virginia

An improved wet-spinning process makes aromatic polyamic acid fibers that contain no voids and can be converted to polyimide fibers that are also free of voids. When made by prior wet-spinning processes, such fibers contain voids. The elimination of voids has been found to improve tensile strength and other tensile properties. The improved polyimide fibers should prove useful in protective clothing, sealing materials, filters for harsh chemical and/or thermal environments, and other applications that take advantage of their excellent chemical resistance, high thermal stability, and good tensile properties.

The polyamic acid is derived from 3,3′, 4,4′-benzophenone-tetracarboxylic dianhydride (BTDA) and 4,4′-oxydianiline (ODA). This polyamic acid is dissolved in dimethyl acetamide to make the spinning resin. In wet spinning, the resin is poured into a stainless-steel cylinder/piston assembly and extruded through a spinneret into a coagulation liquid. The solidifying polyamic acid filament, in what is called "wet gel" form, is drawn through the coagulation liquid onto a first set of cluster rolls, through a water bath, over a second set of cluster rolls, and onto a glass or stainless-steel spool. The spooled wet gel filament is dried in a forced-air or vacuum oven, then converted to polyimide fiber by further heating in a forced-air oven.

The major difference between the improved process and older processes lies in the choice of the compositions and concentration of the coagulation liquid, the inherent viscosity of the resin, the percent of solids in the resin, and the diameter of the filament to obtain a wet gel without voids. Coagulation-liquid and water-bath temperatures and drying oven conditions, chosen to assure good collapse of the wet gel into fiber form, affect the production of solid fibers to a lesser extent. Experiments have shown that to produce solid (that is, void-free) fibers in the coagulation bath, it is necessary to provide the following conditions:

- The resin should have a minimum inherent viscosity of at least 1.6 dl/g and at least 15 percent solids.
- The coagulation liquid should be an aqueous solution of either 70 to 75 percent of ethylene glycol or 70 to 80 percent of ethanol at a temperature of 20 °C.
- Filament diameters should generally be kept below 50 μm.

This work was done by Anne K. St. Clair and Robert M. Ely of **Langley Research Center** *and William E. Dorogy, Jr., of PRC. For further information, Circle 64 on the TSP Request Card.*

This invention is owned by NASA, and a patent application has been filed. Inquiries concerning nonexclusive or exclusive license for its commercial development should be addressed to the Patent Counsel, Langley Research Center [see page 18]. Refer to LAR-14162.

Fast-Acting Rubber-to-Coated-Aluminum Adhesive

This strong adhesive makes clamping unnecessary.

Marshall Space Flight Center, Alabama

A cyanoacrylate adhesive used to join rubber to coated aluminum is easier to apply and more effective than was the neoprene-based adhesive used previously. The neoprene-based adhesive had to be mixed from two components, allowed to set, then mixed frequently while it was applied. Two coats were needed, and the final coat had to dry for several hours before the mating parts were put together. The parts were then clamped together for 1 to 2 h. The old adhesive bonded well in the laboratory but failed repeatedly when used in a production environment. Many times, the entire length of the rubber fell off and had to be rebonded.

The cyanoacrylate adhesive, in contrast, is a one-part material that can be applied in a single coat to aluminum that has been treated previously with an epoxy primer and a top coat. The parts can be mated as soon as the adhesive has been applied; no drying is necessary. The adhesive sets in 5 min. Optionally, an accelerator can be brushed onto the aluminum to reduce the setting time to 30 s. Clamping the parts together then becomes unnecessary.

Specimens of rubber bonded to aluminum with the new adhesive were tested for strength after exposure to room temperature, high temperature and high humidity, subzero temperature, methyl ethyl ketone vapor, and water. Peel-test specimens failed in the rubber, showing that the bond was stronger than the rubber itself was. In lap shear tests, specimens failed in the primer, showing that the bond was also stronger than the primer and top coat were.

The adhesive comes in four formulations, all based on ethyl cyanoacrylate with various amounts of ethylene copolymer rubber, poly(methyl methacrylate), silicon dioxide, hydroquinone, and phthalic anhydride:

- Type I — toughened, medium viscosity, black;
- Type II — toughened, low to medium viscosity, black;
- Type III — toughened, low viscosity, white; and
- Type IV — toughened, high viscosity, clear to slightly cloudy.

This work was done by Dawn A. Comer, Howard Novak, and Mark Vazquez of United Technologies for **Marshall Space Flight Center**. *For further information, Circle 136 on the TSP Request Card.*

Inquiries concerning rights for the commercial use of this invention should be addressed to the Patent Counsel, Marshall Space Flight Center [see page 18]. Refer to MFS-28434.

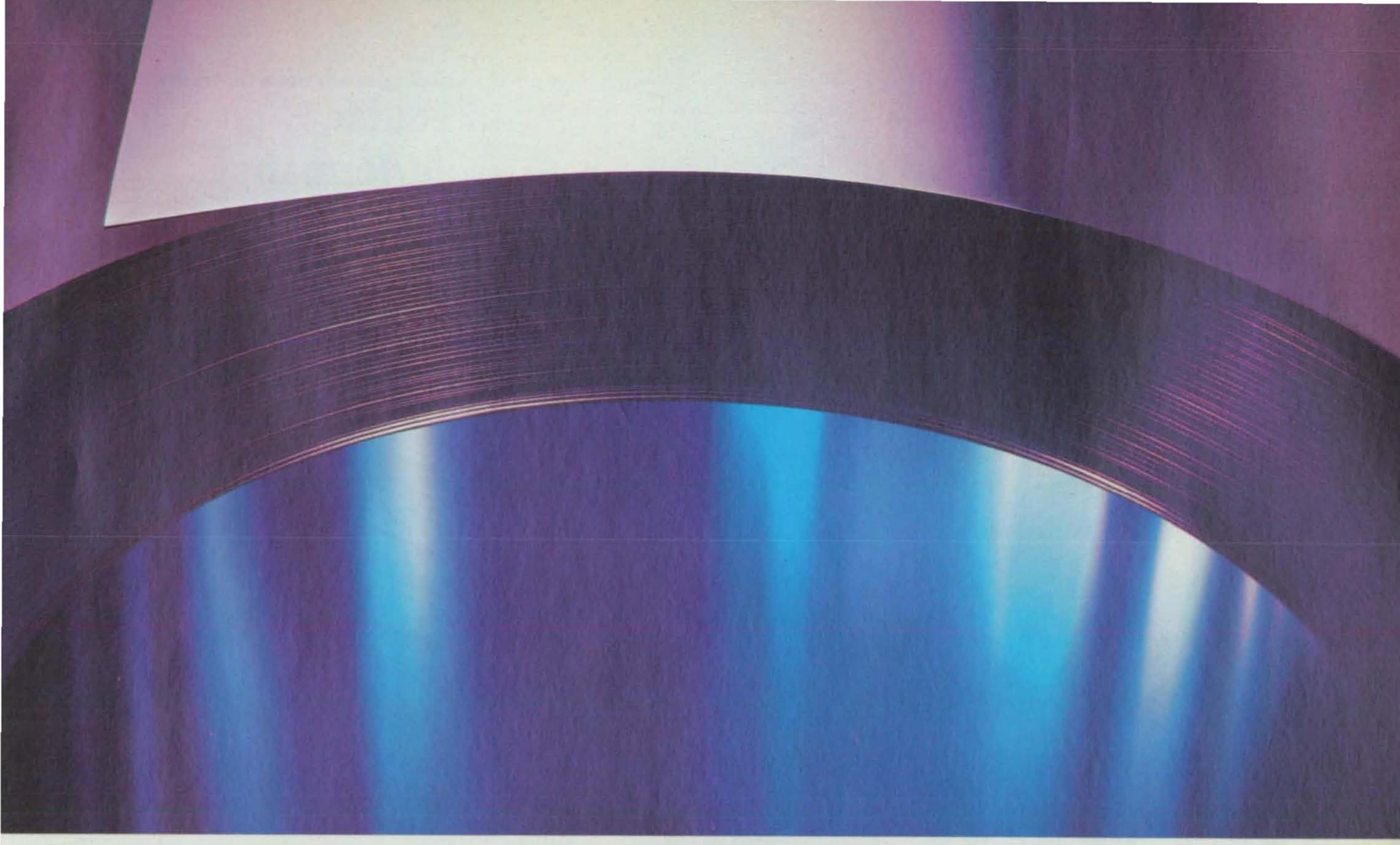

MORE HIGH-PERFORMANCE ALLOYS IN MORE FORMS. BECAUSE YOU KEEP FINDING MORE JOBS FOR THEM.

At Inco Alloys International, you'll find the world's widest selection of high-nickel alloys in the widest range of forms and sizes. Rod, bar, plate, sheet, strip, section, pipe, tubing, wire, and companion welding products. All from one full-line manufacturer, all available through a worldwide network of sales offices and distributor warehouses.

As the pioneers of nickel alloy technology, our scientists invented the alloys whose trademarks are synonymous with quality and performance —MONEL, INCONEL, INCOLOY, INCO, NIMONIC, BRIGHTRAY, and NILO.

These alloys offer superior corrosion resistance, high-temperature strength and other special properties for your most demanding applications, prolonging equipment life and preventing costly repair, replacement and downtime.

A single source for the properties and performance you need, in the forms you need, with the quality assurance and traceability you need, delivered where and when you need them. Inco Alloys International is the only name you need to know.

Write for a free copy of our "Quick Reference Guide." Inco Alloys International, Inc., Huntington, West Virginia 25720. Or, for a quicker reply, FAX us at (304) 526-5441.

MONEL, INCONEL, INCOLOY, INCO, NIMONIC, BRIGHTRAY and NILO are trademarks of the Inco family of companies.

INCO ALLOYS INTERNATIONAL

Circle Reader Action No. 569

Inco Alloys International distributors in the USA: *Castle Metals, Metal Goods, Tubesales, and Williams & Co.* In Canada: *Atlas Alloys and Drummond McCall Inc.*

Tough, High-Performance, Thermoplastic Addition Polymers

A series of addition-type thermoplastics exhibit useful properties.

Langley Research Center, Hampton, Virginia

The development of such toughened high-performance thermosetting polymers as toughened epoxies, bismaleimides (BMI's), PMR polyimides, and acetylene-terminated resins dominates the present approach to the preparation of new polymer composites. Of several possible toughening methods, the synthesis of addition-type thermoplastics (ATT's) is considered to be a very attractive approach.

An ATT is a polymer that has an addition-curing reaction that leads to a linear molecular structure. It is nonclassical in that it has similarities to two major classical categories: thermosets (addition curing with crosslinked structures) and thermoplastics (condensation-reaction curing with linear structures). Because of their addition curing and linear structure, ATT polymers can have toughness, like thermoplastics, and can be easily processed, like thermosets. Work was therefore undertaken to develop a chemical reaction that forms stable aromatic rings in the backbone of an ATT polymer, thereby combining high-temperature performance and thermo-oxidative stability with toughness and easy processibility, and minimizing or eliminating the necessity for the tradeoffs among properties often observed in conventional polymer syntheses.

Tough, high-performance polyimides were made by reacting triple bonds conjugated with an aromatic ring in bisethynyl compounds with the active double bonds in compounds that contained double bonds activated toward the formation of Diels–Alder type adducts, especially bismaleimides, biscitraconimides, benzoquinones, and mixtures thereof. (Addition curing of these products produced highly linear polymeric structures, and heat treatment of the highly linear polymeric structures produced thermally stable aromatic addition-type thermoplastic polyimides.)

By varying the types and ratios of the reagents, an entire series of thermoplastic polyimides and composites (see table) were produced.

A variety of tests and comparisons were conducted, using the new resins and composites made with them. Single lap-shear bond specimens were prepared and tested, using titanium adherends. LaRC-RP80, for example, showed significantly higher adhesive properties than did state-of-the-art bismaleimides. It was found to be significantly tougher than the constituent polymers are, and it ranked highest in toughness among those bismaleimides that have comparable glass-transition temperatures. The neat LaRC-RP80 resin loses only 5 percent of its weight at a temperature of 514 °C, representing the highest thermo-oxidative stability of bismaleimides observed to date. LaRC-RP80 also exhibited outstanding resistance to moisture. Typical bismaleimides have equilibrium moisture absorptions that range from 4 to 6 percent. A value of 2.6 percent was obtained for LaRC-RP80.

Composite	Glass-Transition Temperature, °C		Uptake of Moisture at 25 °C for 2 Weeks, Weight Percent	Thermo-oxidative Stability	
	Dry	Wet		(Isothermal) Percent Loss of Weight after 500 Hours at 232 °C in Air	Temperature, °C, at 5 Percent Loss of Weight in Air by Thermogravimetric Analysis
AS-4/LaRC-RP80	282	258	0.6	0	540
AS-4/LaRC-RP83	275	266	0.5	0	520
AS-4/LaRC-RP57	312	280	0.8	0	560
AS-4/LaRC-RP56	275	272	0.5	0	500
AS-4/LaRC-RP98	287	285	0.9	0	536
AS-4/LaRC-RP99	285	259	0.4	0.5	514
AS-4/LaRC-RP101	310	289	0.9	0.2	585
AS-4/LaRC-RP100	305	190	2.6	0.4	500

Selected Graphite-Fiber/Polymer Composites show desirable combinations of properties.

Prepregs were prepared by winding AS-4 unsized graphite yarn on a drum, then brushing on the resin. The quantity of the resin solution was calculated to yield finished composites containing 60 volume percent fiber. Ten composites were made by this procedure, using various resins. The table gives the properties of the composites. These resins are expected to find utility in a wide variety of aerospace and industrial applications, including the preparation of molding compounds, adhesive compositions, and polymer-matrix composites.

This work was done by Ruth H. Pater, K. Mason Proctor, and John Gleason of **Langley Research Center**, *Cassandra Morgan of PRC-Kentron, and Richard Partos of Analytical Services and Materials, Inc. For further information, Circle 67 on the TSP Request Card.*

This invention is owned by NASA, and a patent application has been filed. Inquiries concerning nonexclusive or exclusive license for its commercial development should be addressed to the Patent Counsel, Langley Research Center [see page 18]. Refer to LAR-10000.

Polyamide-Imides Made From BTDA

Mechanical properties are better than those of the LARC-TPI polyimide.

Langley Research Center, Hampton, Virginia

A new synthesis results in an improved class of tough, thermally stable polyimides containing amide linkages. The new polyamide-imides are potentially useful as matrix resins in graphite-reinforced structures, and as fibers or coating films that can withstand high temperatures.

The synthesis of a polyamide-imide of the new type (see figure) begins with the reaction of isomers of diaminobenzanilide (DABA) with 3,3',4,4'-benzophenonetetracarboxylic dianhydride (BTDA). The resulting polyamide-acid is then thermally converted to the polyamide-imide. In experiments, the initial reactions were carried out in a closed vessel at room temperature at 15 to 20 percent solids content in N,N-dimethyl acetamide (DMAc). The solutions were stirred for about 4 hours after all the BTDA had dissolved in the DMAc. The polyamide-acid solutions were stored in a refrigerator until thermal conversion to the final polymers. For comparison, the polyimide LARC-TPI was synthesized by the same procedure from 3,3',4,4'-BTDA and 3,3'-diaminobenzophenone. (LARC-TPI was chosen as a standard of comparison because it has a similar molecular structure and is already well known.)

Film specimens of the experimental polyamide-acids were cast from solution. Other specimens were prepared as powders, which were then molded and cut into specimens for tension and fracture-toughness tests. The film and molding specimens were heated to convert them to the final polyamide-imides. Chemical, thermal, and mechanical properties of the specimens were then measured.

The new polymers were found to have high glass-transition temperatures, high thermal and oxidative stability, and high resistance to organic solvents (other than DMAc) and water. Polymers based on unsubstituted amide diamines were also observed to exhibit high inherent viscosities, and were easily made into tough, flexible films. However, films of N-methyl substituted amide-imides were brittle, and one of them even exhibited signs of solubility.

Overall, the thermomechanical properties of the experimental polyamide-imides were similar or superior to those of LARC-TPI. A notable exception was the one synthesized from 4,4'-DABA/BTDA, which exhibited a very high tensile modulus and evidence of being semicrystalline.

This work was done by James F. Dezern of **Langley Research Center**. *For further information, Circle 59 on the TSP Request Card. LAR-13942*

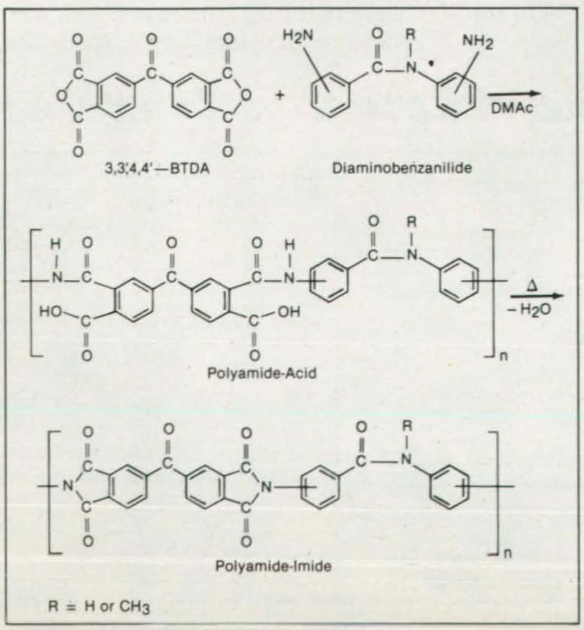

Linear, Aromatic Polyimide/Amides are synthesized from isomers of DABA with 3,3',4,4'-BTDA. The new polymers have thermal and mechanical properties similar to those of the more familiar polyimide LARC-TPI, which has a similiar molecular structure, except that it does not have the amide linkages.

Computer Programs

COSMIC: Transferring NASA Software

COSMIC, NASA's Computer Software Management and Information Center, distributes software developed with NASA funding to industry, other government agencies and academia.

COSMIC's inventory is updated regularly; new programs are reported in *Tech Briefs*. For additional information on any of the programs described here, circle the appropriate TSP number.

If you don't find a program in this issue that meets your needs, call COSMIC directly for a free review of programs in your area of interest. You can also purchase the annual *COSMIC Software Catalog*, containing descriptions and ordering information for available software.

COSMIC is part of NASA's Technology Utilization Network

COSMIC® — *John A. Gibson, Director,*
(404) 542-3265
The University of Georgia, 382 East Broad Street, Athens, Georgia 30602

Computer Programs

These programs may be obtained at a very reasonable cost from COSMIC, a facility sponsored by NASA to make computer programs available to the public. For information on program price, size, and availability, circle the reference number on the TSP and COSMIC Request Card in this issue.

Mathematics and Information Sciences

Surface-Shading Program

Wire-frame, shaded, and function-mapped parts can be created interactively.

The Surface Shading computer program, SURF, was developed in support of the work of Computational Fluid Dynamics (CFD) scientists at NASA Ames Research Center. SURF is part of the CFD graphics software. SURF accepts input in the form of grid and solution files that would otherwise normally be fed to Ames Research Center's version of the PLOT3D software from "flow solver" programs. SURF interactively creates wire-frame, shaded, and function-map parts that can be viewed and then transferred to Ames Research Graphic (ARCGRAPH) standard files, which can be animated with GAS (COSMIC Program ARC-12379).

Such "flow solver" programs as INS3D (COSMIC Program ARC-11794) solve the equations of higher order that govern the characteristics of flight according to the "grid" specifications of the test geometry (e.g., forward swept wing model with surrounding airspace) and simulation conditions (e.g., angle of attack, mach number, and Reynolds number). The numerical solution data thus generated are collected and converted to graphical images of flows, pressure distributions, shock waves, and particle traces via the Ames PLOT3D graphics package.

Although not meant as a substitute for Ames PLOT3D, SURF accepts the PLOT3D input files and provides interactive, mouse-driven manipulation of the resulting graphical images. The mouse-driven menu interface in SURF enables the user to create models that consist of mixtures of different types of parts (including gouraud and smoothly shaded function-mapped parts) that can be interactively viewed, deleted, or put out to ARCGRAPH files.

The color and the specular highlights of gouraud-shaded parts can be adjusted interactively. Shaded parts are created based on sources of light, points of view, and levels of ambient light specified by the user. In addition, the color spectra of function-mapped parts can be adjusted interactively. Legends can be created to show correlations of color and normalized values of functions (i.e., pressure, density, temperature, and mach numbers). Function-mapped parts can be "clipped" in such a way that they show only contours within specified ranges of values. Other features of SURF include the ability to work with several grids and solutions, deletion of grids and/or solutions, support of multigrid files, blanking out the pictures at specified grid points, reading of "planes" or "whole" format files, screen-dump input and output of picture-element files, displays of current grid and part-attribute data, and escape to or from a UNIX software shell.

SURF was developed for the Silicon Graphics IRIS 2000/3000-series workstations running UNIX. The workstation should have at least 4 MBytes of memory, 32 bit planes, z-buffering and z-clipping, and floating-point-hardware support. SURF was written in the C programming language and requires the Silicon Graphics "include" files (e.g., stdio.h, gl.h). SURF can be purchased separately or in a package (COSMIC Program COS-10020) also containing GAS and Ames Research Graphics Systems ARCGRAPH (COSMIC program ARC-12350). SURF was developed in 1988.

This program was written by Todd Plessel of Sterling Software for **Ames Research Center**. *For further information, Circle 42 on the TSP Request Card.*
ARC-12381

Ada Namelist Package

This program accommodates different kinds of variables and mismatches between lists.

The Ada Namelist Package, developed for the Ada programming language, enables a calling program to read and write FORTRAN-style namelist files. A namelist file consists of any number of assignment statements in any order. Features of the Ada Namelist Package are as follows: the handling of any combination of types defined by the user; the ability to read vectors, matrices, and slices of vectors and matrices; the handling of mismatches between variables in the namelist file and those in the programmed list of namelist variables; and the ability to avoid searching the entire input file for each variable.

The principal benefits derived by the user from this software are the following: the ability to read and write namelist-readable files, the ability to detect most file errors in the initialization phase, and an organization that keeps the number of instantiated units to a few packages rather than to many subprograms.

The Ada Namelist Package program is organized similarly to the TEXT_IO program. The package itself is nongeneric. The nongeneric opening portion declares a variety of constants accessible to the user, variables, and subprograms for initializing a namelist, reading and writing strings, and diagnosing errors. Following the opening portion are a group of nested generic packages for reading and writing (1) variables of types defined by the user, including integer, floating-point, fixed-point, and enumeration; and (2) arrays including vectors, matrices, and slices of vectors and matrices.

The source code is available as ASCII text files on a 360K, 5.25-in. (13.3-cm) floppy disk written on an IBM/AT personal computer running under PC DOS, v. 3.1. The size of the largest file is 91,551 bytes. The software was developed using VAX Ada, v. 1.5 under DEC VMS, v. 4.5. It should be portable to any validated Ada compiler, and it should be executable either interactively or in batch. The software was developed in 1989.

This program was written by Allan R. Klumpp of Caltech for **NASA's Jet Propulsion Laboratory**. *For further information, Circle 141 on the TSP Request Card.*
NPO-17984

Mechanics

Calculation of Aeroelastic Transients Using Euler Equations

Conforming grids facilitate calculations of flows about changing shapes.

Ames Research Center, Moffett Field, California

A method for the calculation of transient aeroelastic effects on airplane wings is based on the Euler equations of flow. Aeroelasticity plays an increasingly important role in the design of modern aircraft, which tend to be flexible for high maneuverability. Because wind-tunnel experiments in aeroelasticity are much more expensive than are experiments that involve only flows about rigid models, the advancement of the capability to compute aeroelastic effects can reduce considerably the cost of developing an aircraft.

In establishing the mathematical foundation for the new method, the Euler equations of flow are formulated in strong-conservation-law form to provide for the numerical capturing of shocks. To enhance numerical accuracy and handle boundary conditions more easily, the Euler equations are transformed to general curvilinear coordinates. The governing equations of aeroelastic motion of a flexible wing are obtained via the Rayleigh-Ritz method, in which the aeroelastic displacements are approximated by a finite set of assumed modes. The contribution of each mode to the total motion is derived by Lagrange's equation. Furthermore, it is assumed that the deformation of the continuous wing structure can be represented by deflections at a set of discrete points. This assumption facilitates the use of discrete structural data, such as the modal stiffness matrix and the modal mass matrix. These data can be generated by a finite-element analysis or from experimental influence-coefficient measurements.

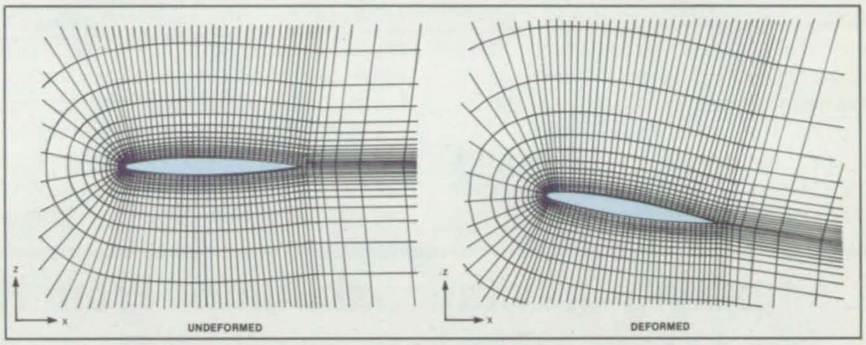

The **Computational Grid** changes to conform to the surface of the wing as the wing deforms in a pitching motion, as shown in this cross section viewed along a wing.

The procedure for the solution of the equations of flow is based on the implicit diagonal algorithm, which in turn is based on a finite-difference scheme suitable for time-accurate computations on dynamic grids. The coupled flow and modal structural equations of motion are solved by use of a simultaneous-integration technique based on the linear-acceleration technique. Dynamic grids that adapt to the deforming shapes of the wing (see figure) are generated by an algebraic grid-generation scheme.

The method was used to predict the unsteady flows about a semi-infinite rectangular wing oscillating in a pitching mode and about a wall-mounted cantilever rectangular wing oscillating in the first bending mode. Aeroelastic responses were computed by use of modal data generated by the finite-element method. The predictions agreed well with experimental data.

This work was done by Guru P. Guruswamy for **Ames Research Center**. *Further information may be found in AIAA paper A88-33775, "Time-Accurate Unsteady Aerodynamic and Aeroelastic Calculations of Wings Using Euler Equations."*

Copies may be purchased [prepayment required] from AIAA Technical Information Services Library, 555 West 57th Street, New York, New York 10019, Telephone No. (212) 247-6500.

ARC-12351

Estimating Liquid and Gas Contents in a Tank

Quantities would be inferred from temperatures and pressure changes.

Lyndon B. Johnson Space Center, Houston, Texas

A general approach to the estimation of the amounts of liquid and gas in a tank is based on measurements of pressure perturbations and temperatures and the use of the thermodynamic relationships among pressures, temperatures, and volumes. Although this approach is approximate and indirect, it is advantageous where such direct and precise methods as the observation of a stationary liquid/gas interface in a gravitational field cannot be used. The thermodynamic approach can be used in the presence or absence of gravitation or acceleration, and regardless of the numbers, shapes, and movements of liquid/gas interfaces in the tank. It could also be useful where the liquid may be stationary but too hazardous to permit direct observation.

Usually, the quantity that one seeks to determine is the volume of liquid in the tank. In this approach, one determines the volume of gas, then subtracts it from the known total volume of the tank to obtain the volume of liquid. To measure the volume of gas, one induces perturbations ΔV in the total volume V, thereby inducing perturbations ΔP in the total pressure P. Then the volume of gas can be computed from

$$V_{gas} = -nP\Delta V/\Delta P$$

where n depends on the amount of heat transferred between the gas and its surroundings during the compression and expansion phases of ΔP and ΔV. The value of n can range from a low of 1 (as in isothermal compression and expansion) at small ΔV to a high equal to the ratio of specific heats of the gas (as in adiabatic compression and expansion — a typical high value of 1.2 to 1.6).

The volume displacement or perturbation ΔV and its rate must be large enough to yield useful ΔP readings in the face of environmental effects, but not so large that the readings are degraded by acoustical noise and limitations of the sensors. A practical choice would lie between these extremes and would result in a value of n between the isothermal and adiabatic extremes. The relationships among ΔP, ΔV, and V_{gas} could be determined theoretically, by calibration measurements on known volumes of liquid and gas, or both.

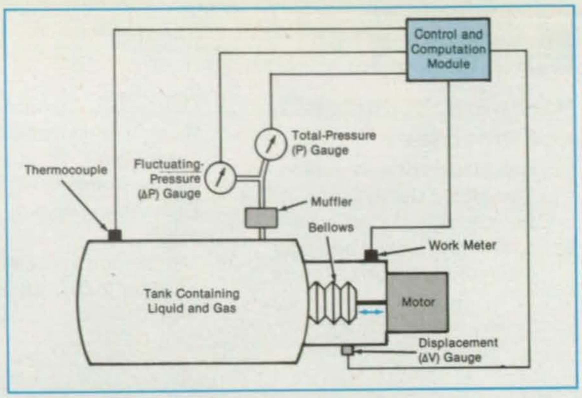

The **Bellows Would Be Alternately Compressed and Expanded** to make the volume of the tank fluctuate. The corresponding fluctuations in pressure would be measured and used to determine the volume of gas and liquid in the tank.

The general method can be implemented in a variety of ways, depending on the type of liquid and the conditions of operation and design of the tank system. For example, as shown in the figure, the volume perturbations could be produced by a small bellows alternately compressed and expanded by a motor. The displacement would be $\lesssim$ 1/1000 of the total volume of the tank. The frequency of displacement could be several cycles per second, but could range several orders of magnitude above or below this value, depending on the type and sophistication of the instruments in the system.

This work was done by Richard T. Walter of **Johnson Space Center** *and Paul Van Buskirk, William Weber, and Richard Froebel of Lockheed Engineering and Sciences Co. For further information, Circle 116 on the TSP Request Card.*

This invention is owned by NASA, and a patent application has been filed. Inquiries concerning nonexclusive or exclusive license for its commercial development should be addressed to the Patent Counsel, Johnson Space Center [see page 18]. Refer to MSC-21500.

Computing Gravitational Bumps From Repeating-Orbit Data

An iterative algorithm exploits sparse-matrix techniques.

NASA's Jet Propulsion Laboratory, Pasadena, California

An iterative, least-squares algorithm efficiently computes estimates of both position errors indicative of the irregularities in the gravitational field of the Earth and the trajectory of a satellite in an orbit that repeats along the same ground track. Such estimates are useful in surveying, navigation, and geophysical research. The algorithm is particularly useful for processing data on the trajectory of a satellite in a low orbit that is tracked via the Global Positioning System (GPS).

The method is based on the repeat orbit technique in which the position of a low Earth orbiter as a function of time is described as the sum of two parts: the first part being an adjustment to the epoch state mapped to current time, the second part being a correction to the position to account for gravity mismodeling. Let $r(t)$ be the adjustment to the current position; we have

$$r(t) = \frac{\partial r}{\partial r_0} r_0 + \frac{\partial r}{\partial v_0} v_0 + \delta(t)$$

where r_0 is the adjustment to the epoch position, v_0 is the adjustment to the epoch velocity, and $\delta(t)$ is the term representing the gravity perturbation. At discrete measurement times, this correction will be called the "Gravity Bin" parameters. The epoch time is using the nominal force model.

The algorithm is intended for use in calculating the gravity-bin parameters from measurements of the positions of a satellite along multiple long arcs (typically, representing time spans of 10 days) that are divided into subarcs. The algorithm exploits the sparse block structure of the measurement matrix (see figure). First, it sets the gravity-bin parameters equal to zero and estimates such arc-dependent parameters as those of the epoch states. This is done arc by arc and typically involves the estimation of a few hundred parameters. The solution is then subtracted from the observed values to get a new set of measurement residuals. The residuals from multiple arcs are combined, and the gravity-bin parameters are estimated. In this step, the arc-dependent parameters are fixed. The number of parameters estimated at one time is typically a few hundred, assuming that the long arc is partitioned into subarcs of time spans of about 2 h.

Once the gravity-bin parameters are estimated, they are subtracted from the measurement residuals. Then the steps are iterated by fixing the gravity-bin parameters and reestimating the arc-dependent parameters, subtracting the solution from the

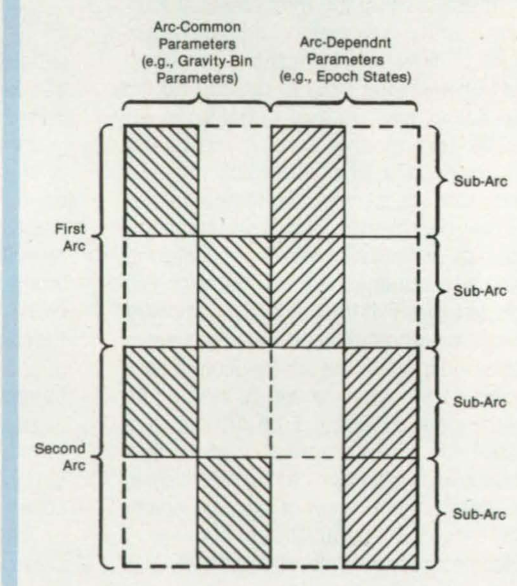

The **Measurement Matrix** for multiple long arcs divided into subarcs has a block structure. For clarity, only two arcs of two subarcs each are shown here. The general case involves arcs ranging in number from 10 to 100. The number of subarcs in each arc ranges from 10 to 127. The matrix is, therefore, very sparse. With proper care, an algorithm can take advantage of this sparseness to reduce the amount of calculation.

residual, fixing the arc-dependent parameters and reestimating the gravity-bin parameters, and subtracting the solution from the residual. This completes the second round of computations. The iteration is repeated until convergence is achieved. At that time, the residuals consist mostly of data noise and any systematic errors not represented in the mathematical model.

This work was done by Jiun-tsong Wu, Sien-Chong Wu, and William I. Bertiger of Caltech for **NASA's Jet Propulsion Laboratory**. *For further information, Circle 26 on the TSP Request Card.*
NPO-17925

Jig for Compression-Relaxation Tests of Plastics

Specimens can be tested in immersion or otherwise manipulated away from the compression tester.

Lyndon B. Johnson Space Center, Houston, Texas

An improved jig facilitates tests of the long-term compression-relaxation properties of plastics. Such tests are useful in quantifying some of the time-dependent properties of polymers, in investigations of the effects of aging, and in ascertaining the service lifetimes of polymeric components.

The jig is designed to accommodate the high moduli of elasticity of some plastics; it is intended in part to replace prior equipment that is unusable because it was designed for testing rubbers, which have low moduli of elasticity. Unlike other equipment designed for long-term tests of plastics, the jig can be removed from a compression-testing machine during a test and immersed in a test fluid. This feature is particularly desirable in testing a polymer that is to be made into compression seals in contact with the fluid. The load on the specimen can be measured at intervals by removing the jig from the fluid, placing it in the compression-testing machine, and obtaining a force-versus-time trace.

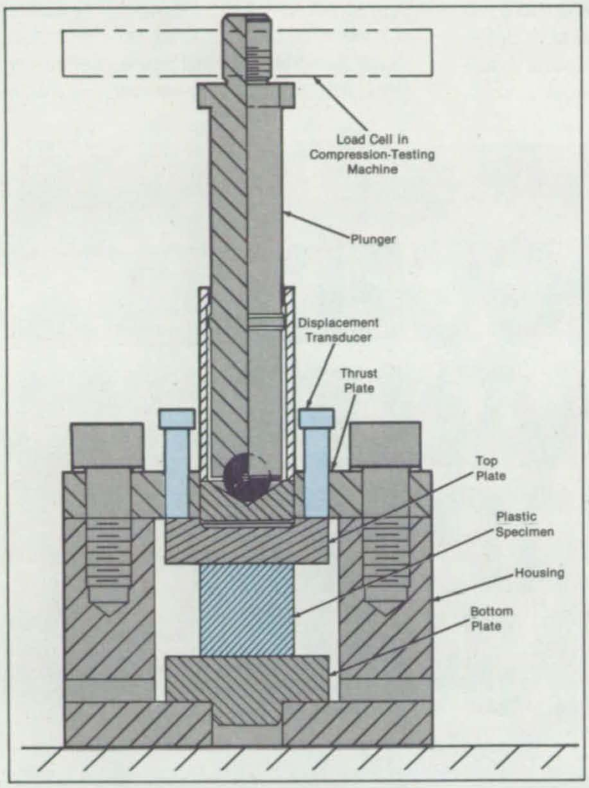

The **Compression-Relaxation-Testing Jig** holds the specimen in compression when it is removed from the compression-testing machine, yet allows the compression force on the specimen to be measured when it is on the machine.

The procedure for use of the jig is the following:

1. Choose the dimensions of the unclamped, uncompressed specimen in conjunction with those of the jig and the top and bottom plates in it (see figure) so that when the specimen is subsequently fully clamped in the jig, with the thrust plate resting on the housing, the specimen will be compressed to the desired degree.
2. Cut the specimen to the chosen length, and place it in the jig between the top and bottom plates, without compressing or clamping.
3. Install the removable linear variable-differential displacement transducers, and place the jig in the compression-testing machine, with the plunger mounted in place to compress the specimen.
4. Set the compression-testing machine to compress the specimen at a rate of about 1 mm per minute, and activate the machine, taking a force-versus-time trace.
5. As soon as the thrust plate comes to rest on the housing and the displacement transducers indicate that the top plate is beginning to separate downward from the thrust plate, stop the compression-testing machine at that position, measure the compression force, and install the bolts that clamp the thrust plate on the housing. The clamped thrust plate will maintain the compression force on the specimen after the machine is backed off.
6. Remove the jig from the compression-testing machine, remove the displacement transducers from the jig, and immerse the jig in the test fluid (if any) during the specified testing time.
7. To monitor the relaxation of force as a function of time during the test, remove the jig from the fluid at intervals, place it in the machine (keeping the specimen clamped), and compress while taking a force-versus-time trace as before. This time, there should be a "knee" in the force-versus-time curve at the point where the specimen starts to be compressed farther and the top plate separates from the thrust plate measured by the pressure transducers. When the knee and separation are reached, stop the machine at this position, measure the force, then remove the jig as before and put it back into the fluid, to remain there until the next measurement. Typically, the relaxed compression force, measured at a given interval is reported as the ratio between that measurement and either the initial measurement or else the measurement at a reference time of, say, one-half hour.

Because the displacement transducers are removed before immersion, this testing technique can be used with electrically conductive as well as nonconductive test fluids. In that the jig does not have to remain in the compression-testing machine throughout the test, this testing technique differs from a standard technique of the American Society for Testing and Materials. This feature offers two advantages in addition to those already mentioned: one is that it is possible to recalibrate the load cell in the compression-testing machine during long tests; the other is that by use of multiple jigs, one can perform simultaneous long-term compression-relaxation tests on multiple specimens with a single compression-testing machine.

This work was done by Richard M. Shelley, James A. Daniel, and Ralph M. Tapphorn of Lockheed Engineering & Sciences for **Johnson Space Center**. *No further documentation is available.*
MSC-21674

Calculating Transient Vibrations of Coupled Substructures

Equations of motion of each substructure are solved independently.

Marshall Space Flight Center, Alabama

A finite-element, numerical-integration method for estimating the transient vibrational response of a structure composed of coupled substructures entails less computation than has been needed in previous methods. The method is applicable to any number and configuration of linearly responding substructures and to both determinate and indeterminate boundary conditions at interfaces between substructures. With little or no additional difficulty, the method is also applicable to changing interface boundary conditions.

In a typical vibrational-response problem, a structure can have several thousand degrees of freedom, and it is impractical to solve the thousands of equations of motion by direct numerical integration. Heretofore, the standard procedure to overcome this obstacle has involved the following procedure: First, one computes the vibrational modes and frequencies of the entire structure by solving an eigenvalue problem (this is still a major problem). The modes are then used to transform from the original discrete physical coordinates to new modal coordinates. Next, in an approximation, the number of equations is reduced by truncating the modal coordinates of higher frequency without significantly reducing the accuracy of the results. One can then make a transformation to a set of uncoupled equations that can be solved easily on present computers.

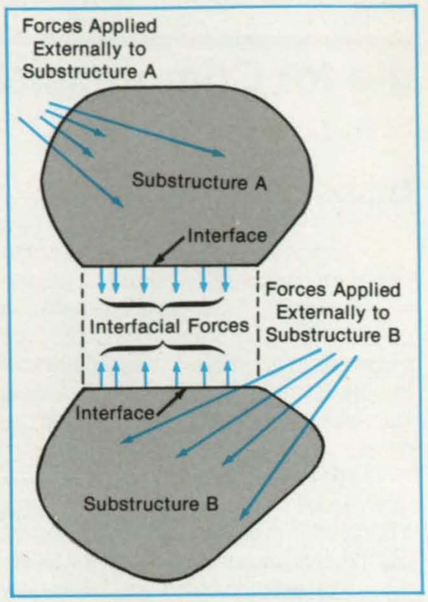

The **Responses of Substructures** to external forces and to the forces of interaction between substructures are computed in the present vibration-analysis method. In previous methods, the response of the entire structure (requiring many more equations) was computed.

In the present method, one does not attempt to solve the complete set of coupled equations for the entire structure. Instead, among other things, one solves the equations of motion for each substructure independently. The interface forces between the substructures are approximated by third-order power series in time. At each time step of the numerical integration, the solution to the equations of motion of each substructure is calculated with all externally applied forces, including the interface forces (see figure), which involve the initially unknown coefficients of the third-order power series in time. These coefficients are evaluated at the end of each time step by enforcing the compatibility of displacements, velocities, and accelerations at the interfaces; this can be done by simple matrix multiplication and is easily accomplished on a computer. Once the coefficients are known, the interface forces and the vibrational response at the end of each time step can be computed.

The procedure is repeated for as many time steps as necessary to span the time of interest. The method is approximate in that interfacial compatibility is enforced only at the ends of the time steps rather than continuously. Therefore, as in most numerical-integration methods, smaller time steps yield more-accurate results.

Because the interfacial compatibility is maintained by use of an interface-compatibility-coefficient matrix, the method is especially suited for use where interface boundary conditions change with time: the matrix is simply changed or regenerated to reflect changes in the boundary conditions between substructures or a change in the size of the time step. Conversely, when no such change is required, there is no need to recompute this matrix. One example of changing boundary conditions is provided by slip/stick motion caused by friction at an interface between substructures. In this case, one would have to monitor the interface forces to determine whether the interface is slipping or sticking and modify the interface-compatibility-coefficient matrix to reflect the new conditions whenever one detected a transition between sticking and slipping.

This work was done by J. R. Admire and J. A. Brunty of **Marshall Space Flight Center.** *Further information may be found in NASA TP-2926 [N90-13444], "A Transient Response Method for Linear Coupled Substructures."*

Copies may be purchased [prepayment required] from the National Technical Information Service, Springfield, Virginia 22161, Telephone No. (703) 487-4650. Rush orders may be placed for an extra fee by calling (800) 336-4700.
MFS-28477

Calculating Flow Through a Helicopter Rotor

The calculated flow is fully coupled with deformations of the rotor blades.

Ames Research Center, Moffett Field, California

A new method for calculating the flow of air through and around a helicopter rotor is incorporated into the General Rotorcraft Aeromechanical Stability Program (GRASP) (a computer program for aeroelastic analysis). The flow induced by the rotor has an important effect on the aeroelastic properties of the helicopter. Because of the combined finite-element/multibody methodology used as the basis for GRASP and because of the need to preserve its modeling flexibility and generality, it was necessary to depart from traditional methods of computing the induced velocity and to develop the new method.

The rotor is treated as an actuator disk, and the flow field as a cylindrical region surrounding the disk (see figure). The axisymmetric flow field in hover or purely vertical ascent or descent is represented by an airmass element. The generalized coordinates of the inflow associated with this element are included in the state vectors of the steady-state and dynamical mathematical models. This means that the steady-state inflow velocity field is calculated in parallel with the deformations of the structure and that this velocity field is fully coupled to the deformed state of the rotor blades. The generalized coordinates of the inflow are introduced into the model in a manner similar to that used to introduce the degrees of freedom of the structure. That is, an air node is introduced to represent the flow field at a point on the axis of symmetry of the flow field.

A rotor blade is represented by an aeroelastic beam element — the primary structural element in GRASP. The calculations of the momentum contributions from the actuator disk are separated from those for the blade element. The airmass element represents only the aerodynamics of the flow field, while the aerodynamics of the blade element are isolated in the aeroelastic beam element. The aerodynamic forces exerted by the flow field on the rotor

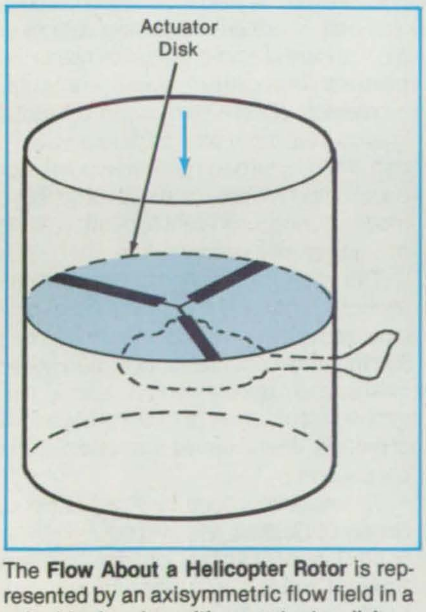

The **Flow About a Helicopter Rotor** is represented by an axisymmetric flow field in a cylindrical region with an actuator disk as the source of the flow.

are calculated for individual subelements within the aeroelastic beam element.

This work was done by Donald L. Kunz of **Ames Research Center** *and Dewey H. Hodges of Georgia Institute of Technology. Further information may be found in NASA TM-100026 [N88-10777], "Analytical Modeling of Helicopter Static and Dynamic Induced Velocity in GRASP."*

Copies may be purchased [prepayment required] from the National Technical Information Service, Springfield, Virginia 22161, Telephone No. (703) 487-4650. Rush orders may be placed for an extra fee by calling (800) 336-4700. *ARC-12202*

Jacobi-Integral Method for Two-Body Problem

Trajectories can be computed more precisely, in fewer steps.

Lyndon B. Johnson Space Center, Houston, Texas

The Jacobi-integral method enables the efficient, accurate computation of the trajectory of a natural satellite or spacecraft perturbed by a component of gravitational potential that depends explicitly on both position and time. In this method, the equations of motion are reformulated to reflect the fact that the total energy is no longer a constant of motion (as it is in prior formulations in which the gravitational potential does not depend explicitly on time).

Instead of the total energy, the Jacobi integral, which is an energylike constant of the motion in this case, is embedded in the Newtonian differential equations of motion. The resulting simplification of the equations makes it possible to compute trajectories more precisely, with fewer numerical steps. With modifications, the Jacobi-integral approach might also be applicable to such terrestrial problems as the motions of rotors and of beams of electrically charged particles in changing electrical and magnetic fields.

Following the path taken in previous research on this topic, the derivation of the modified equations of motion begins with the introduction of the fictitious time variable, s, via the equation

$$\frac{dt}{ds} = t' = r$$

where t = time and r = the radius from the planet (or other source of gravitational potential) to the other object in motion. The substitution of s for t in the basic equations of motion removes singularities. The equations of motion are then linearized to a perturbed-harmonic-oscillator form in which the Laplace vector and the Keplerian energy element are embedded.

The Jacobi integral can be shown, in one example, to yield the Jacobi constant, $J = \boldsymbol{\omega}\mathbf{c}h$, where $\boldsymbol{\omega}$ is the angular velocity of a nonspherical planet that gives rise to the perturbing potential, $\mathbf{c}$ is the angular momentum of the system, and h is the total energy (Keplerian plus perturbing potential). The perturbed-harmonic-oscillator equations of motion are modified so that a modified Jacobi constant appears in place of the Keplerian energy element.

The price for the incorporation of the Jacobi constant is the introduction of a new element — the axial element — and its differential equations. Fortunately, the axial element appears only as a small perturbation term in the differential equations of motion. This facilitates a precise numerical solution.

This work was done by Victor R. Bond, Robert G. Gottlieb, and Michael F. Fraietta of McDonnell Douglas Corp. for **Johnson Space Center**. *For further information, Circle 12 on the TSP Request Card.*
MSC-21623

Higher-Performance Ambient-Temperature Heat Pipe

A porous wick is added to the liquid channel.

Lyndon B. Johnson Space Center, Houston, Texas

The heat pipe shown in the figure is an improved version of the heat pipe described in "High-Performance Ambient-Temperature Heat Pipe" (MFS-26062), *NASA Tech Briefs* Vol. 12, No. 10, page 43. The heat pipe is 3 m long and made of aluminum. It differs from the previous heat pipe in that a lining of sintered aluminum powder has been added to the liquid channel. The new, porous lining results in improved thermal performance.

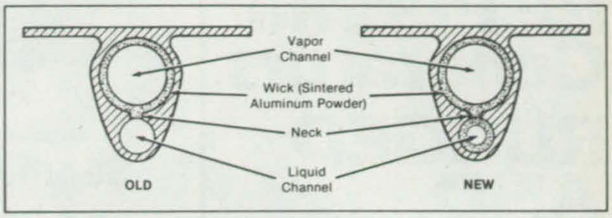

The **New Design** is similar to the previous design except that a porous lining of sintered aluminum has been added to the liquid channel.

This work was done by Donald M. Ernst, Robert M. Shauback and Nelson J. Gernert of Thermacore, Inc., for **Johnson Space Center**. *No further documentation is available.*

In accordance with Public Law 96-517, the contractor has elected to retain title to this invention. Inquiries concerning rights for its commercial use should be addressed to

Nelson J. Gernert
Thermacore, Inc.
780 Eden Road
Lancaster, PA 17601

Refer to MSC-21515, volume and number of this NASA Tech Briefs *issue, and the page number.*

Thermally Actuated Unlatching Mechanism

Differential thermal contraction causes release at a predetermined low temperature.

NASA's Jet Propulsion Laboratory, Pasadena, California

A thermally actuated latch releases a component initially secured to it, when it is cooled to a predetermined temperature lower than the initial temperature. A latch of this type might be used, for example, to retain the cover of a cryogenic aerospace instrument during launch through intermediate cooling. With a nonmoving hook, such a latch might also be used to prevent the door of an industrial furnace from being opened until the furnace cools to a safe temperature.

The latch includes a supporting arm and a spring-loaded hook made of titanium, which has a relatively low coefficient of thermal expansion. It also includes an engaging arm made of epoxy or high-density polyethylene, either of which has a relatively high coefficient of thermal expansion (see figure). As the latch cools, the engaging arm shrinks away from the hook, and the spring drives the hook away from the arm.

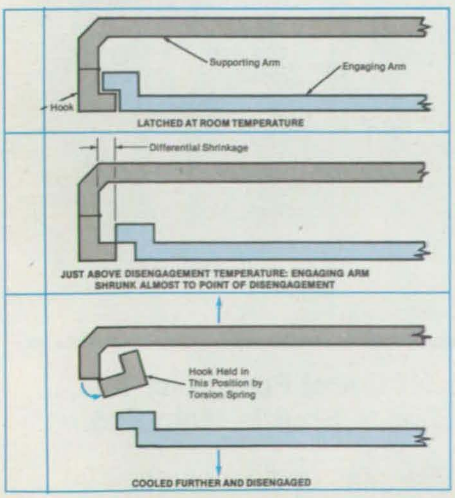

The **Simple Latch** is disengaged by differential thermal contraction of its parts.

The temperature of disengagement depends on the specific design and materials. For the design and materials of the prototype, disengagement occurs when the temperature falls from ambient to −48 °C.

This work was done by Virginia G. Ford of Caltech for **NASA's Jet Propulsion Laboratory**. *For further information, Circle 92 on the TSP Request Card.*
NPO-17601

Machinery

Hardware, Techniques, and Processes

Books and Reports

Segmented Arm for Positioning and Assembly

Control of a large robotic arm relies on conservation of angular momentum.

Lyndon B. Johnson Space Center, Houston, Texas

A proposed segmented robotic arm (see figure) for positioning and assembly of components of large structures would contain motor-and-flywheel angular-momentum devices in each arm segment. These devices would transfer angular momentum to and from the segments of the arm to produce the desired motion of the arm. The arm was conceived for use in outer space, but the concept may also be adaptable to terrestrial uses in which buoyancy cancels the effect of gravitation — for example, floating on or under water.

The application of the torques to particular portions of the arm would be controlled by selectively locking and releasing the rotational joints between the segments. If an angular momentum device in one segment were to fail, the arm could still be used, albeit with some degradation of performance, simply by locking the joint that connects that segment to one of the adjacent segments.

The proposed arm would be about 300 ft (90 m) long and could manipulate components of up to about 1 million pounds (0.5 Gg). The truss structure of each segment would minimize its mass while providing stiffness to support the control and utility systems.

Neglecting friction between the arm and the environment, the total torque about any given joint would be the vector sum of all the individual segment torques. Thus, the more segments there were, the larger would be the effective control torque available at the base of the arm.

The accumulated location errors at the free end of the arm may present a problem. The arm would use position feedback to correct such errors. When the arm is handling a massive object, mechanical oscillations or vibrations could occur if the joints were locked while the load or arm was still moving. Active feedback from sensors that measure local motions would be used to send control signals to the angular-momentum-storage devices to damp any such undesired motions.

This work was done by Reginald B. Berka of **Johnson Space Center**. *For further information, Circle 30 on the TSP Request Card.*
MSC-21512

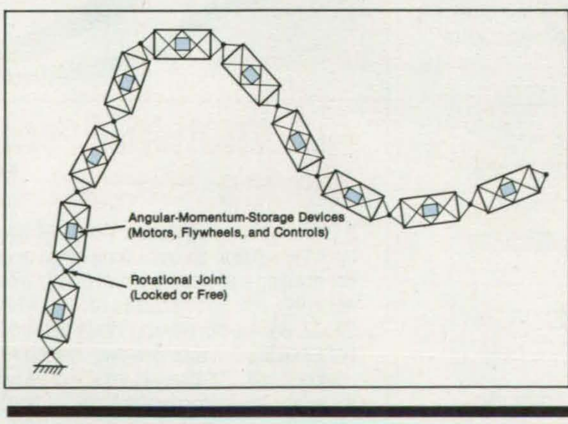

The **Segments of the Robotic Arm** would be moved by transferring angular momentum to and from the segment motors with flywheels.

Books and Reports

These reports, studies, handbooks are available from NASA as Technical Support Packages (TSP's) when a Request Card number is cited; otherwise they are available from the National Technical Information Service.

Jet Boost Pumps for the Space Shuttle Main Engine

Benefits could include increased reliability, simplified ducts, and decreased weight.

A brief report proposes the use of jet boost pumps in conjunction with the main pumps that supply liquid hydrogen and liquid oxygen to the main engine of the Space Shuttle. The present turbine-drive boost pumps are complicated and insufficiently reliable. In contrast, a jet pump is inherently very reliable because the main part of the pump has no moving parts. Moreover, a jet pump can be connected with simpler ducts, and it weighs less.

Jet pumps have been used in a wide variety of applications. In a jet pump, jets of fluid escape through nozzles at high speed from a manifold or plenum at high inlet pressure into a channel filled with the same or a different fluid at a low inlet pressure. Kinetic energy is transferred to the low-pressure flow by mixing, thereby inducing a combined outlet flow at a pressure between the high and low inlet pressures. The principal advantage of this kind of pump is simplicity, and the principal disadvantage is low efficiency.

The report contains several sections. The first section summarizes the principle of operation and previous experience with jet pumps. The next section describes the operation of a representative jet pump, presents some parameters used to describe performance, and discusses the effects of some pump configurations on efficiency.

The next section discusses the increase in temperature of the outlet flow over that of the inlet flow — a manifestation of the efficiency penalty. This causes an increase in the vapor pressure of the outlet fluid, with consequent reduction in the net positive suction head available to the main pump that follows. The increase in temperature is attributed to the kinetic energy lost in the mixing of the two inlet flows, and a conservative design protocol requires the assumption that all mixing losses are converted to heat.

The next section discusses the performance and design of the main pump in connection with the net positive suction head of the flow supplied to it by the jet pump. The last section presents some of the design parameters for the proposed liquid-oxygen and liquid-hydrogen pumps in the Space Shuttle. A comparison with the parameters of the corresponding turbine-drive boost pumps shows that the jet boost pumps should perform better.

This work was done by Sen Y. Meng of Rockwell International Corp. for **Marshall Space Flight Center**. *To obtain a copy of the report, "SSME Jet Pump," Circle 68 on the TSP Request Card.*

Inquiries concerning rights for the commercial use of this invention should be addressed to the Patent Counsel, Marshall Space Flight Center [see page 18]. Refer to MFS-29673.

Fabrication Technology

Hardware, Techniques, and Processes

Coating Solar Cells by Microwave Plasma Deposition

Semiconductor wafers can be processed at temperatures low enough not to harm them.

NASA's Jet Propulsion Laboratory, Pasadena, California

Antireflection films can be deposited on silicon solar cells at high production rates with microwave-enhanced plasma deposition. Microwave energy at a frequency of 2.45 GHz generates a plasma in a mixture of gases, from which a thin film of silicon nitride deposits on silicon substrates. The reaction temperature is relatively low (only 250 °C), and the film deposition rate is more than 500 Å/min — 2 to 5 times faster than in a plasma without microwave enhancement. The quality of the antireflection film is similar to that produced by chemical-vapor deposition.

The deposition is carried out in a quartz chamber (see figure). The neck of the chamber is positioned in a rectangular microwave cavity resonator at a point where the electric field is high. Microwave power is guided by a rectangular waveguide into the cavity. Argon flows into the reactor while silane and ammonia or nitrogen flow over the silicon substrate in the flared portion of the chamber. The application of the microwave field to the argon gas at low pressure forms a high-density excited-state plasma that rapidly dissociates the other gases to form a dense silicon nitride film on the silicon substrate.

The substrate rests on a movable, heated holder. This allows the temperature of the substrate and its position in the chamber to be adjusted for maximum speed and uniformity of deposition. A mechanical pump continuously removes the used reactants from the chamber.

When microwaves rather than the usual 13.56-MHz radio-frequency waves are used to create the plasma, the field in the cavity oscillates so rapidly that the forces on the free electrons change direction before they can travel very far. Therefore, the plasma is not swept to the walls of the reactor. In comparison with lower-frequency plasma systems, the microwave system uses less power and consumes smaller quantities of gas. In addition, the species formed in the plasma are longer lived and can thus dissociate the reactants in a region of the chamber well away from the plasma-generation region. Deposition can thus be done under the most favorable conditions.

This work was done by Behrooz Minaee, Sanjeev R. Chitre, and Narges Zahedi of Superwave Technology Inc., for **NASA's Jet Propulsion Laboratory**. *For further information, Circle 121 on the TSP Request Card.* NPO-17035

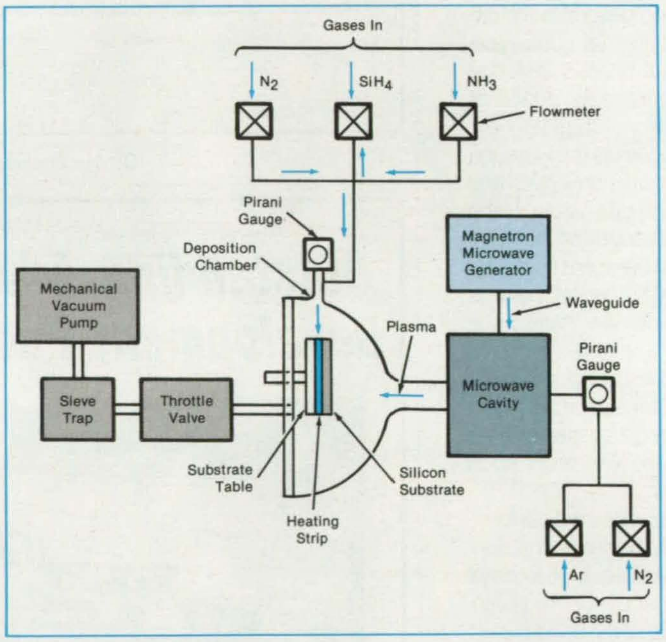

A **Magnetron** produces 2.45-GHz microwaves at a power of 1 kW. Pirani gauges measure the pressure in the deposition chamber while a mechanical vacuum pump removes spent gases. The properties and growth rate of the film depositing on the substrate depend critically on the mix of reactive neutral and ionic species in the plasma. Results are best with a highly activated plasma and moderate bombardment energies.

Making Mullite Fibers by Airgap Wet Spinning

Neither melting nor a dangerous solvent is required.

Marshall Space Flight Center, Alabama

A proposed process would make continuous mullite ($Al_6Si_2O_{13}$) fibers that would retain structural integrity at temperatures up to and somewhat beyond 1,300 °C. Heretofore, mullite fibers have been made by melt spinning (which requires high temperatures) and dry spinning (which requires a dangerous solvent like toluene or benzene).

The proposed process would make highly pure mullite fibers, without melting and without a dangerous solvent. Instead, it would involve airgap wet spinning of an alumina/silica sol/gel mixture. The mixture would be extruded through a single-hole spinneret into a spin bath of deionized water and polyethyleneimine, where it would be converted to gel fiber. Continuing on its way, the gel fiber would be wound onto a package. Later, the gel fiber would be unwound from the spool and fed through a tube furnace, where it would be converted to mullite.

This work was done by Dennis S. Tucker and J. Scott Sparks of **Marshall Space Flight Center**. *No further documentation is available.*

Inquiries concerning rights for the commercial use of this invention should be addressed to the Patent Counsel, Marshall Space Flight Center [see page 18]. Refer to MFS-28431.

Detecting Filler Spaces Under Tiles

An eddy-current probe detects hidden seams, steps, and holes in a metal substrate.

John F. Kennedy Space Center, Florida

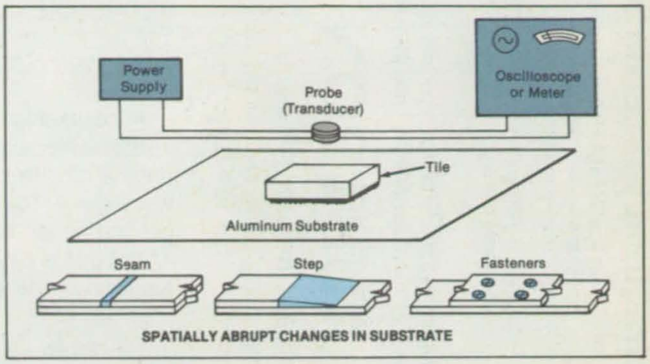

The **Transducer Coil Excites Eddy Currents** in the aluminum substrate material. The response appears on an oscilloscope or meter. Changes in the response indicate spatially abrupt changes in the substrate.

An eddy-current probe nondestructively and indirectly indicates whether screed is present under ceramic tile on an aluminum substrate. The particular eddy-current probe is intended for use on the insulating tiles on the Space Shuttle, but the eddy-current-probe technique has many potential terrestrial applications in nondestructive testing.

The screed, a room-temperature-vulcanizing polymer (RTV), is a filler that provides a smooth surface for bonding the tiles over seams, steps, and fasteners in the aluminum substrate. The screed can deteriorate under the influence of spilled hydraulic fluid, tile-waterproofing compound, and wide-ranging heat cycles, but there is no way of ascertaining from the appearance of the tile surface whether screed underlies the tile. Sometimes, it is necessary to remove tiles where screed may possibly be present, a process that takes 80 worker-hours per tile. Often, tiles are removed in a suspect area only to reveal that no screed has been used there. Moreover, tiles are frequently damaged during removal and replacement.

With the new probe, screed can be detected without removing tiles. Only about 0.5 worker-hour is needed to evaluate one tile. If screed is found, the tile can then be removed so that the RTV can be inspected and repaired. Unnecessary removal — and potential damage — is eliminated.

Pulsed high-frequency current in a coil in the probe induces eddy currents in the aluminum substrate (see figure). The coil detects the magnetic field produced by the eddy currents. The magnetic field can be related to the distance between the probe (which is placed on the outer surface of the tile) and the substrate, and thus indicates indirectly where screed is present. In the prototype instrument, the output signal of the probe is displayed on an oscilloscope, the output of which, in turn, could be fed to a digital voltmeter. In demonstrations, the prototype produced accurate information about the configuration of the substrate under the tiles. It gave repeatable results from test to test and from operator to operator.

This work was done by Paul Mende and David Shinkevich of Lockheed Space Operations Co. and John Scheuer of Lockheed Missiles and Space Co. for **Kennedy Space Center**. *For further information, Circle 130 on the TSP Request Card.*

Inquiries concerning rights for the commercial use of this invention should be addressed to the Patent Counsel, Kennedy Space Center *[see page 18]*. *Refer to KSC-11411.*

Tool for Robotic Resistive Roll Welding

Resistance-welding current starts and stops automatically according to force exerted against the workpiece.

Marshall Space Flight Center, Alabama

A roll-welding attachment for a robot is a simple, inexpensive device that incorporates a modified commercial resistance-welding gun. The roll welder is used to apply brazing foil to a workpiece.

The gun is mounted on a board, and a tungsten-alloy wheel is attached to its electrode holder (see figure). A spring-loaded plate is used for attachment to the end effector of the robot. The hand-operated trigger switch that turns on welding current in the unmodified gun is removed from the interior of the gun and mounted externally on the board, where it is actuated by a spring-

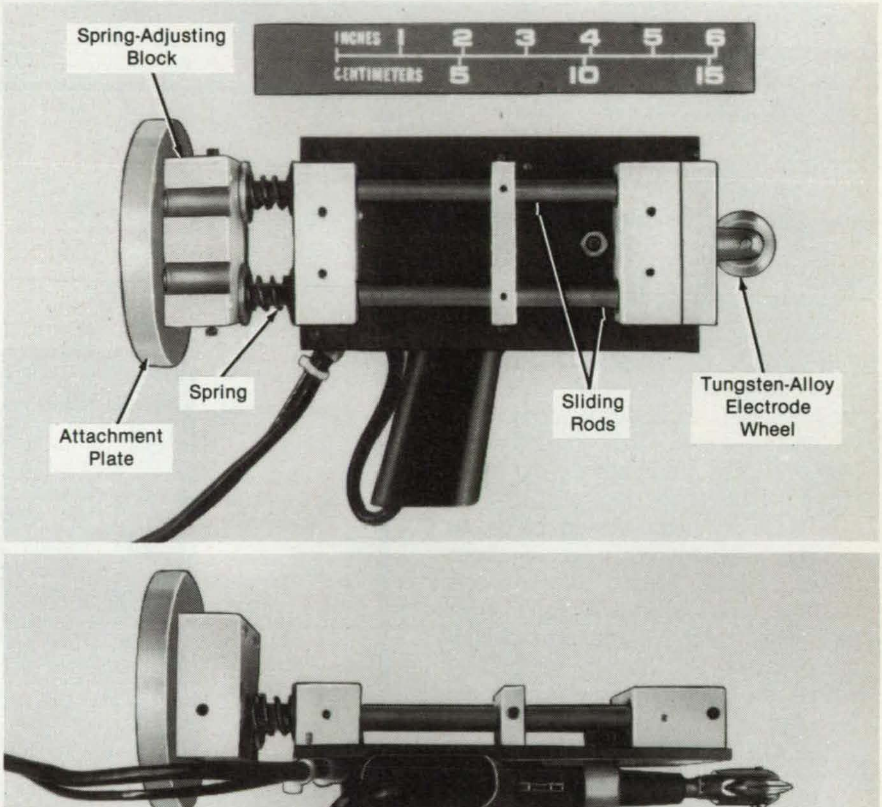

The **Modified Welding Gun** is easily attached to the end effector of a robot. The robot applies the welding force and moves the electrode wheel along the prescribed path.

loaded mechanism and the attachment plate.

The robot applies a force to the attachment plate, thereby compressing the springs and pressing the wheel against the foil on the workpiece. The rods on which the attachment plate are mounted slide into the gun until a tab actuates the switch lever, turning on welding current. The robot then rolls the wheel along the foil to weld it to the workpiece. When the robot removes the force, the springs push the rods and attachment plate outward, turning off the welding current.

This work was done by Jeffrey L. Gilbert of Rockwell International Corp. for **Marshall Space Flight Center**. *No further documentation is available.*

Inquiries concerning rights for the commercial use of this invention should be addressed to the Patent Counsel, Marshall Space Flight Center [see page 18]. Refer to MFS-29660.

Flexible Interior-Impression-Molding Tray

Weld joints in cavities can be examined nondestructively.

Marshall Space Flight Center, Alabama

Yet another device and its method of operation have been added to the variety of techniques for making impression molds of otherwise inaccessible interior surfaces. This latest device is used inside a combustion chamber of complicated shape for the nondestructive evaluation of the qualities of welds, including such features as offset, warping, misalignment of parts, and drop-through.

The device includes a flexible polypropylene tray trimmed to fit the desired interior surface contour. Two neodymium boron magnets ½ in. (12.7 mm) or ¾ in. (19 mm) in diameter and an inflatable bladder are attached to the tray (see figure). In operation, a video borescope (not shown in the figure) is first used to identify the surface to be inspected. Next, the impression-molding material — a quick-setting, very-high-viscosity silicone — is prepared by mixing Citricon base (or equivalent) putty with the amount of accelerator required to obtain a setting time of 10 to 20 minutes.

The tray is loaded with impression-molding material and inserted in the cavity. Viewing the interior of the cavity through the borescope, the technician guides the tray to the surface to be inspected with the aid of two external neodymium boron magnets. Using a 60-cm^3 plastic syringe with a check valve, the technician pumps air into the bladder. The bladder becomes inflated, pressing the flexible tray and its putty against the surface to be inspected. After the 10- to 20-minute setting time, the technician deflates the bladder and extracts the tray from the cavity with the help of a tether. The accurate impression of the wall on the putty is then examined.

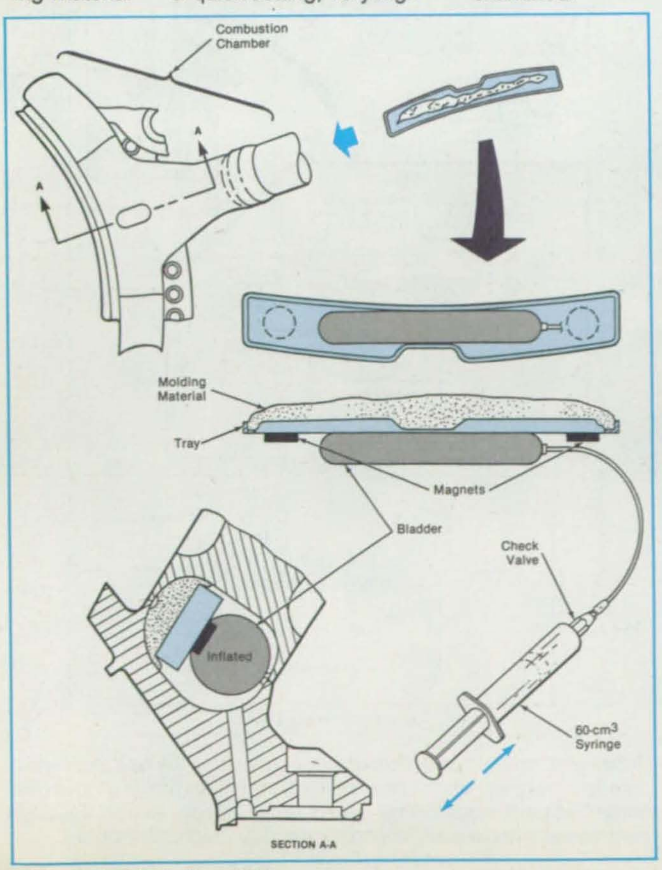

The **Tray and Putty** are inserted in a cavity to make a mold of the interior surface.

This work was done by Jeffrey E. Anders of Rockwell International Corp. for **Marshall Space Flight Center**. *No further documentation is available.*

Inquiries concerning rights for the commercial use of this invention should be addressed to the Patent Counsel, Marshall Space Flight Center [see page 18]. Refer to MFS-29679.

Monitoring Weld Penetration Via Gas Pressure

Jumps in pressure indicate whether full penetration has been achieved or lost.

Marshall Space Flight Center, Alabama

A welding monitor uses pressure on the back side of a weldment to monitor the penetration of the weld. The pressure-monitoring system was devised to ensure full penetration along the full lengths of weld joints, when direct observation of their back sides by visual inspection, x rays, or fiber optics is not possible.

The system operates on the principle that the pressure of the inert purge gas flowing through the cavity on the back of the weldment decreases sharply the instant a weld keyhole is established, indicating full penetration. When the keyhole closes, the pressure rises suddenly, indicating that full penetration has been lost. The information gained by use of the monitor can be used in the initial development of welding parameters or during production as a safeguard.

This work was done by J. Ben Coby, Jr., and Douglas M. Todd by Rockwell International Corp. for **Marshall Space Flight Center.** *No further documentation is available.*

Inquiries concerning rights for the commercial use of this invention should be addressed to the Patent Counsel, Marshall Space Flight Center [see page 18]. Refer to MFS-29683.

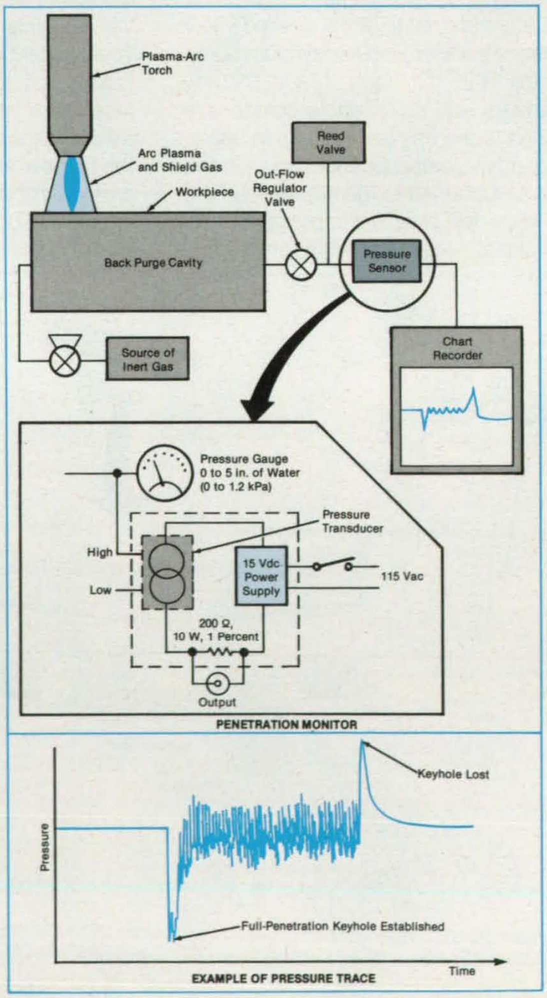

A Sensor Continuously Measures the pressure of the inert gas flowing through the cavity on the back of a weldment. A sudden drop on the pressure chart means that the weld pool has fully penetrated; a sudden rise means that the pool no longer extends through the joint.

Beam Splitter for Welding-Torch Vision System

Illumination for previews could be directed along the torch.

Marshall Space Flight Center, Alabama

A compact welding torch equipped with an along-the-torch vision system includes a cubic beam splitter to direct preview light on the weldment and to reflect light coming from the welding scene for imaging. The beam splitter is integral with the torch; it requires no external mounting brackets. The torch is, therefore, exceptionally compact.

The beam splitter is inside the torch at the right-angle bend in the torch housing (see figure). It directs light from a lamp, in a beam concentric with the welding torch, onto the weld path. It collects the same light after reflection from the workpiece and diverts it into a system of lenses in the torch. A video camera processes the reflected beam and converts it into an image of the weld.

The beam splitter is rugged and withstands vibrations and a wide range of temperatures. It is a commercially available, reasonably priced item that comes in a variety of sizes and optical qualities with antireflection and interference-filter coatings on the desired faces. It can be made to provide 50 percent transmission and 50 percent reflection of the incident light to exhibit minimal ghosting of the image.

This work was done by Jeffrey L. Gilbert of Rockwell International Corp. for **Marshall Space Flight Center**. *No further documentation is available.*
MFS-29641

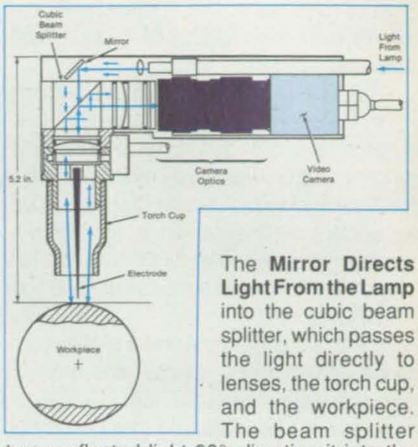

The Mirror Directs Light From the Lamp into the cubic beam splitter, which passes the light directly to lenses, the torch cup, and the workpiece. The beam splitter turns reflected light 90°, directing it into the camera optics.

Making Three-Layer Solid Electrolyte/Electrode Sandwiches

Compositions and particle sizes are adjusted for sintering at a common temperature.

NASA's Jet Propulsion Laboratory, Pasadena, California

A tape-casting-and-sintering process joins two ceramic materials having widely different sintering temperatures into an integral sandwich structure. Although monolithically joined, the layers retain their identities, without migration of constituents.

The method is used to make a three-layer structure composed of outer porous layers of strontium-doped lanthanum manganite and an inner dense layer of yttria-stabilized zirconia (see figure). Such structures could be used to make electrolytic and fuel cells with solid electrolytes for use at high temperatures. In a cell, the porous outer layers are the electrodes, and the dense inner layer is the electrolyte. Other potential applications include oxygen pumps and oxygen sensors.

Ordinarily, tape-cast zirconia powder requires a sintering temperature of at least 1,400 °C to produce a dense layer, whereas manganite powder condenses to an overly dense layer at that temperature. Moreover, manganese migrates into the zirconia layer, adversely affecting electrical properties. In the new method, the sintering temperature of the zirconia is lowered by using a slip composed of submicron-size powder particles with a minimum amount of binder and plasticizer. The sintering temperature of the manganite is raised by using a slip made up of larger, micron-size particles in a large amount of binder and plasticizer.

The strontium-doped lanthanum manganite powder is coarsened by presintering for 2 h at 1,250 °C and crushing the product just enough for it to pass through a 53-μm screen. It is mixed with a commercial polyvinyl butyral binder/plasticizer, stirred without breaking the coarsened particles, degassed, and cast on glass by a tape-casting machine. After drying, the tape contains 50 to 65 percent by volume of ceramic material and 35 to 50 percent organic binder and plasticizer.

Meanwhile, the fine yttria-stabilized zirconia powder is mixed in a solvent with a dispersant such as menhaden fish oil and ball-milled to break up agglomerated particles. The zirconia slip is degassed and spread over the manganite tape by the tape-casting machine.

When the zirconia layer is dry enough not to run when handled, the tape is folded in half so that a double layer of zirconia is sandwiched between two manganite layers. The sandwich is pressed lightly to drive out excess air, then dried in air. The dry sandwich is pressed at 3,000 to 5,000 psi (21 to 34 MPa) and sintered in air for 6 h at 1,300 °C.

At this sintering temperature, the manganite does not decompose, and manganese therefore does not diffuse into the zirconia layer. After sintering, the density of the resulting porous manganite layer is 50 to 60 percent of the theoretical, and the density of the zirconia layer is 98 percent of the theoretical.

This work was done by James E. Schroeder of Caltech for **NASA's Jet Propulsion Laboratory**. *For further information, Circle 135 on the TSP Request Card.*

In accordance with Public Law 96-517, the contractor has elected to retain title to this invention. Inquiries concerning rights for its commercial use should be addressed to

Edward Ansell
Director of Patents and Licensing
Mail Stop 305-6
California Institute of Technology
1201 East California Boulevard
Pasadena, CA 91125

Refer to NPO-17078, volume and number of this NASA Tech Briefs *issue, and the page number.*

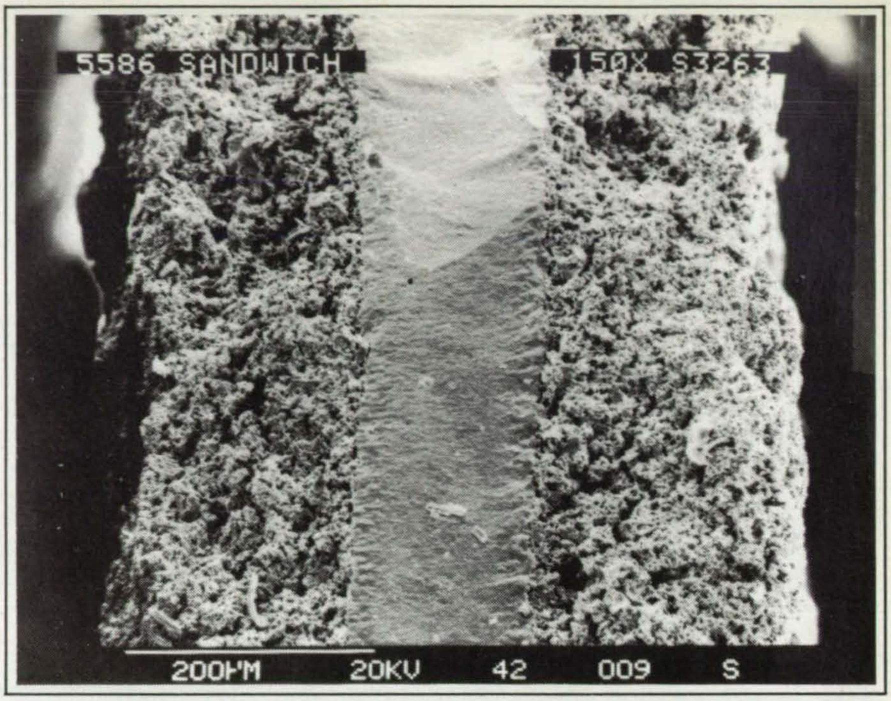

Magnified Cross Sections of the ceramic sandwich show porous strontium-doped lanthanum manganite on the outside and dense yttria-stabilized zirconia on the inside. The layered ceramic is sintered at a temperature 100 °C below the normal sintering temperature for zirconia.

Spacing Windings Evenly in Toroidal Inductors

Leakage inductance is controlled.

NASA's Jet Propulsion Laboratory, Pasadena, California

A technique for winding a toroidal inductor results in even spacing of windings around the toroidal core. Even spacing minimizes the proportion of leakage inductance, especially if the core has relatively low permeability. The new winding technique is useful, for example, in minimizing the leakage inductance of an inductor containing a powder core, intended for use in a power supply operating at a frequency between 250 kHz and 2 MHz.

The new technique involves a three-step winding process. First, the wire (typically, litz wire) to be wound on the core can be covered with shrinkable tubing. (This is not practical in small RF units where only a single wire is used.) Next, the wire is wound on the core through gaps or holes in an alignment disk (or disks) that enforce(s) the desired spacing (see figure). Finally, heat is applied to shrink the tubing, locking the wire in place.

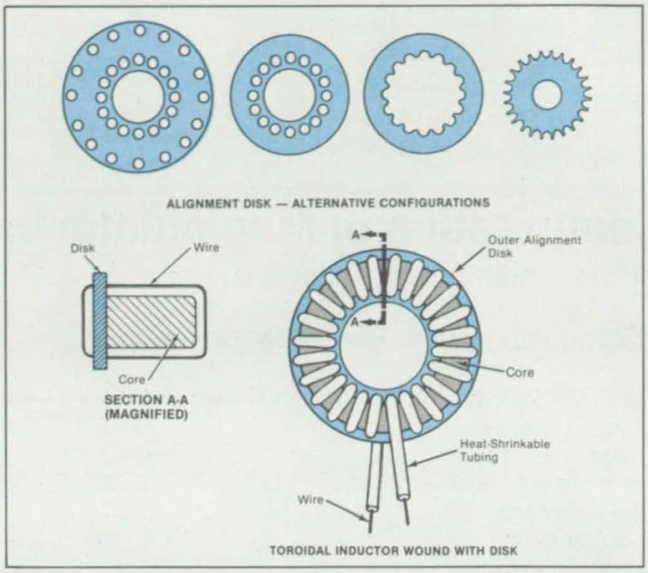

Alignment Disks space the winding evenly, and heat-shrinkable tubing locks it in place. However, shrinkable tubing is not necessary to get good results.

This work was done by W. T. McLyman of Caltech for ***NASA's Jet Propulsion Laboratory****. For further information, Circle 150 on the TSP Request Card.*

This invention is owned by NASA, and a patent application has been filed. Inquiries concerning nonexclusive or exclusive license for its commercial development should be addressed to the Patent Counsel, NASA Resident Office-JPL [see page 18]. Refer to NPO-17830.

Mathematics and Information Sciences

Efficient Computation of Manipulator Inertia Matrix

Real-time control and simulation are enhanced.

NASA's Jet Propulsion Laboratory, Pasadena, California

An improved method for the computation of the manipulator inertia matrix has developed, which is based on the concept of the spatial inertia of composite rigid body (see Figure 1). The computation of the inertia matrix is required for the implementation of the advanced dynamic-control schemes as well as the dynamic simulation of the manipulator motion. The development of this method is motivated by the increasing demand for fast algorithms to provide real-time control and simulation capability and, particularly, the need for faster-than-real-time simulation capability, which will be required in many anticipated space teleoperation applications.

The work starts by discussing two physical interpretations for elements of the inertia matrix, leading to two distinct previously proposed algorithms: i.e., the Composite Rigid-Body (CRB) algorithm and the Newton-Euler Based (NEB) algorithm, with the CRB algorithm being the most efficient. The redundancy in both algorithms is analyzed, and it is shown that the two algorithms are basically equivalent; i.e., they can be transformed to each other. For developing the new algorithm, spatial notation is used, which leads to compact equations and simplifies the algorithmic analysis. Using more classical notation, the final equations of the algorithm are then presented in a coordinate-free form. The choice of optimal frame(s) for projection of the coordinate-free (intrinsic) equations is discussed by analyzing the vectors and the tensors involved in the equations. It is shown that significant efficiency can be achieved by using different frames for projection of different sets of equations. The developed algorithm achieves a greater computational efficiency over the CRB algorithm by eliminating the redundancy in the intrinsic equations as well as by the suitable choice coordinate frame for their projection.

Figure 2 shows a comparison of the efficiency of the developed algorithm (designated as VCRB) and the previously proposed composite rigid-body algorithm (designated as OCRB). The developed algorithm is also more suitable for parallel processing than the CRB algorithm. This is mainly due to the fact that the algorithm achieves a greater computational efficiency by reducing the data dependency in the computation. In a separate report, it is shown that the developed algorithm can be fully parallelized, leading to the computation of the inertia matrix in a time of $O(\log n) + O(1)$ with $O(n^2)$ processors.

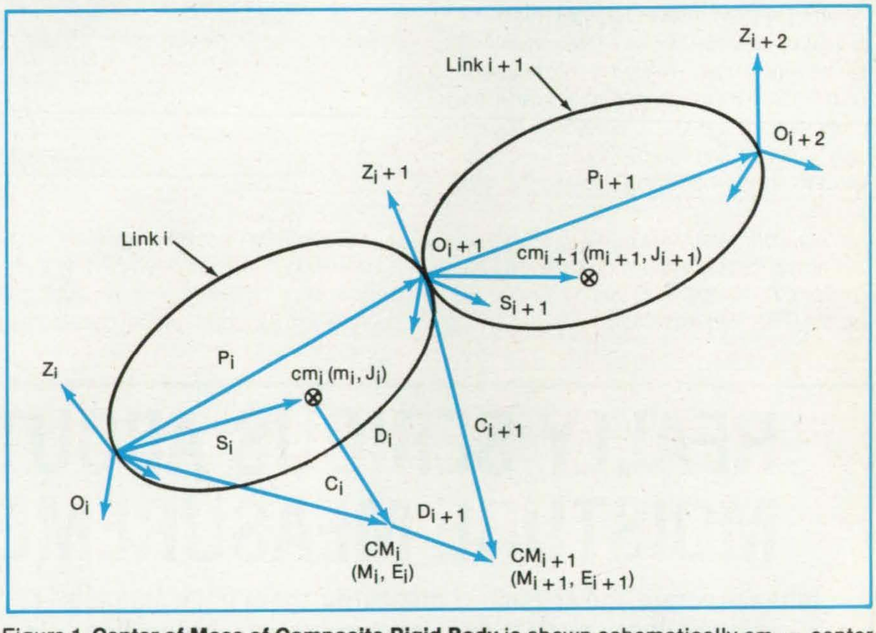

Figure 1. **Center of Mass of Composite Rigid Body** is shown schematically cm_i = center of mass link *i*. CM_i = center of mass composite system composed of link *i* through link *n*.

Algorithm	General		n = 6	
	Multiplication	Addition	Multiplication	Addition
OCRB	$11n^2 + 79n - 21$	$8n^2 + 73n - 39$	849	687
VCRB	$(9/2)n^2 + (231/2)n - 117$	$4n^2 + 88n - 95$	738	595

Figure 2. **Comparison of Computational Costs of Evaluating the Inertia Matrix** shows that the VCRB algorithm is more suitable for parallel processing than the CRB algorithm is.

This work was done by Amir Fijany and Antal K. Bejczy of Caltech for **NASA's Jet Propulsion Laboratory.** *For further information, Circle 51 on the TSP Request Card.*

NPO-17545

Books and Reports

These reports, studies, handbooks are available from NASA as Technical Support Packages (TSP's) when a Request Card number is cited; otherwise they are available from the National Technical Information Service.

Norms and Completeness in Variational Methods

Incomplete bases and incorrect norms can lead to erroneous results.

A paper discusses the significance of norms and completeness in analyses based on the variational principle of mechanics. Such analyses are conducted to determine static deflections and/or vibrations of structures, including complicated ones like spacecraft. In practice, analysts often pay insufficient attention to the requirements for a complete set of basis functions and the correct choice of a norm. The paper illustrates by an example that such a casual approach can lead to erroneous results. One kind of error could occur in an iterative algorithm based on the variational method; the mere fact that the solutions converge does not guarantee that they converge to the correct solution.

The example is that of a simple cantilever beam loaded uniformly along its length. The exact solution for the deflection of the beam is well known; it is a fourth-order polynomial function of position along the beam. A variational-principle solution is sought in the form of a Fourier cosine series. The idea is to choose the coefficients of the cosine terms in such a way as to minimize the total potential energy; that is, the bending energy minus the work performed by the applied loading. Thus, the Fourier cosine terms are the basis functions, and the bending energy is the norm.

Heretofore, many analysts have tacitly assumed that if, as in the case of Fourier cosine terms, the basis functions are members of an infinite family of orthogonal functions and satisfy the geometric boundary conditions, convergence of the variational solution to the correct solution is guaranteed. In this example, the assumption is shown to be false. First, it is shown that the Fourier cosine series that minimizes the total potential energy and that satisfies the geometric boundary conditions differs from the exact fourth-degree polynomial solution. The resolution of the discrepancy lies in the fact that the Fourier cosine terms are complete in the L^2 norm, whereas the problem at hand requires basis functions, which are complete in the energy norm (integral, along the length of the beam, of the square of the second derivative of the deflection with respect to length).

Closer examination shows that the Fourier cosine terms do not constitute a complete set of basis functions for this problem; the additional function x^2 (where x denotes position along the beam) is needed to complete the set. When a term proportional to x^2 is included, the variational solution becomes exact; that is, equivalent to the fourth-degree polynomial along the length of the beam.

This work was done by Joel A. Storch of Caltech for **NASA's Jet Propulsion Laboratory**. *To obtain a copy of the report "Significance of Norms and Completeness in Variationally Based Methods," Circle 5 on the TSP Request Card.*
NPO-18071

Orthogonal Patterns in a Binary Neural Network

When probed by any pattern, the network converges to one of the stored patterns.

A report presents some recent developments in the theory of binary neural networks. The subject matter is relevant to associative (content-addressable) memories and to the recognition of patterns — both of considerable importance in the advancement of robotics and artificial intelligence.

A network of N neurons is represented by N variables x_1 through x_N each capable of taking on one of the two values ± 1. The state of the network is defined in terms of a pattern or vector $\mathbf{x}$ composed of the N variables. The information in M given patterns is stored in synaptic parameters calculated according to

$$T_{i,j} = \sum_{\ell=1}^{M} x_i^{(\ell)} x_j^{(\ell)}$$

where ℓ denotes the ℓth pattern.

The retrieval of information from the network is initiated by applying a probe (initial state) $\mathbf{x}(0)$. Neurons are then selected at random, one at a time, and their states are updated according to

$$x_i(k+1) = \text{sign}\left\{ \sum_{j=1}^{n} T_{i,j}\, x_j(k) \right\}$$

Previous research has shown that the network is globally stable in the sense that, initialized by any probe, it converges to some final state, and that under some conditions stored patterns can be retrieved without error.

To be retrievable, a stored pattern must be an equilibrium point of the network. It is shown that when the stored patterns are mutually orthogonal, they are equilibrium states of the network. The mathematical model is then modified slightly to allow storage of only mutually orthogonal patterns. The state of the network, initialized by any probe, is shown to converge to a pattern in the space, called the "memory space," spanned by the stored patterns.

There can be, at most, N orthogonal patterns. It is shown that when the stored patterns satisfy a certain coding condition, they are the only members of the memory space. The maximum number of such code words is shown to be $(2N)^{1/2}$, in agreement with a previous empirical observation.

A particular code-construction method is proposed. A network loaded with such code acts as a decoder. The stored patterns are shown to have basins of attraction of Hamming radius $N/(2M)$. When initialized within this range of a stored pattern, the state of the network converges with probability 1 to that pattern in less than a neural-update-cycle time. When the probe falls outside this range, the probability of retrieving the nearest stored pattern can still be increased to 1 by repeatedly running the network with the same probe.

This work was done by Yoram Baram of **Ames Research Center**. *To obtain a copy of the report, "Orthogonal Patterns in Binary Neural Network," Circle 48 on the TSP Request Card.*
ARC-12454

Life Sciences

Hardware, Techniques and Processes

Intramuscular Contact Lead Filled With Conductive Solution

The solution would maintain electrical conduction even when wires fail.

NASA's Jet Propulsion Laboratory, Pasadena, California

A proposed sheath for a braided-wire intramuscular conductor would preserve electrical continuity even if the wire breaks, as such wires often do because of corrosion and repeated flexing in the chemically and mechanically active environment of the human body. Such braided wires are used to deliver electrical stimuli to muscles in biomedical research on human and animal physiology, the development of prostheses, the regeneration of nerves and muscles, and artificial implants.

The sheath would be a tube of polyethylene terephthalate (Mylar or equivalent) or other plastic and would be surrounding a braided titanium or platinum wire (see figure). The sheath would contain an electrically conductive (e.g., salt) solution so that the wire is immersed in a conductive liquid. The solution would wet the wire but not the sheath. If the wire should break at any point along its length, the liquid would maintain electrical conduction, and the wire could still deliver electrical pulses. The electrically insulating sheath would prevent electrical leakage to the surrounding tissue.

The sheathed wire would be implanted surgically with the aid of a device that resembles a catheter. According to calculations, the stress of a representative 0.4-in. (0.1-cm) diameter sheath bent to a 2-in. (5-cm) radius would be 5,000 lb/in.^{2} (34 MPa), the endurance limit of Mylar.

This work was done by Robert M. Bamford and James A. Hendrickson of Caltech for **NASA's Jet Propulsion Laboratory**. *For further information, Circle 99 on the TSP Request Card. NPO-17186*

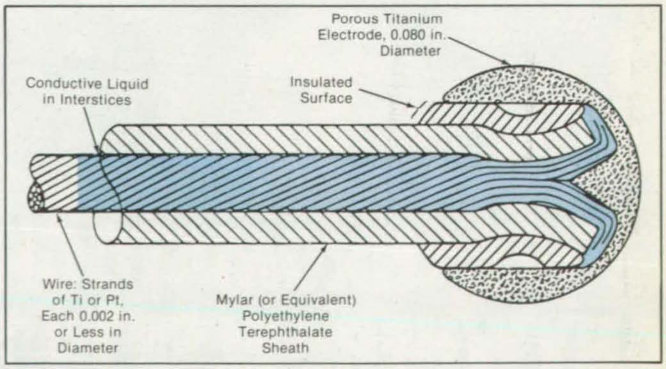

A **Plastic Sheath Would Surround** a conductive solution in which a braided wire would be immersed. At the end of the cable, the wire and sheath would be crimped together and press-fit in a porous titanium electrode.

New on the Market

Rockwell Communication Systems, Dallas, TX, has developed a five-channel **Global Positioning System receiver** measuring 2 1/2" x 4". The NavCore V can provide 3D position information worldwide for OEM applications in the automotive, marine, agriculture, mining, and consumer electronics industries, and could be employed in a handheld unit for personal navigation. It features a gallium arsenide receiver front-end, a high-speed digital signal processor, and a low-power navigation microprocessor.
Circle Reader Action Number 800.

Master Bond Inc., Hackensack, NJ, has introduced a room-temperature **curing adhesive** for bonding applications from -51° to +232° C. The EP33 adhesive produces high-strength bonds which resist thermal cycling and chemicals. It is 100 percent reactive, contains no diluents or solvents, and adheres to metals, glass, ceramics, wood, vulcanized rubbers, and most plastics.
Circle Reader Action Number 792.

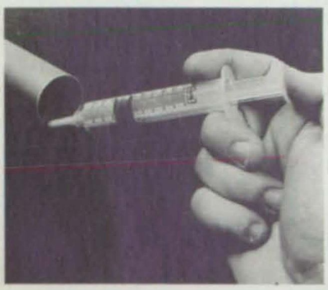

WH Brady Thin Film Products, Milwaukee, WI, has introduced BRADYTOUCH™ plastic transparent **touch screens** for industrial, medical, and telecommunications applications. Available in both matrix and analog formats, the lightweight screens can be used with any flat CRT, LCD, plasma, or electroluminescent display panel. They are constructed with an optical adhesive that reduces reflection and refraction.
Circle Reader Action Number 796.

A new **insertion magnetic flowmeter** from Metron Technology, Boulder, CO, accurately measures the flow rate of conductive liquids in line sizes from 3 to 80 inches. Meter electronics yield either 4 to 20 mA or pulse output and can be mounted remotely. A high-pressure retractor allows installation and removal without line shutdown or depressurization.
Circle Reader Action Number 794.

Sensor Products Inc., New York City, has created Pressurex™, a tactile **pressure detecting film** for determining compression magnitude and dispersion between contact surfaces. When subjected to pressure, the film turns a shade of red whose intensity indicates the force applied. By comparing the film to a color-calibrated spectrum chart, the user can quickly determine the compression force. If greater sensitivity is needed, the Pressurex densitometer can scan the film to produce a pressure distribution map. Pressurex comes in four sensitivities for pressure detection up to 18,000 lb/in^2, and operates in a variety of temperature and humidity conditions.
Circle Reader Action Number 790.

A new line of **brushless DC motors** from American Precision Industries, Oceanside, CA, features rare-earth magnets for high performance and high speeds at a variety of speed controls; quiet operation; and Hall-effect commutation. The motors meet MIL-I-45208A and NASA 5300-4 (1C) and can be customized. Applications include computer per-ipherals, laser scanners, medical and lab equipment, pumps, material handling equipment, and test and measurement instrumentation.
Circle Reader Action Number 798.

Polydamp™ melamine foam (PMF), a **sound-absorbing composite** produced by Polymer Technologies Inc., Newark, DE, functions under a temperature range of -45° to +200° C and will not drip or produce excess flame and smoke when ignited. PMF comprises a melamine foam core sandwiched between a film facing and a pressure-sensitive adhesive backing. The composite weighs 0.7 lbs/sq ft and adheres to metals, plastics, foams, and many other surfaces.
Circle Reader Action Number 786.

The Seriplex™ **control system** offered by Automated Process Control, Jackson, MS, can replace hundreds of control wires with one four-wire cable. A single cable lined with intelligent I/O modules is connected to a computer or PLC to control hundreds of sensors and loads. The modules have built-in communications, logic, and I/O control, and can operate as a stand-alone interconnect between an operator and hundreds of remote I/O devices without a CPU or PLC.
Circle Reader Action Number 784.

Advanced Photonix Inc., Los Angeles, CA, has produced large-area **avalanche photodetection devices** (APDs) designed to replace photomultiplier tubes in low-light-level applications. The rugged solid-state devices consume one-tenth the power of photomultiplier tubes, allowing for a much smaller power source. And unlike the glass tubes, APDs are not affected by magnetic fields, and therefore do not need shielding. In combination with scintillation crystals, the devices can be used in radiation detection, and also offer applications in scanners, industrial process controls, and military systems, including laser tracking and guidance.
Circle Reader Action Number 778.

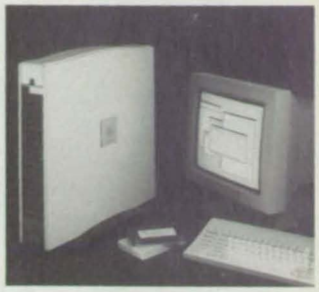

A new **neurocomputer system** can speed learning in neural networks 1000 fold, according to the manufacturer, Adaptive Solutions Inc., Beaverton, OR. Application developers can use the system to solve pattern recognition problems in optical character recognition, machine vision, speech recognition, and robotic and process control. It consists of a server, a neurocomputer for a UNIX network, and a robust software development environment called CodeNet.
Circle Reader Action Number 788.

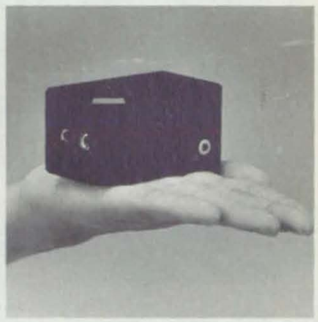

Hamamatsu Photonic Systems of Bridgewater, NJ, has introduced a picosecond **photodetector** that replaces the head, power supply, and cables currently used as an oscilloscope accessory. The model C4258 consists of a large-area photodiode with associated high-frequency circuitry and power source in a single compact case. It operates from 450 to 870 nm, making it useful for monitoring mode-locked lasers such as argon iron and Ti sapphire.
Circle Reader Action Number 782.

Conductus Inc., Sunnyvale, CA, has developed a process for manufacturing **Josephson junctions**, the key elements in most superconductive electronic circuits, including those used in signal processing, sensor, and digital applications. Employing conventional photolithographic techniques, the fabrication process creates reproducible grain boundary Josephson junctions on a wafer scale, and can be extended to complex superconductive integrated circuits.
Circle Reader Action Number 780.

New on the Market

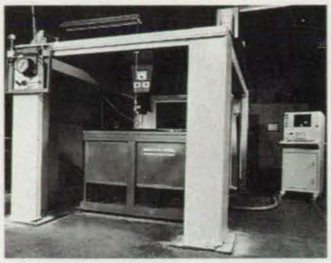

Ingersoll-Rand, Baxter Springs, KS, has introduced a moving gantry system for **waterjet cutting** of composites, plastics, glass, metals, and other materials. Suited for semi-automated production, the computer-driven system provides a contouring accuracy of ±0.015" per axis over total travel. The steel grid cutting area has a 125 lb/ft² load capacity and can cut large-scale pieces.
Circle Reader Action Number 776.

A new **deposition system for producing thin films** has been developed by Jet Process Corp., New Haven, CT. The jet vapor deposition (JVD) process uses a supersonic jet flow of inert carrier gas formed by a nozzle directed into a low-vacuum chamber to create uniform thin films at high rates and low temperatures. It deposits thin films of a variety of metals, oxides, nitrides, semiconductors, and organics, and can be used to coat wires, tapes, fibers, and inside channels and tubes.
Circle Reader Action Number 768.

Ei/Engineering Information Inc., New York City, has introduced Ei Page One™, a **CD-ROM database** containing citations from engineering journals and conference proceedings worldwide. Updated monthly, the database covers publications from 3000 engineering societies, commercial publishers, research and development organizations, university presses, and government agencies. Readers can scan the table of contents or skip to a journal of interest and call up successive issues or articles.
Circle Reader Action Number 770.

Smart Touch™, a **flat-panel operator interface** from Total Control Products Inc., Berkeley, IL, replaces push buttons, pilot lights, thumbwheels, panel meters, and alarm displays with touch-actuated graphic controls. The built-in CAD editor produces graphic characters such as lines, circles, fan shapes, squares, tiled squares, and filled patterns. Only five inches deep, the flat-panel display has a resolution of 640 x 400 pixels.
Circle Reader Action Number 772.

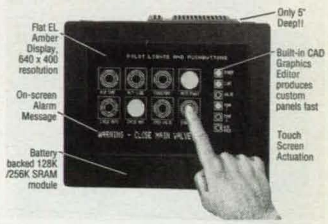

A new line of portable **thermal imaging radiometers** is offered by Inframetrics Inc., North Billerica, MA. Features include an integrated floppy disk image recorder, built-in image processing, an embedded color LCD display, backlit controls, and electric cooling, which eliminates the need for liquid nitrogen.
Circle Reader Action Number 774.

Monolithic Systems Corp., Englewood, CO, has introduced the MicroVGA 452, a **half-length card which enhances VGA monitor resolution**. An anti-aliasing technique reduces stair-stepping to provide straight lines, smooth circles and arcs, and near photo-realistic images. It provides a resolution of 1536 x 1280 with 742,813 colors on a standard (640 x 480) monitor.
Circle Reader Action Number 766.

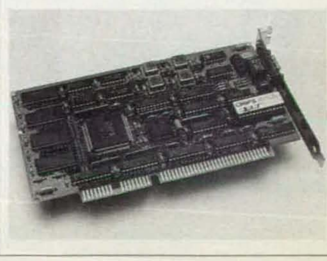

New Literature

West Instruments, East Greenwich, RI, has released a four-color brochure on its Gardsman **microprocessor-based controllers** which offer up to 32 loops with continuous adaptive self-tuning and pre-tune algorithms. A multi-loop, 32-character LED provides deviation bar graph display for up to 32 loops simultaneously. The Gardsman recipe feature allows all data to be stored on a solid-state memory card.
Circle Reader Action Number 712.

Zero Plastics, Chicopee, MA, has published a catalog of standard and custom plastic thermoformed and rotationally-molded **cases for commercial and military applications**. Illustrations and color photographs highlight design features, benefits, suggested applications, and accessories and options.
Circle Reader Action Number 710.

A free catalog from Applied Microsystems Corp., Redmond, WA, offers **microprocessor development tools** for embedded design projects. It features in-circuit emulators, source level debuggers, and a variety of software tools and utilities. Application articles available through the catalog describe how to develop microprocessor-based designs.
Circle Reader Action Number 706.

Kinney Vacuum Co., Canton, MA, has published a guide to selecting **vacuum pumps** based on vacuum pressure and capacity. It includes formulas for factoring gas load and pump down-time into capacity calculations, and features a color-coded selector chart that describes Kinney's vacuum pumps, boosters, and booster/pump combinations.
Circle Reader Action Number 702.

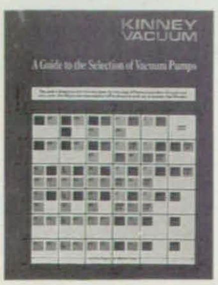

A 20-page catalog of **optical interference filters and coatings** for laser, absorption, and fluorescence spectroscopy is available from Omega Optical Inc., Brattleboro, VT. It provides details on physical theory, coating design, and spectral characteristics, and includes a glossary of optics terms and a conversion table of absorbance versus percent transmittance. Instrumental considerations such as signal-to-noise ratio and incident angle effects are presented along with physical configurations.
Circle Reader Action Number 714.

A 412-page handbook of **linear motion products** from Star Linear Systems, Charlotte, NC, provides engineering specifications for round shaft linear bearings, ball rail linear motion guides, and precision rolled and ground ballscrews. Over 130 pages are dedicated to high-precision linear positioning tables with ballscrew, timing belt, or rodless cylinder drive packages.
Circle Reader Action Number 708.

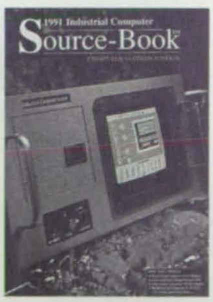

More than 500 **industrial computer systems** and data acquisition, industrial control, and communication products for the IBM PC/XT/AT are featured in a free publication from Industrial Computer Source, San Diego, CA. New product offerings include 20/15/10 slot rack and bench-top chassis, 8 and 15 slot chassis with electroluminescent displays, 486/25 MHz and 386/25/33 MHz CPU cards, and LabTech Notebook with ICONview.
Circle Reader Action Number 704.

General Dynamics Space Systems Div., San Diego, CA, has published a four-color brochure on its **materials and processes facilities** for integrated testing and analysis. It describes and illustrates the company's laboratories dedicated to mechanical and physical properties, cryogenics, engineering processes, composites processing, liquid oxygen compatibility testing, surface science and x-ray analysis, printed circuit boards, and nondestructive testing. Data sheets list each facility's capabilities and equipment.
Circle Reader Action Number 724.

Solutions for engineering, laboratory, and process control applications are detailed in *PC Instrumentation for the 90s*, a new publication from United Electronic Industries, Watertown, MA. It includes technical information for **data acquisition boards, systems, and software**. The board software, called Status, provides data acquisition at a maximum board throughput and features windowing, a graphic interface, pulldown menus, and context-sensitive help.
Circle Reader Action Number 720.

A free catalog from Global Specialties, New Haven, CT, highlights **electronic testing and prototyping equipment**. New products include digital multimeters, test instruments, power supplies, frequency counters, breadboards, and PC prototyping cards. It also features a handheld multimeter, three logic analysis test kits, and a digitally-synthesized function generator.
Circle Reader Action Number 716.

Electronic Devices Inc., Yonkers, NY, has issued a 152-page catalog of **rectifier bridges, low- and high-voltage diodes, and high-voltage assemblies**. It contains specifications for hundreds of silicon rectifiers, and includes new products such as x-ray diodes, in-line PC mount bridges in 10 and 40 amp ratings, high-current single- and three-phase bridges, and miniature high-voltage diodes, arrays, and multipliers.
Circle Reader Action Number 726.

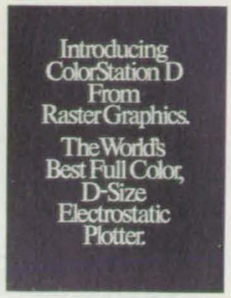

The ColorStation, a 400-dpi, D-size **electrostatic plotter**, is spotlighted in a new brochure from Raster Graphics Inc., Sunnyvale, CA. The brochure describes ColorStation's Silicon Imaging Bar™, a writing head which eliminates streaking and striations, and its patented paper transport system, which automatically loads paper from a roll, cuts it, and anchors it to a belt while the image is written, eliminating registration marks on the media. The free publication also covers software compatibility and has a features/benefits comparison chart.
Circle Reader Action Number 728.

A four-color brochure from Grumman Data Systems, Woodbury, NY, describes **logistics information systems** that support CALS standards and Open System Interconnect (OSI) protocols. It explores such programs as the Defense Logistics Services Center Modernization Program, the US Navy Rapid Acquisition of Manufactured Parts system, and Phase I of the US Army CALS program. The systems are installed without interruption of existing operations by means of special transitioning techniques.
Circle Reader Action Number 722.

Keithley Instruments, Cleveland, OH, has published a handbook of **low-voltage measurement techniques**. Each of its four main sections—metrology, superconductivity, component evaluation, and materials research—illustrate three measurement applications. The handbook also discusses physical phenomena such as Johnson noise, thermoelectric potentials, and magnetic fields, as well as their effects on low-level signals.
Circle Reader Action Number 718.

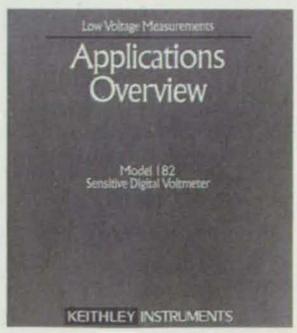

Subject Index

A

B

C

D

E

F

G

H

I

Advertisers Index

*RAC stands for **Reader Action Card**. For future information on these advertisers, please circle the RAC number on the Reader Action Card in this issue. This index has been compiled as a service to our readers and advertisers. Every precaution is taken to insure its accuracy, but the publisher assumes no liability for errors or omissions.

NASA Tech Briefs, ISSN 0145-319X , USPS 750-070, copyright © 1991 in U.S., is published monthly by Associated Business Publications Co., Ltd., 41 E. 42nd St., New York, NY 10017-5391. The copyrighted information does not include the individual tech briefs which are supplied by NASA. Editorial, sales, production and circulation offices at 41 East 42nd Street, New York, NY 10017-5391. Subscription for non-qualified subscribers in the U.S., Panama Canal Zone, and Puerto Rico, $75.00 for 1 year; $125.00 for 2 years; $200.00 for 3 years. Single copies $10.00. Foreign subscriptions one-year U.S. Funds $150.00. Remit by check, draft, postal, express order or VISA, MasterCard, or American Express. Other remittances at sender's risk. Address all communications for subscriptions or circulation to NASA Tech Briefs, 41 East 42nd Street, New York, NY 10017-5391. Second-class postage paid at New York, NY and additional mailing offices.

POSTMASTER: Please send address changes to NASA Tech Briefs, 41 East 42nd Street, Suite 921, New York, NY 10017-5391

Photo courtesy Diatek Corp.

A new infrared thermometer measures energy emitted from the eardrum.

Mission Accomplished

Through the technology transfer process, many of the systems, methods, and products pioneered by NASA are reapplied in the private sector, obviating duplicate research and making a broad range of new products and services available to the public.

Adopting infrared sensor technology developed for space missions, the Diatek Corporation of San Diego has produced an aural thermometer that gauges body temperature in two seconds or less. Accurate to within two-tenths of a degree, the Model 7000 thermometer measures heat emitted from the patient's tympanic membrane, or eardrum. This technique saves nursing time and enhances patient comfort, according to Lee Lyman, Diatek's chief operating officer, and enables fast temperature-taking of the critically ill, incapacitated, or newborn.

A nurse inserts the plastic-covered probe into the opening of the patient's ear canal and presses a button activating the sensor. The probe detects infrared radiation emitted from the eardrum and converts it into electricity, which is then converted by a microprocessor into the corresponding body temperature and displayed on a liquid crystal screen. The aural device reduces the risk of cross-infection because it avoids contact with mucous membranes, Lyman said, and because it employs disposable probe covers.

The Model 7000's optical sensor was designed by Diatek engineers, then refined with help from NASA's Jet Propulsion Laboratory (JPL). The company's challenge was to design the optical components so the one-piece, handheld instrument could make rapid and accurate measurements, Lyman explained. Through NASA's Technology Affiliates Program, which lends NASA expertise to US firms developing new technology-based products, Diatek consulted JPL scientists who have used infrared sensors to remotely measure the temperatures of planets and stars. JPL also aided in mechanical analysis of the thermometer design, according to Dr. James Rooney, manager of the Technology Affiliates Program.

Introduced in February, the Model 7000 is targeted for acute-care hospitals and alternative health care sites such as Surgi-Centers, nursing homes, blood banks, and cancer and burn centers. Diatek estimates the clinical thermometry market at $126 million worldwide, and expects 60 percent of all clinical thermometers to use infrared sensors by 1997. ❑

For further information about NASA's Technology Affiliates Program, contact:
Dr. James Rooney
Jet Propulsion Laboratory
4800 Oak Grove Drive
Pasadena, CA 91109

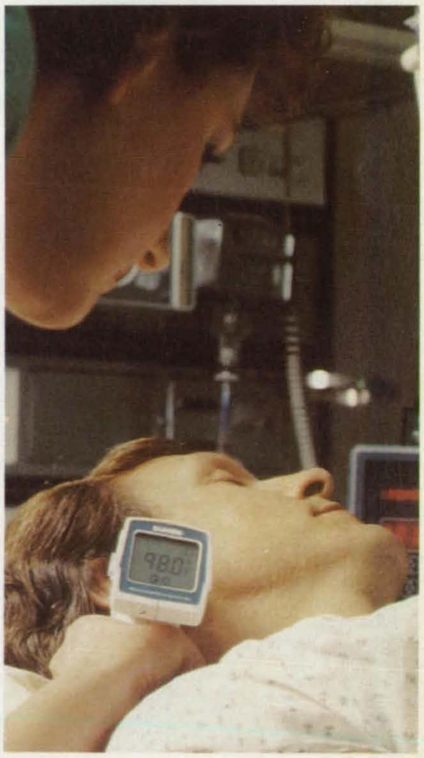

Photo courtesy Diatek Corp.

The Model 7000's infrared sensor delivers temperature readings in either Centigrade or Fahrenheit in two seconds or less.